WAVEGUIDE QED IN THE SQUEEZED VACUUM

A Dissertation

by

JIEYU YOU

Submitted to the Office of Graduate and Professional Studies of
Texas A&M University
in partial fulfillment of the requirements for the degree of

DOCTOR OF PHILOSOPHY

Chair of Committee,	M. Suhail Zubairy
Committee Members,	Alexei Sokolov
	Aleksei Zheltikov
	Philip R. Hemmer
Head of Department,	Grigory Rogachev

May 2020

Major Subject: Physics

ABSTRACT

The well-known Purcell effect shows that the spontaneous decay rate of an emitter can be affected by the electromagnetic environment with which the emitters interact. One of the most famous and popular examples is the squeezed vacuum. Although the squeezed vacuum does not change the density of states of the electromagnetic modes, it can modify the decay rate as well as the dephasing rate of the emitters. The interaction between a single atom and the squeezed vacuum has been widely studied, while only a few publications deal with the multiple-atom system. Despite the fact that the dipole-dipole interaction induced by ordinary vacuum depends on the relative separation of atoms, there are only a few papers studying the impact of atomic separation in the squeezed vacuum. In this dissertation, we show that the interaction induced by the squeezed vacuum depends on the center of mass positions of the atoms, which is essentially different from that in the ordinary vacuum. We also illustrate how to choose the coordinate system to make the center of mass position reasonable and well-defined.

Although the squeezed vacuum theory has been widely studied, it is impractical to generate a broadband squeezed vacuum reservoir which squeezes all modes in the 3-dimensional (3D) space. Recently, photon transport in a one-dimensional (1D) waveguide coupled to quantum emitters (well known as "waveguide-QED") has attracted much attention due to its possible applications in quantum device and quantum information. In contrast to the 3D case, squeezing in 1D is more experimentally feasible. Suppression of the spontaneous decay rate and the linewidth of the resonance fluorescence atom has been experimentally demonstrated in a 1D microwave transmission line coupled to a single artificial atom. However many-body interaction in a 1D waveguide QED system coupled to the squeezed vacuum has still not yet been studied. In this dissertation, we apply our theory to the 1D waveguide-QED system with the squeezed reservoir. Contrary to the traditional result that the dephasing rate of a single atom is a constant, our calculation shows that the dephasing rate is actually position-dependent. As the dipole-dipole interaction is involved in the atomic system, both the atomic separation and center of mass position have impacts on the decay

rate, dephasing rate, and the emitted resonance fluorescence spectrum. Moreover, the stationary maximum entangled NOON state can be achieved if atomic transition frequency is resonant with the center frequency of the squeezed vacuum.

In light of the fact that two qubits can be treated as a whole to be a four level atomic system, we also study the dynamics of Ξ-type atoms driven by a squeezed vacuum. We get the interesting result that the atomic system's steady state is a pure state, and a complete population inversion can occur when the coupling between the atomic dipole and the squeezed vacuum satisfy some certain conditions. We also mathematically prove that the steady state of a many-body system is nothing else but the direct product of that in the single atom case even when dipole-dipole interaction is involved.

DEDICATION

To my mother, Aihua Hu, and my father, Sijian You.

ACKNOWLEDGMENTS

I would like to thank my advisor, Dr. M. Suhail Zubairy, for giving me the opportunity to learn from him. He is so patient, erudite, and full of knowledge that I could not have finished this dissertation without his instruction and guidance. I also want to thank Dr. Marlan O. Scully, the leader of IQSE (The Institute for Quantum Science and Engineering) for supporting me with HEEP fellowship and inviting me to Wyoming summer school, where I could learn from many world famous physicists. Thanks also to my colleagues Dr. Zeyang Liao, Dr. Xiaodong Zeng, Dr. Shengwen Li, Dr. Phililp R. Hemmer, Dr. Girish Agarwal, and Dr. Fuli Li for their collaboration. Their help was essential in many of my projects. It has been my great pleasure to work with and learn from them. I also want to extend my gratitude to the department faculty who taught me physics courses and the staff who helped me prepare for my defense.

CONTRIBUTORS AND FUNDING SOURCES

Contributors

This work was supported by a dissertation committee consisting of Professor M. Suhail Zubairy, Alexei Sokolov, and Aleksei Zheltikov of the Department of Physics and Atronomy and Professor Philip R. Hemmer of the Department of Electrical & Computer Engineering.

All work conducted for the dissertation was completed by the student independently.

Funding Sources

Graduate study was supported HEEP fellowship, a grant from the Qatar National Research Fund (QNRF) under NPRP project 8-352-1-074, and a grant from King Abdulaziz City for Science and Technology(KACST).

NOMENCLATURE

IQSE	The Institute for Quantum Science and Engineering
TAMU	Texas A&M University
QED	Quantum electrodynamics
3D	three dimensional
TE modes	traverse electric modes
TM modes	traverse magnetic modes

TABLE OF CONTENTS

Page

ABSTRACT ii

DEDICATION iv

ACKNOWLEDGMENTS v

CONTRIBUTORS AND FUNDING SOURCES vi

NOMENCLATURE vii

TABLE OF CONTENTS viii

LIST OF FIGURES x

1. INTRODUCTION 1

2. SQUEEZED VACUUM RESERVOIR AND TRADITIONAL RESERVOIR THEORY ... 4

   2.1 Introduction to the squeezed vacuum 4
   2.2 Traditional reservoir theory 14

3. A MODIFIED RESERVOIR THEORY IN THE SQUEEZED VACUUM 20

   3.1 A new master equation from a modified mode function 20
   3.2 Master equation in the quasi-one-dimensional waveguide 31
   3.3 Dynamics of a single qubit 40
   3.4 Dynamics of multiple qubits coupled by the dipole-dipole interaction 41
   3.5 Generalization to multi-level atoms 43

4. THE STEADY STATE PROPERTIES OF ATOMS IN THE SQUEEZED VACUUM 50

   4.1 Quantum entanglement of two qubits 50
   4.2 Resonance fluorescence of a group of atoms 54
   4.3 The steady state population inversion of a single Ξ-type atom by the squeezed vacuum 58
   4.4 The steady state population inversion of multiple Ξ-type atoms by the squeezed vacuum 60

5. CAVITY-CAVITY INTERACTION IN THE SQUEEZED VACUUM 69

   5.1 General master equation of cavity-cavity interaction 69
   5.2 Steady state of non-resonant cavities 74

5.3 Steady state of resonant cavities 76

6. SUMMARY AND CONCLUSIONS 79

REFERENCES 81

LIST OF FIGURES

FIGURE Page

2.1 The error ellipse for the squeezed vacuum. 6

2.2 An SPDC scheme with the Type I output. 8

2.3 The photon number distribution for the single mode squeezed vacuum. 9

2.4 An SPDC scheme with the Type II output. 10

2.5 The photon number distribution for the two-mode squeezed vacuum. 12

2.6 The phase matching condition in SPDC process. 15

3.1 Demonstration for squeezing all modes in a single direction. The Electromagnetic wave propagates in two opposite directions, so two pumps are needed to squeeze all modes. 23

3.2 (a) Schematic setup for waveguide-QED in the 1D squeezed vacuum where the vacuum is squeezed from both directions. (b) The dispersion relations inside the waveguide. Here the atomic transition frequency is $\frac{1.2c\pi}{a}$, which is below the cut-off frequency of TE_{11} mode. Considering the fact that the atomic dipole moment is along y-axis and $E_y \neq 0$ only for TE_{10}, we only need to consider TE_{10} mode in our calculation. 32

3.3 (a) The dephasing dynamics of a single emitter in the squeezed vacuum. The black and red solid curves are the results of σ_x and σ_y, respectively. The blue dotted line is the result when there is no squeezing (thermal reservoir). (b) The dephasing rates of σ_x and σ_y as a function of the emitter position. For (a)&(b), the squeezing parameters are chosen to be $r = 0.5$. 39

3.4 Two-emitter case: Transverse polarization decay of the first emitter as a function of time. (a) $r_{12} = 0.5\lambda_{0z}$ for superscript (1) and $r_{12} = 1.0\lambda_{0z}$ for superscript (2), $r = 0.5$ and $r_c = 0$; (b) population decay as a function of time when $r_{12} = 0.5\lambda_{0z}$, $r = 0.5$ and $r_c = 0$. Solid lines are the results in squeezed vacuum and the dotted lines are the results in the thermal reservoir with $N = \sinh^2(r)$. Here the dynamics of ρ_{++} and ρ_{--} are highly identical. (c) Dephasing rate as a function of atom separation with the center of mass fixed at $r_c = 0$. (d) Dephasing rate as a function of center of mass position with atom separation fixed at $r_{ij} = \lambda_{0z}$, where the two-atom case is plotted in solid lines and the five-atom case is plotted in dashed lines. .. 42

4.1 (a) Concurrence evolution of different initial states in squeezed vacuum, where $r = 1$, $r_c = 0$, and $r_{12} = 0.25\lambda_{0z}$. (b) Fidelity evolution of different initial states in the same environment. 52

4.2 (a) Concurrence of the steady state as a function of average photon number $N = \sinh(r)^2$ and the position of the center mass $r_c = \frac{r_1+r_2}{2}$.(b) The impact of r_c's fluctuations on concurrence for different average photon number N. Δr_c is the distance from $\frac{n}{4}\lambda_{0z}$ to the position where the entanglement vanishes. 55

4.3 Resonance fluorescence spectrum of the two-emitter system inside a 1D waveguide. For better comparison, the spectra are normalized to the intensity at $\omega = \omega_0$ with the coherent elastic scattering singularity removed. Coherent driving Rabi frequency is $\Omega_R = 4\gamma$. In (a) and (b), the solid curves are the spectra for the coupled emitters, while the dashed curves are the spectra without emitter-emitter coupling. Parameters: (a) $r_1 = 0, r_2 = 0.01\lambda_{0z}$, squeezing parameter $r = 0.5$. (b) $r_1 = 0, r_2 = 0.25\lambda_{0z}$, $r = 0.5$. (c) $r_1 = 0, r_2 = \lambda_{0z}, \phi = \pi/2$, $r = 0.5$ for black line, $r = 1$ for red line. (d) $r_1 = -0.125\lambda_{0z}, r_2 = 0.125\lambda_{0z}$ for the red line, $r_1 = -0.25\lambda_{0z}, r_2 = 0.25\lambda_{0z}$ for the black line. $\phi = 0, r = 0.5$. 56

4.4 (a) The steady state population distribution for different μ_{ab} and μ_{bc}. The squeezing parameter $r = 1$ and the squeezing is perfect ($M = \sqrt{N(N+1)}$). (b) The steady state population distribution for non-ideal squeezed vacuum which is characterized by the ratio of M and $\sqrt{N(N+1)}$. The squeezing parameter $r = 1$, and $\gamma_{ab} = \frac{1}{4}\gamma_{bc}$. 61

4.5 The allowed population flow in the squeezed vacuum..... 62

4.6 (a) Fidelity evolution with different atomic separations. The atomic separations of λ_0, $0.1\lambda_0$, $0.2\lambda_0$ are plotted. Squeezing parameter $r = 1$, decay rate $\frac{\gamma_1}{\gamma_2} = \frac{1}{4}$ and time unit $\tau = 1/\sqrt{\gamma_{ab}\gamma_{bc}}$ is the geometric mean of the transition $|a\rangle \to |b\rangle$ and $|b\rangle \to |c\rangle$'s spontaneous emission rates in ordinary vacuum. (b) Fidelity evolution with different squeezing parameters. Decay rate $\frac{\gamma_1}{\gamma_2} = \frac{1}{4}$, and atomic separation $r_{12} = \lambda_0$. (c) Fidelity evolution with different decay rates. Squeezing parameter $r = 1$, and atomic separation $r_{12} = \lambda_0$. 64

5.1 (a) Schematic setup: two single-mode cavities are placed inside the waveguide with the broadband squeezed vacuum incident from both ends. 74

1. INTRODUCTION[1]

Due to the well known Purcell effect [1], the spontaneous decay rate of an emitter can be modified by engineering the electromagnetic bath environment with which the emitters interact. One example of bath engineering is the squeezed vacuum. Although the squeezed vacuum does not change the density of the electromagnetic modes, it can still modify the decay rate of the emitter [2, 3, 4]. A single emitter interacting with the squeezed vacuum has been widely studied [5, 6, 7]. However, there are only a few publications dealing with multiple emitters interacting with squeezed vacuum. Among these works, most are considering the case where emitters are separated by much less than an optical wavelength which is the well known Dicke model [8]. It is shown that in a broadband squeezed vacuum, emitter system evolves into a state whose properties are similar to those of the squeezed vacuum. Only a very few papers study the case when the separation between the emitters becomes important [9, 10, 11]. It is found that the dipole-dipole interaction induced by ordinary vacuum depends on the relative emitter separation, while the interaction induced by the squeezed vacuum depends on the center of mass coordinate of the emitters. Since it depends on the position of the center of mass, the choice of the coordinate system should be no longer arbitrary. However, it is not yet clearly illustrated in these literature on how to choose the coordinate system. Actually, the dependence on the absolute position comes from the fact that the squeezed vacuum is not vacuum but generated by a coherent light source. The phase of a coherent source is important for the dynamics of the emitter system [12] and it is seldom considered in the previous literature[9, 10, 11]. People usually thought this phase can be included in the phase of the correlation function. However, the phase in the correlation function is usually treated as a constant, while it can be a function of position. In addition, the previous calculations mainly consider a broadband squeezing in all directions of the 3-dimensional (3D) space which is difficult to be experimentally realized.

[1]Parts of the Abstract and this section are reprinted with permission from: "Waveguide QED in the Squeezed Vacuum" by Jieyu You et al, 2018. Physical Review A, 97, 023810, Copyright 2018 by the American Physical Society and "Steady-state population inversion of multiple Ξ-type atoms by the squeezed vacuum in a waveguide" by Jieyu You, Zeyang Liao, and M. Suhail Zubairy, 2019. Physical Review A, 100, 013843, Copyright 2019 by the American Physical Society

Recently, photon transport in a one-dimensional (1D) waveguide coupled to quantum emitters (well known as “waveguide-QED") has attracted much attention due to its possible applications in quantum device and quantum information [13, 14, 15, 16, 17, 18, 19, 20, 21, 22, 23, 24, 25]. In these previous studies, the photon modes in the waveguide are usually considered to be ordinary vacuum modes. The case when the waveguide modes are squeezed is seldom studied. In contrast to the 3D case, squeezing in 1D is more experimentally feasible. Suppression of the radiative decay of atomic coherence and the linewidth of the resonance fluorescence have been experimentally demonstrated in a 1D microwave transmission line coupled to single artificial atom [26, 27, 28, 29]. However, many-body interaction in a 1D waveguide-QED system coupled to squeezed vacuum has not yet been studied.

In this dissertation we consider the phase of the squeezing source and rederive the master equation for multi-atom dynamics in the squeezed vacuum based on the Weisskopf-Wigner approximation. We show that while the collective dipole-dipole interaction due to the ordinary vacuum depends on the emitter separation, the collective two-photon decay rate due to the squeezed vacuum largely depends on the center of mass position of the emitters relative to the squeezing source. We then apply this theory to the 1D waveguide-QED system with squeezing reservoir. Contrary to the traditional result that the dephasing rate of a single atom in the squeezed vacuum is a constant [4, 30], our calculation shows that the dephasing rate is actually position-dependent. As dipole-dipole interaction is involved, both emitter separation and center of mass coordinate can affect the decay rate, dephasing rate and the emitted resonance fluorescence spectrum. In addition, we also show that stationary quantum entanglement can be prepared in this system by the squeezing reservoir. The stationary maximum entangled NOON state can be approached if the center-of-mass of the emitters is at certain position.

Considering the fact that two qubits can be treated as a four-level system, the stationary NOON state implies the occurrence of population inversion in the steady state. The concept of population inversion is of fundamental importance in laser physics because the population inversion is a key step of generating laser. However, the population inversion can never exist for a system at thermal

equilibrium because of the spontaneous emission. The achievement of population inversion therefore requires pushing the system into a non-equilibrated state [31]. Thus, the spontaneous emission must be inhibited in order to maintain the population inversion in a steady state. In 1946, Purcell showed that the spontaneous decay rate of an emitter can be modified by engineering the electromagnetic bath environment with which the emitters interact [1]. One famous example of bath engineering is the squeezed vacuum which leads to many novel effects and techniques in quantum optics and atomic spectroscopy. The reduction of quantum fluctuations below vacuum level by the squeezed vacuum yields many interesting phenomenons, for example, the suppression of dephasing rate in one direction and enhancment in the other for a two-level emitter [2, 3, 4, 7, 8, 9, 10, 11], the subnatural linewidth of resonance fluorescence [32, 29], and improvement of an atomic clock using squeezed vacuum [33]. The entanglement nature of the squeezed vacuum also leads to interesting results like pairwise excitation of atomic states [34, 35, 36]. In 1993, Ficek and Drummond studied the dynamical properties of a single three-level atom in the squeezed vacuum where they showed that a single three-level atom in the cascade configuration coupled to squeezed modes in a cavity can reach steady state with level population inversion relative to the ordinary laser spectroscopy [37, 38, 39]. In their model, they found a population inversion of about 78%.

In this dissertation, we consider multiple Ξ-type atoms coupled to a broadband squeezed vacuum in the quasi-1D waveguide where all resonant modes can be technically squeezed. We show that for a single atom, it can always reach a population inversion of almost 100% or any other ratio as long as the direction of its transition dipole moment is properly set. We also mathematically prove that this result can be generalized to arbitrary number of atoms coupled to each other through dipole-dipole interaction, which may be a scenario for studying two-photon laser or collective atomic effect.

2. SQUEEZED VACUUM RESERVOIR AND TRADITIONAL RESERVOIR THEORY

In this section, we will first introduce the basic properties of the squeezed vacuum and why it draws so much interests from researchers. Then we will discuss the traditional way to study the interaction between the atomic system and the squeezed vacuum reservoir. Finally, we will generalize the theory to multi-atom system where the dipole-dipole interaction is included.

2.1 Introduction to the squeezed vacuum

If two operators satisfy the commutation relation $[\hat{A}, \hat{B}] = i\hat{C}$, then according to the Heisenberg uncertainty relation, it follows that

$$\left\langle (\Delta\hat{A})^2 \right\rangle \left\langle (\Delta\hat{B})^2 \right\rangle \geq \frac{1}{4}|\langle\hat{C}\rangle|^2 \tag{2.1}$$

Thus, either $\left\langle (\Delta\hat{A})^2 \right\rangle \geq \frac{1}{2}|\langle\hat{C}\rangle|$ or $\left\langle (\Delta\hat{B})^2 \right\rangle \geq \frac{1}{2}|\langle\hat{C}\rangle|$ must be satisfied. A state is defined to be squeezed if one of the following is satisfied:

$$\left\langle (\Delta\hat{A})^2 \right\rangle < \frac{1}{2}|\langle\hat{C}\rangle| \quad or \quad \left\langle (\Delta\hat{B})^2 \right\rangle < \frac{1}{2}|\langle\hat{C}\rangle| \tag{2.2}$$

Consider the case for quadrature operator where

$$\begin{aligned} \hat{A} = \hat{X}_1 &= \frac{1}{2}\left(\hat{a} + \hat{a}^\dagger\right) \\ \hat{B} = \hat{X}_2 &= \frac{1}{2i}\left(\hat{a} - \hat{a}^\dagger\right) \end{aligned} \tag{2.3}$$

then we have

$$\left[\hat{X}_1, \hat{X}_2\right] = \frac{i}{2} \tag{2.4}$$

For a coherent state $|\alpha\rangle$, we have $\left\langle \left(\Delta\hat{X}_1\right)^2 \right\rangle = \left\langle \left(\Delta\hat{X}_2\right)^2 \right\rangle = 1/4$ which is the same as that in ordinary vacuum. Thus, quadrature squeezing, which satisfies one of the equations in Eq.(2.2), has even less noise than vacuum. One way to generate such a quadrature squeezing state is hitting

the squeeze operator

$$\hat{S}(\xi) = \exp\left[\frac{1}{2}\left(\xi^* a^2 - \xi a^{\dagger 2}\right)\right] \tag{2.5}$$

on vacuum state $|0\rangle$, which is called "the single mode squeezed vacuum". The fluctuation of the squeezed vacuum can be calculated as follows:

$$\begin{aligned}\left\langle\left(\Delta\hat{X}_1\right)^2\right\rangle &= \frac{1}{4}\left[\cosh^2 r + \sinh^2 r - 2\sinh r\cosh r\cos\theta\right] \\ \left\langle\left(\Delta\hat{X}_2\right)^2\right\rangle &= \frac{1}{4}\left[\cosh^2 r + \sinh^2 r + 2\sinh r\cosh r\cos\theta\right]\end{aligned} \tag{2.6}$$

To study the role of θ, we define the rotated quadrature operators $\hat{Y}_1$ and $\hat{Y}_2$ as follows:

$$\begin{pmatrix}\hat{Y}_1 \\ \hat{Y}_2\end{pmatrix} = \begin{pmatrix}\cos\theta/2 & \sin\theta/2 \\ -\sin\theta/2 & \cos\theta/2\end{pmatrix}\begin{pmatrix}\hat{X}_1 \\ \hat{X}_2\end{pmatrix} \tag{2.7}$$

Substituting Eq.(2.6) , we have

$$\begin{aligned}\left\langle\left(\Delta\hat{Y}_1\right)^2\right\rangle &= \frac{1}{4}e^{-2r} \\ \left\langle\left(\Delta\hat{Y}_2\right)^2\right\rangle &= \frac{1}{4}e^{2r}\end{aligned} \tag{2.8}$$

which can be represented in Fig. 2.1. Thus, for the squeezed vacuum, squeezing occurs along $\theta/2$ in the phase space.

The most famous approach to generate the above squeezed vacuum is based on degenerate parametric process through nonlinear optical crystal, which is shown in Fig. 2.2 . A degenerate parametric down-converter pumped by a field of frequency ω_P can split photons of that field into a pair of entangled "signal" photons with the same frequency $\omega_P/2$. This process is called degenerate parametric down-conversion with the Hamiltonian as below:

$$\hat{H} = \hbar\omega\hat{a}^\dagger\hat{a} + \hbar\omega_{\mathrm{P}}\hat{b}^\dagger\hat{b} + i\hbar\chi^{(2)}\left(\hat{a}^2\hat{b}^\dagger - \hat{a}^{\dagger 2}\hat{b}\right) \tag{2.9}$$

where b is the pump mode operator, a is the signal mode operator, and $\chi^{(2)}$ is the second-order

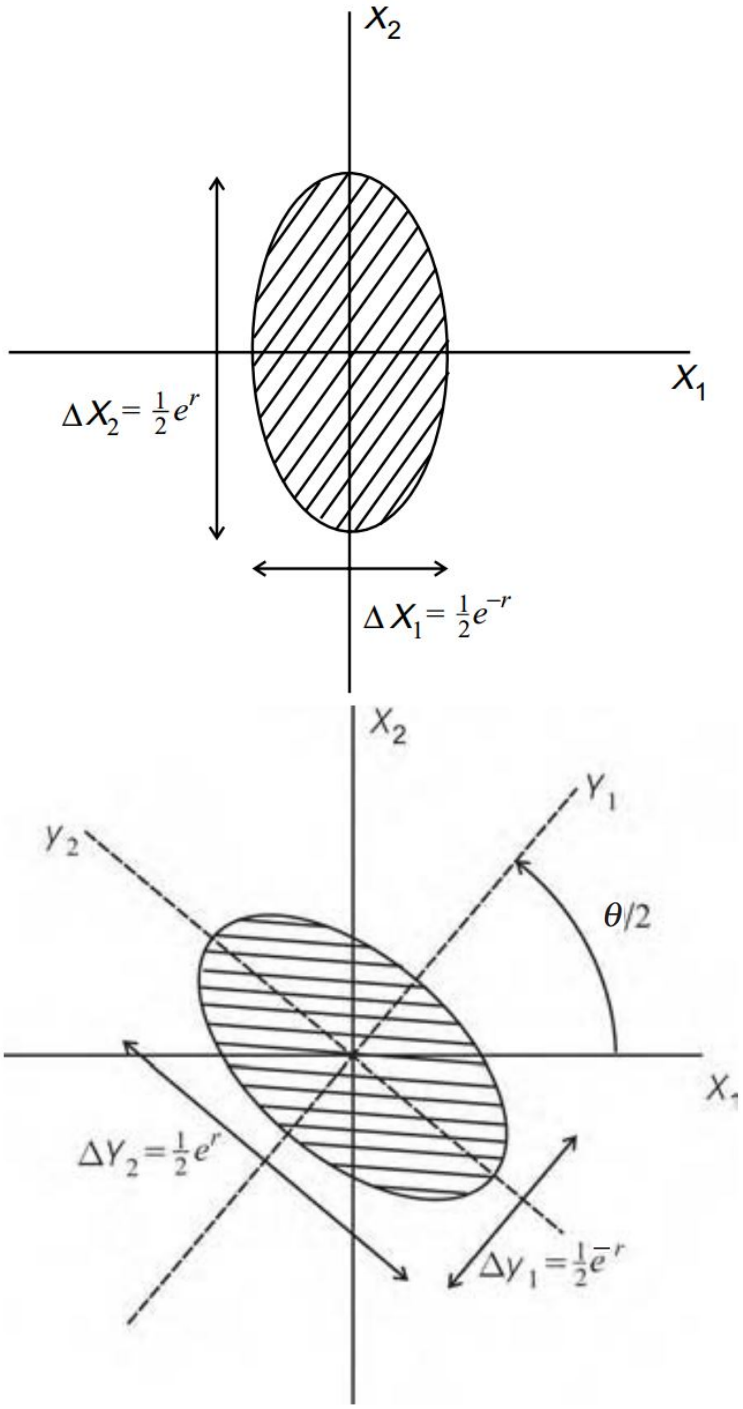

Figure 2.1: The error ellipse for the squeezed vacuum. (a) $\theta = 0$. (b) A general value of θ. Reproduced with permission of The Licensor through PLSclear. Original author: Christopher Gerry, Peter Knight, Introductory Quantum Optics. Copyright by Cambridge University Press.[40]

nonlinear susceptibility of the device. When the pump field is a strong classical field, we can make the "parametric approximation" whereby the operators $\hat{b}$ and $\hat{b}^\dagger$ can be replace by $\beta e^{-i\omega_{\rm P}t}$ and $\beta^* e^{i\omega_{\rm P}t}$, respectively. Thus, the Hamiltonian in Eq.(2.9) can be reduced to

$$\hat{H}^{(\rm PA)} = \hbar\omega\hat{a}^\dagger\hat{a} + i\hbar\left(\eta^*\hat{a}^2 e^{i\omega_{\rm P}t} - \eta\hat{a}^{\dagger 2}e^{-i\omega_{\rm P}t}\right) \tag{2.10}$$

with $\eta = \chi^{(2)}\beta$. This Hamiltonian can be simplified further in the interaction picture since energy is conserved $\omega_{\rm P} = 2\omega$:

$$\hat{H}_{\rm I} = i\hbar\left(\eta^*\hat{a}^2 - \eta\hat{a}^{\dagger 2}\right) \tag{2.11}$$

Thus, the associated evolution operator $\hat{U}_1(t) = \exp\left(-i\hat{H}_1 t/\hbar\right) = \exp\left(\eta^* t\hat{a}^2 - \eta t\hat{a}^{\dagger 2}\right)$ is exactly the squeezed operator in Eq.(2.5) with $\xi = 2\eta t$.

The degenerate four-wave mixing where two pump photons are converted into two signal photons of the same frequency can also be used to generate the squeezed vacuum, which relies on the third order nonlinear susceptibility of the device. The calculation is almost identical to the above process. The photon number statistics of the above squeezed vacuum is interesting. Hitting Eq. (2.5) on vacuum gives

$$|\xi\rangle = \frac{1}{\sqrt{\cosh r}}\sum_{m=0}^{\infty}(-1)^m\frac{\sqrt{(2m)!}}{2^m m!}e^{im\theta}(\tanh r)^m|2m\rangle \tag{2.12}$$

whose photon number probability vanishes for all odd photon numbers, as shown in Fig. 2.3.

Quantum damping is a very significant topic in quantum optics, which is caused by interacting with a system with a large number of degrees of freedom. Such a system is called reservoir. For example, Atomic decay and decoherence is caused by electromagnetic interaction between atomic dipole and radiative fields. Engineering the reservoir requires modifying the infinite number of modes in the reservoir. For vacuum, all the electromagnetic modes are in the ground state with zero photon. For black body radiation in a thermal equilibrium at temperature T, the photon number distribution in each mode can be described by the Bose-Einstein distribution[30]. For the single-mode squeezed vacuum, it is implausible to engineer a reservoir with all modes in the single-mode squeezed vacuum state because different modes requires different materials and pump fields of

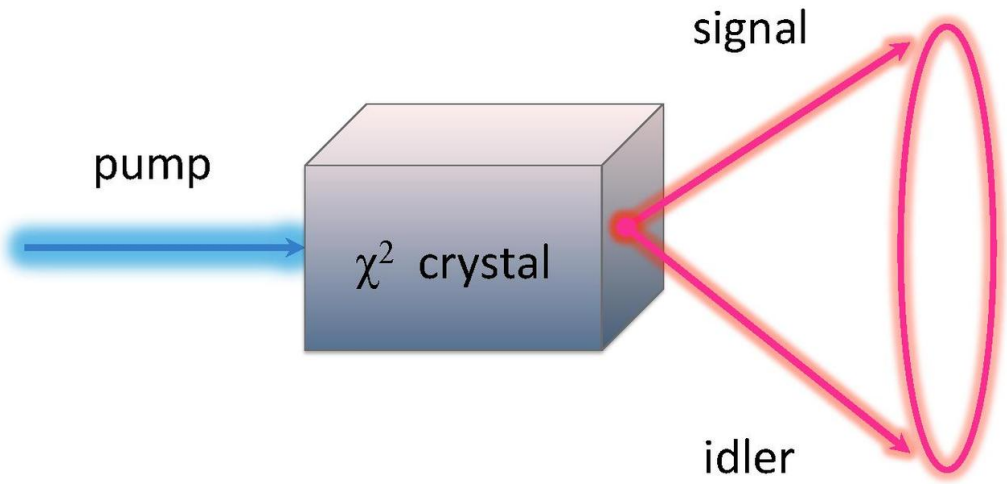

Figure 2.2: An SPDC scheme with the Type I output. This figure is licensed under the Creative Commons Attribution-Share Alike 3.0 Unported license: `https://en.wikipedia.org/wiki/File:Scheme_of_spontaneous_parametric_down-conversion.pdf`[41].

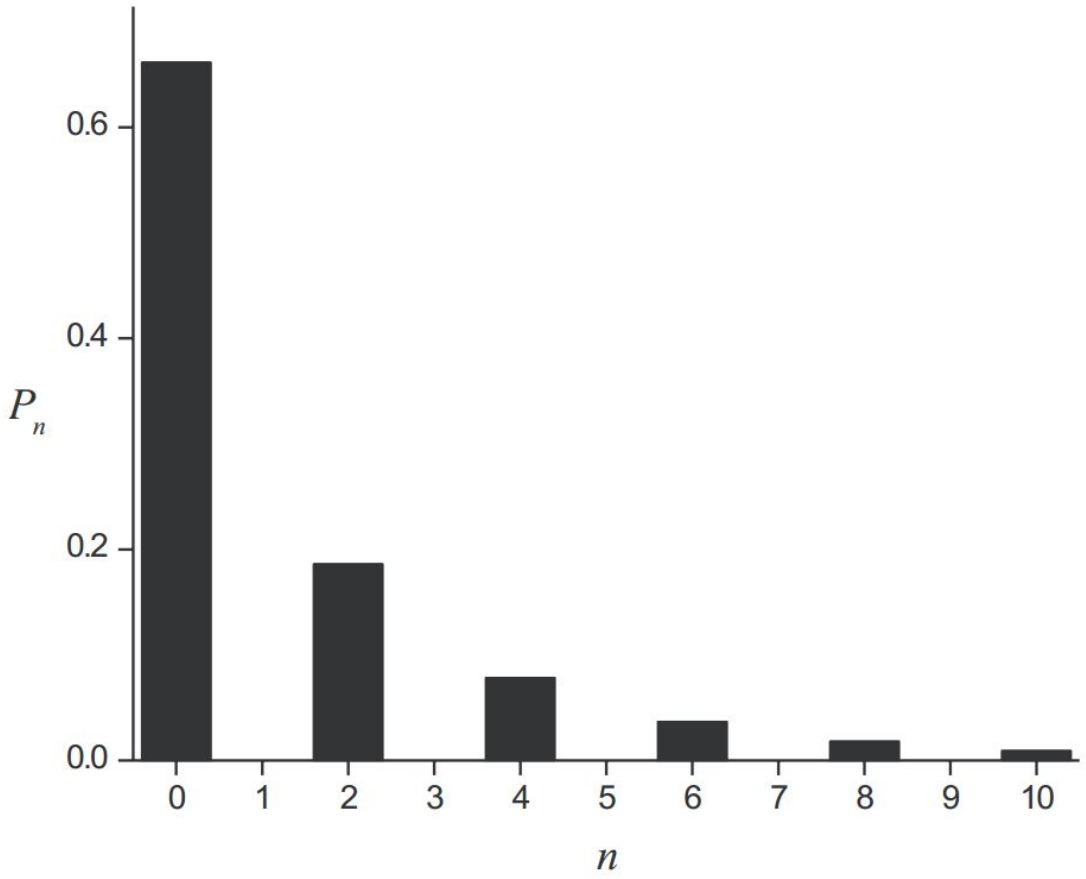

Figure 2.3: The photon number distribution for the single mode squeezed vacuum. Reproduced with permission of The Licensor through PLSclear. Original author: Christopher Gerry, Peter Knight, Introductory Quantum Optics. Copyright by Cambridge University Press.[40]

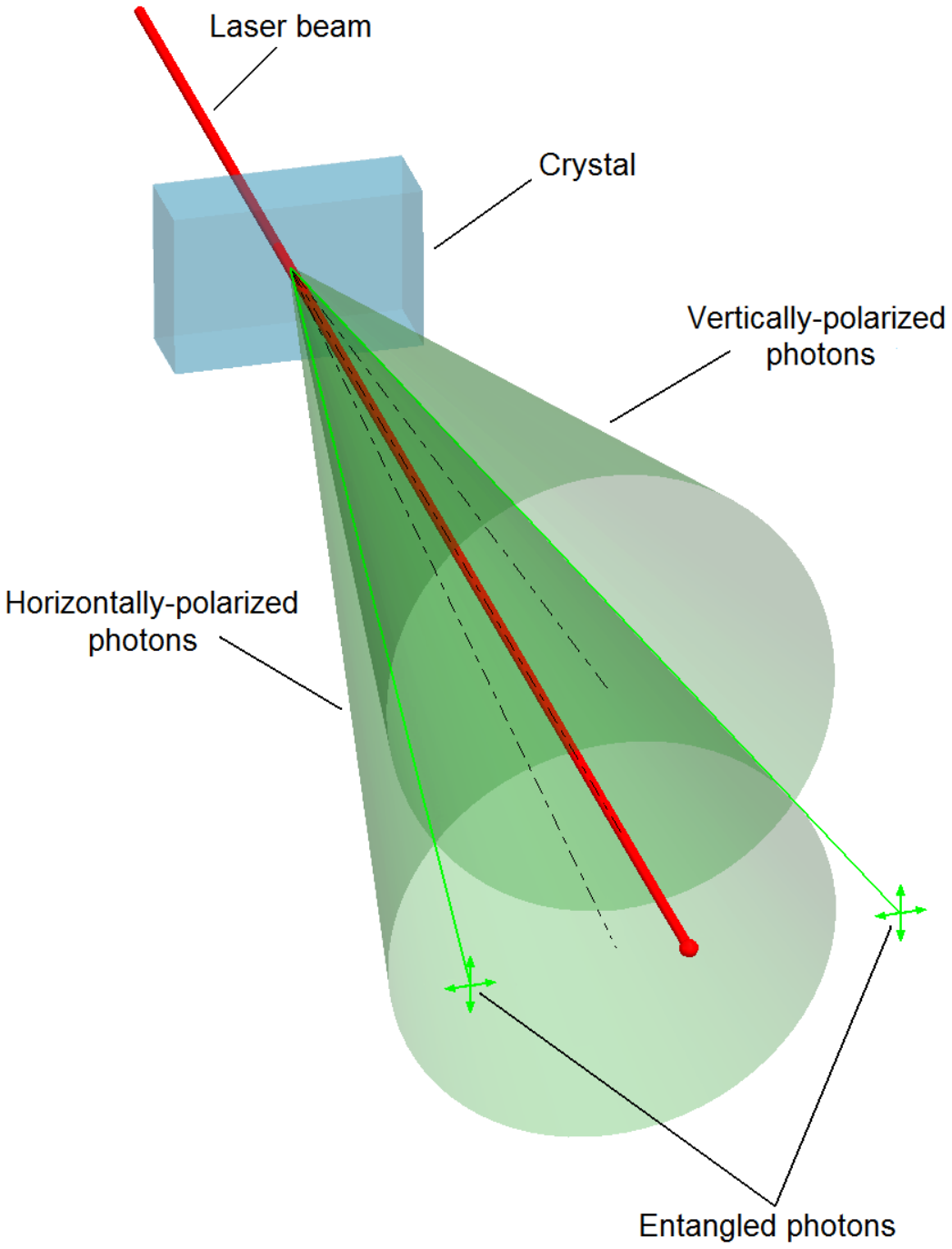

Figure 2.4: An SPDC scheme with the Type II output. This figure is licensed under the Creative Commons Attribution-Share Alike 3.0 Unported license: `https://en.wikipedia.org/wiki/File:Scheme_of_spontaneous_parametric_down-conversion.pdf`[41]

different frequency. To engineer such a squeezed vacuum reservoir, we need two-mode squeezed vacuum. The two-mode squeezed vacuum can be generated by the spontaneous parametric down-conversion process described by the following Hamiltonian:

$$\hat{H} = \hbar\omega_a \hat{a}^\dagger \hat{a} + \hbar\omega_b \hat{b}^\dagger \hat{b} + \hbar\omega_{\mathrm{P}} \hat{c}^\dagger \hat{c} + i\hbar\chi^{(2)} \left(\hat{a}\hat{b}\hat{c}^\dagger - \hat{a}^\dagger \hat{b}^\dagger \hat{c} \right) \tag{2.13}$$

which is the non-degenerate form of (2.10), with the process shown in Fig. 2.4. We can impose the same parametric approximation to replace c by $\gamma e^{-i\omega_P t}$ and define $\eta = \chi^{(2)}\gamma$. Then the Hamiltonian becomes

$$\hat{H}^{(\mathrm{PA})} = \hbar\omega_a \hat{a}^\dagger \hat{a} + \hbar\omega_b \hat{b}^\dagger \hat{b} + i\hbar \left(\eta^* e^{i\omega_{\mathrm{P}} t} \hat{a}\hat{b} - \eta e^{-i\omega_{\mathrm{P}} t} \hat{a}^\dagger \hat{b}^\dagger \right) \tag{2.14}$$

Considering the energy should be conserved for this three-wave mixing process, we have the following Hamiltonian in the interaction picture:

$$\hat{H}_{\mathrm{I}} = i\hbar \left(\eta^* \hat{a}\hat{b} - \eta \hat{a}^\dagger \hat{b}^\dagger \right) \tag{2.15}$$

Thus, the associated evolution operator is

$$\hat{U}_1(t,0) = \exp\left[-i\hat{H}_1 t/\hbar \right] \tag{2.16}$$

Defining $\xi = \eta t$, we have the two-mode squeezed vacuum

$$|\xi\rangle_2 = \hat{U}_1(t,0)|\xi\rangle_2 = \hat{S}_2(\xi)|0,0\rangle = \exp\left(\xi^* \hat{a}\hat{b} - \xi \hat{a}^\dagger \hat{b}^\dagger \right) |0,0\rangle \tag{2.17}$$

Expanding the exponential operator, we have

$$|\xi\rangle_2 = \frac{1}{\cosh r} \sum_{n=0}^{\infty} (-1)^n e^{in\theta} (\tanh r)^n |n,n\rangle \tag{2.18}$$

It is interesting that this two-mode squeezed vacuum state is a photon number entangled state with photons in the correlated modes always generated by pair, as shown in Fig. 2.5

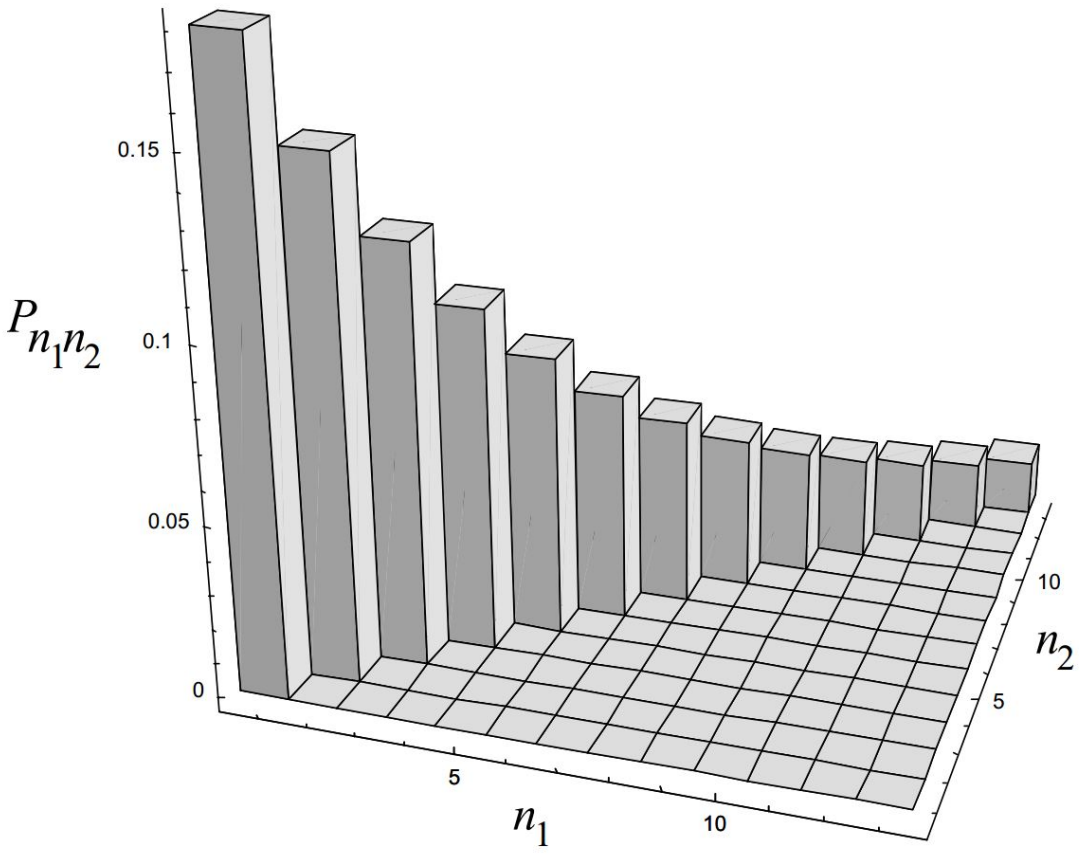

Figure 2.5: The photon number distribution for the two-mode squeezed vacuum. Reproduced with permission of The Licensor through PLSclear. Original author: Christopher Gerry, Peter Knight, Introductory Quantum Optics. Copyright by Cambridge University Press.[40]

However, when we only focus on one mode by taking the partial trace of the other mode, we can find that each mode seems to be in the thermal state:

$$\begin{aligned}\hat{\rho}_a &= \sum_{n_b=0}^{\infty} \langle n_b|\xi\rangle_2 \langle \xi|_2 |n_b\rangle \\ &= \frac{1}{\cosh r} \sum_{n_a=0}^{\infty} (-1)^{n_a} e^{i n_a \theta} (\tanh r)^{n_a} |n_a\rangle\langle n_a|\end{aligned} \tag{2.19}$$

whose photon number distribution is

$$P_n = \langle n\,|\hat{\rho}|\,n\rangle = \frac{(\tanh r)^{2n}}{(\cosh r)^2} \tag{2.20}$$

which is exactly the Boltzmann distribution with the average photon number $\langle n\rangle = \sinh^2 r$. The two-mode squeezed vacuum is also a squeezed state. Considering the following quadrature operators:

$$\begin{aligned}\hat{X}_1 &= \frac{1}{2^{3/2}} \left(\hat{a} + \hat{a}^\dagger + \hat{b} + \hat{b}^\dagger\right) \\ \hat{X}_2 &= \frac{1}{2^{3/2}\hat{i}} \left(\hat{a} - \hat{a}^\dagger + \hat{b} - \hat{b}^\dagger\right)\end{aligned} \tag{2.21}$$

which satisfies the commutation relation $\left[\hat{X}_1, \hat{X}_2\right] = i/2$, we have the fluctuations as follows:

$$\begin{aligned}\left\langle \left(\hat{X}_1\right)^2 \right\rangle &= \frac{1}{4}\left[\cosh^2 r + \sinh^2 r - 2\sin r \cosh r \cos\theta\right] \\ \left\langle \left(\hat{X}_2\right)^2 \right\rangle &= \frac{1}{4}\left[\cosh^2 r + \sinh^2 r + 2\sin r \cosh r \cos\theta\right]\end{aligned} \tag{2.22}$$

This is identical to Eq. (2.6). Thus, the two-mode squeezed vacuum is also a squeezed state. If all modes are squeezed in the above way, the reservoir is called the squeezed vacuum reservoir.

However, it is worth nothing that generating the two-mode squeezed vacuum in all modes with the same mid frequency ω_0 and the same squeezing parameter r is still experimentally impossible due to many reasons. The most significant reason is that, both the three-wave mixing and four-wave mixing must satisfy the phase-matching condition so that both energy and momentum must be conserved, as depicted in Fig. 2.6. Thus, it is theoretically impossible to squeeze all modes in all directions in the 3D space with one pump field. Furthermore, even those squeezed modes

do not have a uniform squeezing parameter r, since the second-order nonlinear susceptibility $\chi^{(2)}$ depends on the frequency of the output field. Hence in experiments, the concept of "broadband squeezed light" is used. Instead of the single-mode quadrature operators in Eq. (2.3) or two-mode quadrature operators in Eq. (2.21), collective quadrature operators are considered:

$$\begin{aligned}\hat{X}_1^{(\mathrm{c})}(t) &= \frac{1}{2}\left[\hat{E}^{(+)}(t) + \hat{E}^{(-)}(t)\right] \\ \hat{X}_2^{(\mathrm{c})}(t) &= \frac{1}{2i}\left[\hat{E}^{(+)}(t) - \hat{E}^{(-)}(t)\right]\end{aligned} \tag{2.23}$$

where the annihilation part is $\hat{E}^{(+)}(\mathbf{r},t) = i\sum_{\mathbf{k},s}\sqrt{\frac{\hbar\omega}{2V\epsilon_0}}\mathbf{e}^{(s)}\hat{a}^{(s)}(\mathbf{k})e^{i\mathbf{k}\cdot\mathbf{r}-i\omega_k t}$ and the creation part is $\hat{E}^{(-)}(\mathbf{r},t) = -i\sum_{\mathbf{k},s}\sqrt{\frac{\hbar\omega}{2V\epsilon_0}}\overline{\mathbf{e}}^{(s)}\hat{a}^{\dagger(s)}(\mathbf{k})e^{-i\mathbf{k}\cdot\mathbf{r}+i\omega_k t}$. If we have the following commutation relation measured from experiments

$$\left[\hat{E}^{(+)}(t), \hat{E}^{(-)}(t)\right] = C \tag{2.24}$$

then we have

$$\left[\hat{X}_1^{(\mathrm{c})}, \hat{X}_2^{(\mathrm{c})}\right] = \frac{i}{2}C \tag{2.25}$$

Thus, the broadband squeezing is defined if

$$\left\langle \left(\Delta\hat{X}_i^{(\mathrm{c})}\right)^2 \right\rangle < \frac{1}{4}|C|$$

is satisfied for $i = 1$ or $i = 2$.

2.2 Traditional reservoir theory

Considering the fact that a reservoir is a system with a large number of degrees of freedom, the reservoir can be interpreted as an open system. Thus, if an atom in the excited state interacts with the reservoir, the atom will decay to the ground state with photon emitted to the reservoir and never re-absorbed by the atom, which is called quantum damping. Since the reservoir requires so many degrees of freedom to be fully described, we can apply Markovian assumption on this process that

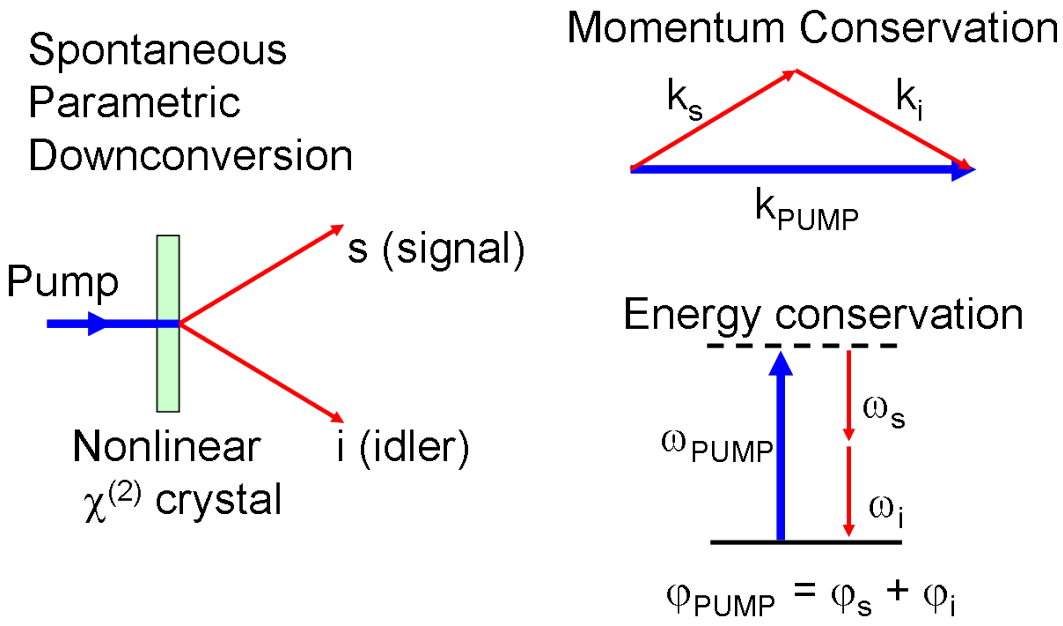

Figure 2.6: The phase matching condition in SPDC process. This figure is licensed under the Creative Commons Attribution-Share Alike 3.0 Unported license: `https://upload.wikimedia.org/wikipedia/commons/7/74/Spontaneous_Parametric_Downconversion.png`[41].

the damping destroys memory of the past. Thus, for a system represented as ρ^S interacting with a reservoir represented as ρ^F, its evolution can be described by the following equation[30]:

$$\begin{aligned}\dot{\rho^S} = &-\frac{i}{\hbar}Tr_R[V(t), \rho^S(0)\otimes\rho^F(0)] \\ &-\frac{1}{\hbar^2}Tr_R\int_0^t [V(t),[V(t-\tau),\rho^S(t-\tau)\otimes\rho^F(0)]]d\tau\end{aligned} \tag{2.26}$$

where $V(t)$ is the interaction Hamiltonian in the interaction picture. For a two-level system (qubit) in free space, the interaction Hamiltonian is

$$V(t) = \boldsymbol{d}\cdot\boldsymbol{E} = \hbar[\boldsymbol{\mu}S^\dagger(t) + \boldsymbol{\mu}^* S^-(t)]\cdot[\boldsymbol{u}_{\boldsymbol{ks}}(\boldsymbol{r}_i)\hat{a}_{\boldsymbol{ks}}(t) + \boldsymbol{u}^*_{\boldsymbol{ks}}(\boldsymbol{r}_i)\hat{a}^\dagger_{\boldsymbol{ks}}(t)] \tag{2.27}$$

where $S^- = |b\rangle\langle a|$ is the lowering operator and $S^+ = |a\rangle\langle b|$ is the raising operator of the qubit. In the interaction picture, we have $S_i^{\pm}(t) = S_i^{\pm} e^{\pm i\omega_0 t}$, $\hat{a}_{\boldsymbol{k}s}(t) = \hat{a}_{\boldsymbol{k}s} e^{-i\omega_{\boldsymbol{k}s} t}$, and $\hat{a}^\dagger_{\boldsymbol{k}s}(t) = \hat{a}^\dagger_{\boldsymbol{k}s} e^{i\omega_{\boldsymbol{k}s} t}$. $\boldsymbol{u}_{\boldsymbol{k}s}(\boldsymbol{r}_i)$ is the mode function which is typically given by

$$\boldsymbol{u}_{\boldsymbol{k},s}(\boldsymbol{r}_i) = \sqrt{\frac{\omega_{\boldsymbol{k},s}}{2\epsilon_0 \hbar V}} \boldsymbol{e}_{\boldsymbol{k},s} e^{i\boldsymbol{k}\cdot\boldsymbol{r}_i} \tag{2.28}$$

where s indicates the polarization. For a thermal reservoir which is described by the density operator

$$\rho_R = \prod_{\mathbf{k},\mathbf{s}} \left[1 - \exp\left(-\frac{\hbar v_k}{k_{\mathrm{B}} T}\right)\right] \exp\left(-\frac{\hbar v_k b^\dagger_{\mathbf{k}} b_{\mathbf{k}}}{k_{\mathrm{B}} T}\right) \tag{2.29}$$

where k_B is the Boltzmann constant and T is the thermal equilibrium temperature, we have

$$\begin{aligned}
\langle a_{\boldsymbol{k},s} \rangle = \left\langle a^\dagger_{\boldsymbol{k},s} \right\rangle &= 0 \\
\left\langle a^\dagger_{\boldsymbol{k},s} a_{\boldsymbol{k}',s'} \right\rangle &= \bar{n}_{k,s} \delta_{\boldsymbol{k}'\boldsymbol{k}} \delta_{ss'} \\
\left\langle a_{\boldsymbol{k},s} a^\dagger_{\boldsymbol{k}',s'} \right\rangle &= (\bar{n}_{k,s} + 1) \delta_{\boldsymbol{k}'\boldsymbol{k}} \delta_{ss'} \\
\left\langle a^\dagger_{\boldsymbol{k},s} a^\dagger_{\boldsymbol{k}',s'} \right\rangle &= \langle a_{\boldsymbol{k},s} a_{\boldsymbol{k}',s'} \rangle = 0
\end{aligned} \tag{2.30}$$

where $\bar{n}_{\boldsymbol{k},s}$ is the average photon number with $\bar{n}_{\boldsymbol{k},s} = \frac{1}{\exp\left(\frac{\hbar v_k}{k_{\mathrm{B}} T}\right) - 1}$. Substituting them into Eq.(2.26) and applying Wigner-Weisskopf approximation, we have

$$\begin{aligned}
\frac{d\rho^S}{dt} = &-\frac{1}{2}\gamma(N+1)\left(\rho^S S^+ S^- + S^+ S^- \rho^S - 2S^- \rho^S S^+\right) \\
&-\frac{1}{2}\gamma N \left(\rho^S S^- S^+ + S^- S^+ \rho^S - 2S^+ \rho^S S^-\right)
\end{aligned} \tag{2.31}$$

where $\gamma = \frac{1}{4\pi\epsilon_0}\frac{4\omega^3\mu^2}{3\hbar c^3}$ is the spontaneous decay rate and N is the average photon number in the resonant frequency mode. Analyzing each element in Eq.(2.31), we have

$$\begin{aligned}
\dot{\rho}_{aa} &= -\left(N+1\right)\gamma\rho_{aa} + N\gamma\rho_{bb} \\
\dot{\rho}_{ab} &= \dot{\rho}^*_{ba} = -\left(N+\frac{1}{2}\right)\gamma\rho_{ab} \\
\dot{\rho}_{bb} &= -N\gamma\rho_{bb} + \left(N+1\right)\gamma\rho_{aa}
\end{aligned} \tag{2.32}$$

At $T = 0$, this reduces to

$$\begin{aligned}
\dot{\rho}_{aa} &= -\gamma\rho_{aa} \\
\dot{\rho}_{ab} &= -\tfrac{\gamma}{2}\rho_{ab} \\
\dot{\rho}_{bb} &= \gamma\rho_{aa}
\end{aligned} \tag{2.33}$$

In general, for N_a multi-level atoms interacting with the electromagnetic field, the total Hamiltonian can be written as

$$H = H_A + H_F + H_{AF} \tag{2.34}$$

where the atomic free Hamiltonian is

$$H_A = \sum_{l=1}^{N_a}\sum_{e=a,b,c}\hbar\omega_{e,l}\left|e_l\right\rangle\left\langle e_l\right| \tag{2.35}$$

with $|e_l\rangle$ representing the energy state of the lth atom with energy $\hbar\omega_{e,l}$. The Hamiltonian of the EM field is

$$H_F = \sum_{\boldsymbol{k}s}\hbar\omega_{\boldsymbol{k}s}(\hat{a}^\dagger_{\boldsymbol{k}s}\hat{a}_{\boldsymbol{k}s} + \frac{1}{2}) \tag{2.36}$$

where $\hat{a}_{\boldsymbol{k}s}$ and $\hat{a}^\dagger_{\boldsymbol{k}s}$ are the annihilation and creation operators of the filed mode with wavevector $\boldsymbol{k}$ and polarization s. The interaction Hamiltonian in the electric-dipole approximation is

$$H_{AF} = -i\hbar\sum_{\boldsymbol{k}s}\sum_{i}\sum_{l=1}^{N_a}[\boldsymbol{\mu}_{l,i}\cdot\boldsymbol{u}_{\boldsymbol{k}s}(\boldsymbol{r}_{l,i})S^+_{l,i}\hat{a}_{\boldsymbol{k}s} + \boldsymbol{\mu}^*_{l,i}\cdot\boldsymbol{u}_{\boldsymbol{k}s}(\boldsymbol{r}_{l,i})S^-_{l,i}\hat{a}_{\boldsymbol{k}s} - H.c.] \tag{2.37}$$

where i denotes the ith atomic transition. Transforming the total Hamiltonian H into the interac-

tion picture, and substituting them into Eq.(2.26), considering the thermal reservoir described in Eq.(2.30), we have the following equation[42]: (The calculation will be derived in a very detailed manner in section 2, here we just jump to the conclusion)

$$\begin{aligned}\frac{d\rho^S}{dt} =& -i\sum_{ijkl}\Lambda_{ijkl}[S^+_{i,j}S^-_{k.l},\rho^S]e^{i(\omega_j-\omega_l)t} \\ &-\frac{1}{2}\sum_{ijkl}\gamma_{ijkl}(1+N)(\rho^S S^+_{i,j}S^-_{k.l}+S^+_{i,j}S^-_{k.l}\rho^S-2S^-_{k.l}\rho^S S^+_{i,j})e^{i(\omega_j-\omega_l)t} \\ &-\frac{1}{2}\sum_{ijkl}\gamma_{ijkl}N(\rho^S S^-_{i,j}S^+_{k.l}+S^-_{i,j}S^+_{k,l}\rho^S-2S^+_{k,l}\rho^S S^-_{i,j})e^{-i(\omega_j-\omega_l)t}\end{aligned} \tag{2.38}$$

The collective energy shifts Λ_{ijkl} and decay rates γ_{ijkl} due to the ordinary vacuum are given by [43, 42]

$$\begin{aligned}\Lambda_{ijkl} =& \frac{3}{4}\sqrt{\gamma_{ij}\gamma_{kl}}\{-(1-\cos^2\alpha)\frac{\cos(k_0r_{ik})}{k_0r_{ik}} \\ &+(1-3\cos^2\alpha)[\frac{\sin(k_0r_{ik})}{(k_0r_{ik})^2}+\frac{\cos(k_0r_{ik})}{(k_0r_{ik})^3}]\} \\ \gamma_{ijkl} =& \sqrt{\gamma_{ij}\gamma_{kl}}F(k_0r_{ik})\end{aligned} \tag{2.39}$$

where subscripts i,k label the atom index, $j(l)$ labels the transitions of the $ith(kth)$ atom, $\gamma = \frac{\omega_0^3\mu^2}{3\pi\epsilon_0\hbar c^3}$ is the spontaneous decay rate of the atom in ordinary vacuum and $F(x) = \frac{3}{2}\{(1-\cos^2\alpha)\frac{\sin x}{x}+(1-3\cos^2\alpha)[\frac{\cos x}{x^2}-\frac{\sin x}{x^3}]\}$.

However, if we apply the above calculations to a single atom interacting with the squeezed vacuum, we will have some weird result. Since we have

$$\begin{aligned}\langle a_{\boldsymbol{k},s}\rangle = \left\langle a^\dagger_{\boldsymbol{k},s}\right\rangle &= 0 \\ \left\langle a^\dagger_{\boldsymbol{k},s}a_{\boldsymbol{k}',s'}\right\rangle &= \sinh^2 r\delta_{\boldsymbol{k}'\boldsymbol{k}}\delta_{ss'} \\ \left\langle a_{\boldsymbol{k},s}a^\dagger_{\boldsymbol{k}',s'}\right\rangle &= \cosh^2 r\delta_{\boldsymbol{k}'\boldsymbol{k}}\delta_{ss'} \\ \left\langle a^\dagger_{\boldsymbol{k},s}a^\dagger_{\boldsymbol{k}',s'}\right\rangle &= -e^{-i\theta}\cosh(r)\sinh(r)\delta_{\boldsymbol{k}',2\boldsymbol{k}_0-\boldsymbol{k}}\delta_{ss'} \\ \langle a_{\boldsymbol{k},s}a_{\boldsymbol{k}',s'}\rangle &= -e^{i\theta}\cosh(r)\sinh(r)\delta_{\boldsymbol{k}',2\boldsymbol{k}_0-\boldsymbol{k}}\delta_{ss'}\end{aligned} \tag{2.40}$$

Substituting them into Eq.(2.26), we have

$$\begin{aligned}\frac{d\rho^S}{dt} &= \sinh(r)\cosh(r)\gamma'(S^+\rho^S S^+ + H.c.) \\ &- \frac{1}{2}\gamma\cosh^2(r)(\rho^S S^+S^- + S^+S^-\rho^S - 2S^-\rho^S S^+) \\ &- \frac{1}{2}\gamma\sinh^2(r)(\rho^S S^-S^+ + S^-S^+\rho^S - 2S^+\rho^S S^-)\end{aligned} \tag{2.41}$$

with $\gamma'_{ij} = \gamma F(2k_0 r))$. However, although the position of atom is well-defined, its coordinate is ill-defined since there is no requirement on the origin of the coordinate system. This value varies from 0 to γ by the value of r, which is not physical. For example, if we choose $r = 0$, then $\gamma'_{ij} = \gamma$ which is the perfect squeezing; if r is the zero point of $F(2k_0 r)$, Eq.(2.41) reduces to the thermal reservoir as Eq.(2.31). As we mentioned before, the choice of r completely depends on the coordinate system, which can be built arbitrarily. Thus, the above theory cannot be applied on the squeezed vacuum, and putting forward a modified theory is the main goal of this dissertation.

3. A MODIFIED RESERVOIR THEORY IN THE SQUEEZED VACUUM[1]

In the last section, we discussed about the limitation of the traditional reservoir theory when it is applied on the squeezed vacuum. In this section, we will bring forward a modified theory. We will show that this theory works properly with the squeezed vacuum, and remains consistent with the traditional theory in the thermal reservoir case. We will discuss the new behaviors of the system based on our new theory.

3.1 A new master equation from a modified mode function

First of all, we need to analyze the origin of the unphysical quantity γ' in Eq.(2.41), and here we start from the most typical single-qubit case with transition frequency ω. The interaction Hamiltonian is

$$V(t) = -i\hbar \sum_{\boldsymbol{ks}} [\boldsymbol{\mu} \cdot \boldsymbol{u}_{\boldsymbol{ks}}(\boldsymbol{r}) S^+(t) \hat{a}_{\boldsymbol{ks}}(t) + \boldsymbol{\mu}^* \cdot \boldsymbol{u}_{\boldsymbol{ks}}(\boldsymbol{r}) S^-(t) \hat{a}_{\boldsymbol{ks}}(t) - H.c.] \tag{3.1}$$

with the mode function

$$\boldsymbol{u}_{\boldsymbol{ks}}(\boldsymbol{r}) = \sqrt{\frac{\omega_{\boldsymbol{ks}}}{2\epsilon_0 \hbar V}} \boldsymbol{e}_{ks} e^{i\boldsymbol{k}\cdot\boldsymbol{r}} \tag{3.2}$$

Considering that $\langle a_{\boldsymbol{k},s} \rangle = \left\langle a^\dagger_{\boldsymbol{k},s} \right\rangle = 0$ for both thermal reservoir and the squeezed vacuum reservoir, we can drop the first term in Eq. (2.26), so we have the master equation

$$\begin{aligned} \frac{d\rho^S}{dt} =& -\frac{1}{\hbar^2} \int_0^t d\tau Tr_F \{[V(t), [V(t-\tau), \rho^S(t-\tau)\rho^F\} \\ =& -\frac{1}{\hbar^2} \int_0^t d\tau Tr_F \{V(t)V(t-\tau)\rho^S(t-\tau)\rho^F + \rho^S(t-\tau)\rho^F V(t-\tau)V(t) \\ & - V(t)\rho^S(t-\tau)\rho^F V(t-\tau) - V(t-\tau)\rho^S(t-\tau)\rho^F V(t)\}. \end{aligned} \tag{3.3}$$

[1]Part of this section is reprinted with permission from: "Waveguide QED in the Squeezed Vacuum" by Jieyu You et al, 2018. Physical Review A, 97, 023810, Copyright 2018 by the American Physical Society and "Steady-state population inversion of multiple Ks-type atoms by the squeezed vacuum in a waveguide" by Jieyu You, Zeyang Liao, and M. Suhail Zubairy, 2019. Physical Review A, 100, 013843, Copyright 2019 by the American Physical Society.

which is of the second order in the interaction Hamiltonian $V(t)$ and mode function $\boldsymbol{u_{ks}}(\boldsymbol{r}_i)$. To make the derivation simple in form, we define

$$D(t) = [\boldsymbol{\mu} \cdot \boldsymbol{u}_{\boldsymbol{k},s}(r) S^{\dagger}(t) + \boldsymbol{\mu}^* \cdot \boldsymbol{u}_{\boldsymbol{k},s}(r) S^{-}(t)] \tag{3.4}$$

so the interaction Hamiltonian Eq.(3.1) becomes

$$V(t) = -i\hbar \sum_{\boldsymbol{ks}} [D(t) a_{\boldsymbol{ks}}(t) - D^{+}(t) a^{\dagger}_{\boldsymbol{ks}}(t)] \tag{3.5}$$

Here we just show the way to deal with the first term in Eq.(3.3), the remaining terms can be calculated in the same way. For the first term, we have

$$\begin{aligned}
&-\frac{1}{\hbar^2}\int_0^t d\tau Tr_F\{V(t)V(t-\tau)\rho^S(t-\tau)\rho^F\} \\
&= \int_0^t d\tau \sum_{\boldsymbol{ks},\boldsymbol{k's'}} \{D(t)D(t-\tau)Tr_F[\rho^F a_{ks}(t) a_{k's'}(t-\tau)] - D(t)D^{+}(t-\tau)Tr_F[\rho^F a_{ks}(t) a^{\dagger}_{k's'}(t-\tau)] \\
&\quad - D^{+}(t)D(t-\tau)Tr_F[\rho^F a^{\dagger}_{ks}(t) a_{k's'}(t-\tau)] + D^{+}(t)D^{+}(t-\tau)Tr_F[\rho^F a^{\dagger}_{ks}(t) a^{\dagger}_{k's'}(t-\tau)]\}\rho^S(t-\tau)\}.
\end{aligned} \tag{3.6}$$

Using the correlation functions Eq.(2.40), we have the following result under the rotating wave approximation (RWA):

$$
\begin{aligned}
&-\frac{1}{\hbar^2}\int_0^t d\tau Tr_F\{V(t)V(t-\tau)\rho^S(t-\tau)\rho^F\} \\
=&\sum_{\boldsymbol{k}s,\boldsymbol{k}'s'}\int_0^t d\tau\{\boldsymbol{\mu}\cdot\boldsymbol{u}_{\boldsymbol{k}s}(r)S^+e^{i\omega t}\boldsymbol{\mu}\cdot\boldsymbol{u}_{\boldsymbol{k}'s'}(r)S^+e^{i\omega(t-\tau)}e^{-i(\omega_{\boldsymbol{k}s}+\omega_{\boldsymbol{k}'s'})t+i\omega_{\boldsymbol{k}'s'}\tau} \\
&\times[-\sinh(r)\cosh(r)\delta_{\boldsymbol{k}',2\boldsymbol{k}_0-\boldsymbol{k}}\delta_{ss'}] \\
&-\boldsymbol{\mu}\cdot\boldsymbol{u}_{\boldsymbol{k}s}(r)S^+e^{i\omega t}\boldsymbol{\mu}^*\cdot\boldsymbol{u}^*_{\boldsymbol{k}'s'}(r)S^-e^{-i\omega(t-\tau)}e^{-i\omega_{\boldsymbol{k}'s'}\tau}\cosh^2 r\delta_{\boldsymbol{k}\boldsymbol{k}'}\delta_{ss'} \\
&-\boldsymbol{\mu}^*\cdot\boldsymbol{u}_{\boldsymbol{k}s}(r)S^-e^{-i\omega t}\boldsymbol{\mu}\cdot\boldsymbol{u}^*_{\boldsymbol{k}'s'}(r)S^+e^{i\omega(t-\tau)}e^{-i\omega_{\boldsymbol{k}'s'}\tau}\cosh^2 r\delta_{\boldsymbol{k}\boldsymbol{k}'}\delta_{ss'} \\
&-\boldsymbol{\mu}^*\cdot\boldsymbol{u}^*_{\boldsymbol{k}s}(r)S^-e^{-i\omega t}\boldsymbol{\mu}\cdot\boldsymbol{u}_{\boldsymbol{k}'s'}(r)S^+e^{i\omega(t-\tau)}e^{i\omega_{\boldsymbol{k}'s'}\tau}\sinh^2 r\delta_{\boldsymbol{k}\boldsymbol{k}'}\delta_{ss'} \\
&-\boldsymbol{\mu}\cdot\boldsymbol{u}^*_{\boldsymbol{k}s}(r)S^+e^{i\omega t}\boldsymbol{\mu}^*\cdot\boldsymbol{u}_{\boldsymbol{k}'s'}(r)S^-e^{-i\omega(t-\tau)}e^{i\omega_{\boldsymbol{k}'s'}\tau}\sinh^2 r\delta_{\boldsymbol{k}\boldsymbol{k}'}\delta_{ss'} \\
&+\boldsymbol{\mu}^*\cdot\boldsymbol{u}^*_{\boldsymbol{k}s}(r)S^-e^{-i\omega t}\boldsymbol{\mu}^*\cdot\boldsymbol{u}^*_{\boldsymbol{k}'s'}(r)S^-e^{-i\omega(t-\tau)}e^{i(\omega_{\boldsymbol{k}s}+\omega_{\boldsymbol{k}'s'})t-i\omega_{\boldsymbol{k}'s'}\tau} \\
&\times[-\sinh(r)\cosh(r)\delta_{\boldsymbol{k}',2\boldsymbol{k}_0-\boldsymbol{k}}\delta_{ss'}]\}\rho^S(t-\tau)
\end{aligned}
\tag{3.7}
$$

For the second to the fifth terms, $\boldsymbol{u}_{\boldsymbol{k}s}(r)\boldsymbol{u}^*_{\boldsymbol{k}'s'}(r)$'s positional dependence is canceled. However, the first depends on $e^{i\boldsymbol{k}\cdot\boldsymbol{r}}$ and the sixth term depends on $e^{i\boldsymbol{k}\cdot\boldsymbol{r}}$. This is not an issue for the thermal reservoir since $\langle a_{\boldsymbol{k},s}a_{\boldsymbol{k}',s'}\rangle=\langle a^\dagger_{\boldsymbol{k},s}a^\dagger_{\boldsymbol{k}',s'}\rangle=0$ so these two terms vanish. For the squeezed vacuum, these terms are positional dependent. What's more, since there is no constraint on the choice of coordinate system, r can be arbitrary which yields the arbitrary value of the first and sixth terms in the above equation. This unphysical behavior originates from the definition of the mode function in Eq.(3.2). However, this formula is so famous that it appears in almost every textbook on quantum mechanics and quantum mechanics, so challenging it should be very cautious. We noticed that the usage of Eq. (3.2) is always related to the quantization of radiation field with the running wave boundary condition, for example in Quantum Optics by M.O. Scully and M.S. Zubairy[30]. However, if the standing wave boundary condition is applied, $e^{i\boldsymbol{k}\cdot\boldsymbol{r}}$ should be replace by $\cos(\boldsymbol{k}\cdot\boldsymbol{r})$ or $\sin(\boldsymbol{k}\cdot\boldsymbol{r})$. Thus, equation (3.2) can only be used when the space translational symmetry is satisfied. In the thermal reservoir, the space translational symmetry is satisfied. However, this is not the case

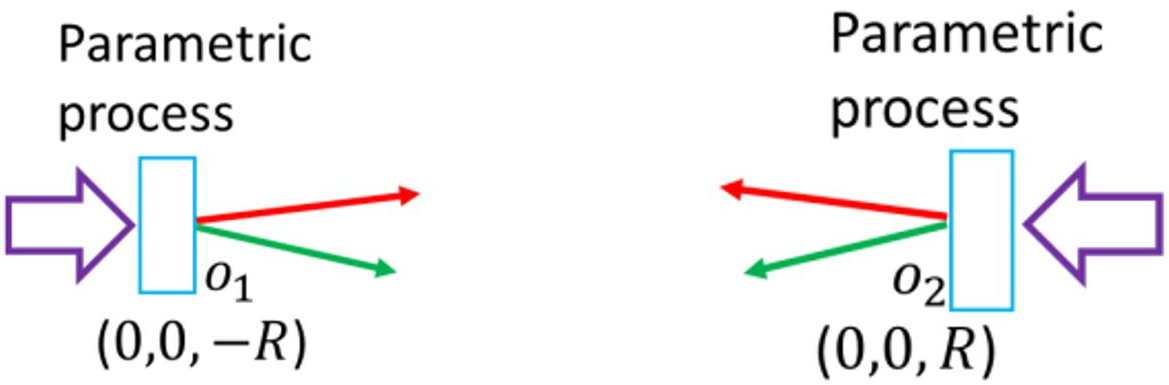

Figure 3.1: Demonstration for squeezing all modes in a single direction. The Electromagnetic wave propagates in two opposite directions, so two pumps are needed to squeeze all modes.

for the squeezed vacuum reservoir. Considering the squeezed vacuum reservoir in one dimensional case, two pump beams interacting with the nonlinear crystal from opposite directions are needed to form a broad-band squeezed vacuum, which is shown in Fig. 3.1. Due to the existence of the nonlinear crystal and the pump field, the space translational symmetry is broken. Thus, we cannot use Eq. (3.2) as the mode function. Here we propose a new mode function which incorporate both the existence of the squeezing source and the nature of running wave of the squeezed vacuum:

$$\boldsymbol{u}_{\boldsymbol{k},s}(\boldsymbol{r}_i) = \sqrt{\frac{\omega_{\boldsymbol{k},s}}{2\epsilon_0\hbar V}}\boldsymbol{e}_{ks}e^{i\boldsymbol{k}\cdot(\boldsymbol{r}_i-\boldsymbol{o}_{\boldsymbol{k},s})} \tag{3.8}$$

where $\boldsymbol{o}_{\boldsymbol{k}s}$ includes the effects of the initial phase and the position of the squeezing source with wavevector $\boldsymbol{k}s$. Here we need to make two assumptions: first, one specific mode is generated from a single source, i.e., mode $\boldsymbol{k}s$ is only generated from the source located at $\boldsymbol{o}_{\boldsymbol{k}s}$; second, the phases of all modes can be well defined by $\boldsymbol{k}\cdot(\boldsymbol{r}-\boldsymbol{o}_{\boldsymbol{k}s})$. In the ordinary vacuum or thermal reservoir, there is no source and we can set $\boldsymbol{o}_{\boldsymbol{k}s}=0$, so the mode function shown in Eq. (3.8) is reduced to the normal cases as Eq. (3.2). In fact, $\boldsymbol{o}_{\boldsymbol{k}s}$ can be any value since their effects will be canceled in Eq. (3.6). Considering the fact that the squeezed vacuum is generated by the pump field from different directions, $\boldsymbol{o}_{\boldsymbol{k}s}$ should be different for different modes.

Next, we will derive the master equation from Eq. (3.6) based on the new mode function

Eq.(3.8). We start from a more general case where atoms are not identical but $\omega_i \approx \omega_j$, and we make the squeezing center frequency $\omega_0 = \sum_i \omega_i/l$. Then we can rewrite the interaction Hamiltonian as

$$V(t) = -i\hbar \sum_{\boldsymbol{k}s} [D(t)a_{\boldsymbol{k}s}(t) - D^+(t)a^\dagger_{\boldsymbol{k}s}(t)], \tag{3.9}$$

where

$$D(t) = \sum_i [\boldsymbol{\mu}_i \cdot \boldsymbol{u}_{\boldsymbol{k},s}(r_i) S_i^\dagger(t) + \boldsymbol{\mu}_i^* \cdot \boldsymbol{u}_{\boldsymbol{k},s}(r_i) S_i^-(t)] \tag{3.10}$$

Therefore, we have

$$\begin{aligned}
\frac{d\rho^S}{dt} =& -\frac{1}{\hbar^2}\int_0^t d\tau Tr_F\{[V(t),[V(t-\tau),\rho^S(t-\tau)\rho^F\} \\
=& -\frac{1}{\hbar^2}\int_0^t d\tau Tr_F\{V(t)V(t-\tau)\rho^S(t-\tau)\rho^F + \rho^S(t-\tau)\rho^F V(t-\tau)V(t) \\
& - V(t)\rho^S(t-\tau)\rho^F V(t-\tau) - V(t-\tau)\rho^S(t-\tau)\rho^F V(t)\}.
\end{aligned} \tag{3.11}$$

Here we just show how to deal with the first term in Eq.(3.11), the remaining terms can be calculated in the same way. For the first term, we have

$$\begin{aligned}
& -\frac{1}{\hbar^2}\int_0^t d\tau Tr_F\{V(t)V(t-\tau)\rho^S(t-\tau)\rho^F\} \\
=& \int_0^t d\tau \sum_{\boldsymbol{k}s,\boldsymbol{k}'s'} \{D(t)D(t-\tau)Tr_F[\rho^F a_{ks}(t)a_{k's'}(t-\tau)] - D(t)D^+(t-\tau)Tr_F[\rho^F a_{ks}(t)a^\dagger_{k's'}(t-\tau)] \\
& - D^+(t)D(t-\tau)Tr_F[\rho^F a^\dagger_{ks}(t)a_{k's'}(t-\tau)] + D^+(t)D^+(t-\tau)Tr_F[\rho^F a^\dagger_{ks}(t)a^\dagger_{k's'}(t-\tau)]\}\rho^S(t-\tau)\}.
\end{aligned} \tag{3.12}$$

Considering that the time scale t_0 we care satisfies $\omega_0 t_0 \gg 1$, the average effects of the oscillations terms like $e^{i\omega t}$ are ceased. Thus, we impose the rotating wave approximation(RWA), which

discards all terms containing $e^{i\omega t}$. Using Eq.(3.10) and the correlation function Eq.(2.40), we have

$$
\begin{aligned}
&-\frac{1}{\hbar^2}\int_0^t d\tau Tr_F\{V(t)V(t-\tau)\rho^S(t-\tau)\rho^F\} \\
=&\sum_{ij}\sum_{\boldsymbol{k}s,\boldsymbol{k}'s'}\int_0^t d\tau\{\boldsymbol{\mu}_i\cdot\boldsymbol{u}_{\boldsymbol{k}s}(r_i)S_i^+e^{i\omega_i t}\boldsymbol{\mu}_j\cdot\boldsymbol{u}_{\boldsymbol{k}'s'}(r_j)S_j^+e^{i\omega_j(t-\tau)}e^{-i(\omega_{\boldsymbol{k}s}+\omega_{\boldsymbol{k}'s'})t+i\omega_{\boldsymbol{k}'s'}\tau} \\
&\times[-\sinh(r)\cosh(r)\delta_{\boldsymbol{k}',2\boldsymbol{k}_0-\boldsymbol{k}}\delta_{ss'}] \\
&-\boldsymbol{\mu}_i\cdot\boldsymbol{u}_{\boldsymbol{k}s}(r_i)S_i^+e^{i\omega_i t}\boldsymbol{\mu}_j^*\cdot\boldsymbol{u}_{\boldsymbol{k}'s'}^*(r_j)S_j^-e^{-i\omega_j(t-\tau)}e^{-i\omega_{\boldsymbol{k}'s'}\tau}\cosh^2 r\delta_{\boldsymbol{k}\boldsymbol{k}'}\delta_{ss'} \\
&-\boldsymbol{\mu}_i^*\cdot\boldsymbol{u}_{\boldsymbol{k}s}(r_i)S_i^-e^{-i\omega_i t}\boldsymbol{\mu}_j\cdot\boldsymbol{u}_{\boldsymbol{k}'s'}^*(r_j)S_j^+e^{i\omega_j(t-\tau)}e^{-i\omega_{\boldsymbol{k}'s'}\tau}\cosh^2 r\delta_{\boldsymbol{k}\boldsymbol{k}'}\delta_{ss'} \\
&-\boldsymbol{\mu}_i^*\cdot\boldsymbol{u}_{\boldsymbol{k}s}^*(r_i)S_i^-e^{-i\omega_i t}\boldsymbol{\mu}_j\cdot\boldsymbol{u}_{\boldsymbol{k}'s'}(r_j)S_j^+e^{i\omega_j(t-\tau)}e^{i\omega_{\boldsymbol{k}'s'}\tau}\sinh^2 r\delta_{\boldsymbol{k}\boldsymbol{k}'}\delta_{ss'} \\
&-\boldsymbol{\mu}_i\cdot\boldsymbol{u}_{\boldsymbol{k}s}^*(r_i)S_i^+e^{i\omega_i t}\boldsymbol{\mu}_j^*\cdot\boldsymbol{u}_{\boldsymbol{k}'s'}(r_j)S_j^-e^{-i\omega_j(t-\tau)}e^{i\omega_{\boldsymbol{k}'s'}\tau}\sinh^2 r\delta_{\boldsymbol{k}\boldsymbol{k}'}\delta_{ss'} \\
&+\boldsymbol{\mu}_i^*\cdot\boldsymbol{u}_{\boldsymbol{k}s}^*(r_i)S_i^-e^{-i\omega_i t}\boldsymbol{\mu}_j^*\cdot\boldsymbol{u}_{\boldsymbol{k}'s'}^*(r_j)S_j^-e^{-i\omega_j(t-\tau)}e^{i(\omega_{\boldsymbol{k}s}+\omega_{\boldsymbol{k}'s'})t-i\omega_{\boldsymbol{k}'s'}\tau} \\
&\times[-\sinh(r)\cosh(r)\delta_{\boldsymbol{k}',2\boldsymbol{k}_0-\boldsymbol{k}}\delta_{ss'}]\}\rho^S(t-\tau)
\end{aligned}
\tag{3.13}
$$

Assuming all $\boldsymbol{o}_{\boldsymbol{k}s}$ are located on the spherical surface with distance D to the origin $(0,0,0)$, for the thermal terms (the second to the fifth terms), we can replace the summation of discrete modes with the integral of continuous modes in the free space in the limit of $L\to\infty$:

$$
\sum_{\boldsymbol{k}}\to\frac{L^3}{(2\pi)^3}\int k^2dk\int_{\Omega_k}
\tag{3.14}
$$

In Ref. [42], it has been shown that the integral can be calculated as

$$
\frac{L^3}{(2\pi)^3}\int k^2dk\int_{\Omega_k}\sum_s\boldsymbol{\mu}_i\cdot\boldsymbol{u}_{\boldsymbol{k}s}(r_i)\boldsymbol{\mu}_j^*\cdot\boldsymbol{u}_{\boldsymbol{k}s}^*(r_j)\approx\frac{\sqrt{\gamma_i\gamma_j}}{2\pi\omega_0^3}\int_0^\infty d\omega\omega^3F(kr_{ij})
\tag{3.15}
$$

with

$$
\begin{aligned}
F(kr_{ij})&=\frac{3}{2}\{[1-\cos^2\alpha]\frac{sin(kr_{ij})}{kr_{ij}}+[1-3\cos^2\alpha][\frac{\cos(kr_{ij})}{(kr_{ij})^2}-\frac{sin(kr_{ij})}{(kr_{ij})^3}]\} \\
\gamma_i&=\frac{\omega_i^3\mu_i^2}{3\pi\epsilon_0\hbar c^3}
\end{aligned}
\tag{3.16}
$$

where $\boldsymbol{r}_{ij} = \boldsymbol{r}_i - \boldsymbol{r}_j$, $r_{ij} = |\boldsymbol{r}_{ij}|$, α is the angle between $\boldsymbol{r}_{ij}$ and $\boldsymbol{\mu}_i$, and the approximation in Eq.(3.15) becomes equality when $\omega_1 = \omega_2$. We can also show that

$$\begin{aligned} &\frac{L^3}{(2\pi)^3}\int k^2 dk \int_{\Omega_k} \sum_s \boldsymbol{\mu}_i \cdot \boldsymbol{u}_{\boldsymbol{k}s}(r_i)\boldsymbol{\mu}_j \cdot \boldsymbol{u}_{\boldsymbol{2k_0}-\boldsymbol{k},s}(r_j) \\ \approx &\frac{\sqrt{\gamma_i\gamma_j}}{2\pi\omega_0^3}\int_0^\infty d\omega\omega^2\sqrt{\omega(2\omega_0-\omega)}F(k_0|\frac{k}{k_0}\boldsymbol{r}_{ij}+2\boldsymbol{r}_j|)e^{2ik_0R} \end{aligned} \tag{3.17}$$

where R is the distance from the sources to the center mass of two atoms, and the approximation becomes equality when $\omega_1 = \omega_2$. Next, we will show how to calculate the first and the second terms in Eq.(3.13), and the remaining terms can be approached in the same way. Using Eq.(3.15), the second term in Eq.(3.13) can be simplified as

$$\begin{aligned} &\sum_{\boldsymbol{k}s}\int_0^t d\tau \boldsymbol{\mu}_i \cdot \boldsymbol{u}_{\boldsymbol{k}s}(r_i)S_i^+ e^{i\omega_i t}\boldsymbol{\mu}_j^* \cdot \boldsymbol{u}_{\boldsymbol{k}s}^*(r_j)S_j^- e^{-i\omega_j(t-\tau)}e^{-i\omega_{\boldsymbol{k}s}\tau}\cosh^2 r\rho^S(t-\tau) \\ &= \cosh^2 r\frac{\sqrt{\gamma_i\gamma_j}}{2\pi\omega_0^3}\int_0^t d\tau\int_0^\infty d\omega\omega^3 F(kr_{ij})e^{i(\omega_i-\omega_j)t}e^{i(\omega_j-\omega_k)\tau}S_i^+S_j^-\rho^S(t-\tau) \end{aligned} \tag{3.18}$$

with $F(kr_{ij})$ given in Eq.(3.16). We here calculate the integral of the first term in $F(kr_{ij})$ ($i \neq j$) and the other terms can be calculated similarly.

$$\begin{aligned} &\cosh^2 r\frac{\sqrt{\gamma_i\gamma_j}c^4}{2\pi\omega_0^3}\frac{3}{2}\int_0^t d\tau\int_0^\infty dk k^3\frac{sinkr_{ij}}{kr_{ij}}e^{i(\omega_j-\omega_k)\tau}S_i^+S_j^-\rho^S(t-\tau)e^{i(\omega_i-\omega_j)t} \\ &= \cosh^2 r\frac{\sqrt{\gamma_i\gamma_j}c^4}{2\pi\omega_0^3}\frac{3}{2}\int_0^t d\tau\int_{-\infty}^\infty dk k^2\frac{1}{2ir_{ij}}(e^{i(k-k_j)r_{ij}+ik_jr_{ij}} - e^{-i(k-k_j)r_{ij}-ik_jr_{ij}}) \\ &\times e^{-i(k-k_j)c\tau}S_i^+S_j^-\rho^S(t-\tau)e^{i(\omega_i-\omega_j)t} \\ &\approx \cosh^2 r\frac{\sqrt{\gamma_i\gamma_j}c^4}{2\pi\omega_0^3}\frac{3}{2}\int_0^t d\tau k_j^2\frac{1}{ir_{ij}}[\delta(r_{ij}-c\tau)e^{ik_jr_{ij}} - \delta(r_{ij}+c\tau)e^{-ik_jr_{ij}}]S_i^+S_j^-\rho^S(t-\tau)e^{i(\omega_i-\omega_j)t} \\ &\approx \cosh^2 r\frac{\sqrt{\gamma_i\gamma_j}c^4}{2\pi\omega_0^3}\frac{3}{2}k_j^2\frac{\pi}{icr_{ij}}e^{ik_jr_{ij}}S_i^+S_j^-\rho^S(t)e^{i(\omega_i-\omega_j)t} \\ &\approx \frac{3}{4}\sqrt{\gamma_i\gamma_j}\cosh^2 r\frac{e^{ik_0r_{ij}}}{ik_0r_{ij}}S_i^+S_j^-\rho^S(t)e^{i(\omega_i-\omega_j)t} \end{aligned} \tag{3.19}$$

In the second line of the equations, we replace $\int_0^\infty dk$ by $\int_{-\infty}^\infty dk$ since the main contribution comes

from the frequency around ω_0 and the negative frequency part leads to fast-oscillating term such that its integration $\int_0^t d\tau$ vanishes. From the second line to the third line, the Weisskopf-Wigner approximation[30] is applied and k is replaced by k_j because the contribution comes mainly from the resonant frequency. From the third line to the fourth line, we assume that the two atoms are very close that the time-retarded effect can be neglected. In the last line, we use the fact that $\omega_i \approx \omega_0$

The other terms in Eq.(3.18) can be calculated in a similar way, and the result is given by

$$\frac{\sqrt{\gamma_i\gamma_j}}{2\pi\omega_0^3}\int_0^t d\tau\int_0^\infty dkk^3F(kr_{ij})e^{i(\omega_i-\omega_j)t}e^{i(\omega_j-\omega_k)\tau}S_i^+S_j^-\rho^S(t-\tau)=(\frac{1}{2}\gamma_{ij}+i\Lambda_{ij})S_i^+S_j^-\rho^S(t)e^{i(\omega_i-\omega_j)t} \tag{3.20}$$

where

$$\begin{aligned}\Lambda_{ij}&=\frac{3}{4}\sqrt{\gamma_i\gamma_j}\{-(1-\cos^2\alpha)\frac{\cos(k_0r_{ij})}{k_0r_{ij}}+(1-3\cos^2\alpha)[\frac{sin(k_0r_{ij})}{(k_0r_{ij})^2}+\frac{\cos(k_0r_{ij})}{(k_0r_{ij})^3}]\}\\ \gamma_{ij}&=\sqrt{\gamma_i\gamma_j}F(k_0r_{ij})\end{aligned} \tag{3.21}$$

All the other terms with the combination of S_i^+ and S_i^- can also be calculated in the same way. Thus, all the thermal terms and oscillation terms in Eq.(3.6) can be given.

Next we need to calculate the squeezed vacuum terms containing $S_i^+S_j^+$ or $S_i^-S_j^-$. Here we calculate the first term in Eq.(3.6) as an example. Inserting Eq.(3.17), the first term of Eq.(3.6) yields

$$\begin{aligned}&\sum_{\boldsymbol{k}s,\boldsymbol{k'}s'}\int_0^t d\tau\int d^3k\{\boldsymbol{\mu}_i\cdot\boldsymbol{u}_{2\boldsymbol{k}_0-\boldsymbol{k},s}(r_i)\boldsymbol{\mu}_j\cdot\boldsymbol{u}_{\boldsymbol{k}s}(r_j)e^{i(\omega_{\boldsymbol{k}s}-\omega_j)\tau}S_i^+S_j^+\rho^S(t-\tau)\\ &=\frac{\sqrt{\gamma_i\gamma_j}c^4}{2\pi\omega_0^3}\int_0^t d\tau\int_0^{2k_0}dkk^2\sqrt{k(2k_0-k)}F(k_0|\frac{k}{k_0}\boldsymbol{r}_{ij}+2\boldsymbol{r}_j|)e^{i(\omega_k-\omega_j)\tau}S_i^+S_j^+\rho^S(t-\tau)e^{2ik_0R}\\ &\approx\frac{\sqrt{\gamma_i\gamma_j}c}{2\pi}\int_0^t d\tau\int_{-\infty}^\infty dkF(k_0|\frac{k}{k_0}\boldsymbol{r}_{ij}+2\boldsymbol{r}_j|)e^{i(\omega_k-\omega_0)\tau}S_i^+S_j^+\rho^S(t-\tau)e^{2ik_0R}\end{aligned} \tag{3.22}$$

From the second line to the third line, we make the following approximations: (1) The integral limit

is extended to $\pm\infty$ because the principal part is near $\omega_k \approx \omega_i$. (2) $k^2\sqrt{k(2k_0-k)}$ is pulled out of the integral as a constant k_0^3 according to the Weisskopf-Wigner approximation. To calculate one term with fixed i, j, we need to rebuild the coordinate system where $\boldsymbol{r}_i + \boldsymbol{r}_j = 0$ for $i \neq j$(We need to build different coordinate systems for different pairs of i, j). For example, we here consider the first two atoms, $i, j = 1, 2$. When $i = j$, this term directly gives $\frac{1}{2}\gamma \cosh^2 rF(2k_0|\boldsymbol{r}_j|)S_i^+ S_i^+ \rho^S(t)$. When $i \neq j$, since there is a singular point at $k = k_0$, the calculation is a little bit more complicated but can still be calculated. We have the following integrals:

$$\begin{aligned}
&\int_{-\infty}^{\infty} dk \frac{\sin kr_{ij}}{kr_{ij}} e^{-ikc\tau} = \frac{\pi}{r_{ij}}\theta_1(r_{ij} - c\tau), \\
&\int_{-\infty}^{\infty} dk \Big[\frac{\cos kr_{ij}}{(kr_{ij})^2} - \frac{\sin kr_{ij}}{(kr_{ij})^3}\Big] e^{-ikc\tau} = \frac{\pi(c\tau - r_{ij})(c\tau + r_{ij})}{2r_{ij}^3}\theta_2(r_{ij} - c\tau),
\end{aligned} \tag{3.23}$$

where $\theta_{1,2}(x)$ are step functions: $\theta_{1,2}(x) = 0$ when $x < 0$, $\theta_{1,2}(x) = 1$ when $x > 0$, and $\theta_1(0) = 1/2$ and $\theta_2(0) = 0$. Since $F(k_0|\frac{k}{k_0}\boldsymbol{r}_{ij} + 2\boldsymbol{r}_j|) = F((k - k_0)r_{12})$, we have

$$\begin{aligned}
&\int_0^t d\tau \int_{-\infty}^{\infty} dk F([(k - k_0)r_{12}]e^{i(\omega_0 - \omega_k)\tau}\rho^S(t - \tau) \\
&= \int_0^{\frac{r_{ij}}{c}} d\tau \frac{3}{2}[(1 - \cos^2\alpha)\frac{\pi}{r_{ij}} + (1 - 3\cos^2\alpha)\frac{\pi(c\tau - r_{ij})(c\tau + r_{ij})}{2r_{ij}^3}]\rho^S(t - \tau) \\
&\approx \frac{\pi}{c}\rho^S(t).
\end{aligned} \tag{3.24}$$

In Eq.(3.24), the emitter separation is assumed to be small and the Markovian approximation is applied such that $\rho^S(t - \tau) \approx \rho^S(t)$. Hence, Eq.(3.22) gives $\sinh r \cosh r \frac{\gamma'_{ij}}{2} S_i^+ S_j^+ \rho^S(t)$ with $\gamma'_{ij} = e^{2ik_0 R}\gamma F(k_0|\boldsymbol{r}_i + \boldsymbol{r}_j|)$ after transforming the above results to the original coordinate system(Although replacing k by k_0 in Eq.(3.22)'s last line yields the same result, it is not always safe to do so since $F(x)$ is an oscillating function). Having dealt with all the squeezed vacuum terms,

we can get the final master equation in the 3D free space for arbitrary number of qubits:

$$\begin{aligned}\frac{d\rho^S}{dt} =& -\frac{1}{2}\sum_{\alpha=\pm}\sum_{i,j}\gamma'_{ij}M(\rho^S S_i^\alpha S_j^\alpha + S_i^\alpha S_j^\alpha \rho^S - 2S_j^\alpha \rho^S S_i^\alpha) \\ &-\frac{1}{2}\sum_{i,j}\gamma_{ij}(1+N)(\rho^S S_i^+ S_j^- + S_i^+ S_j^- \rho^S - 2S_j^- \rho^S S_i^+)e^{i(\omega_i-\omega_j)t} \\ &-\frac{1}{2}\sum_{i,j}\gamma_{ij}N(\rho^S S_i^- S_j^+ + S_i^- S_j^+ \rho^S - 2S_j^+ \rho^S S_i^-)e^{-i(\omega_i-\omega_j)t} \\ &-i\sum_{i\neq j}\Lambda_{ij}[S_i^+ S_j^-, \rho^S]e^{i(\omega_i-\omega_j)t}\end{aligned} \tag{3.25}$$

where the last three terms agree with the traditional reservoir theory in the thermal reservoir case, and the first term is the collective decay due to the squeezed vacuum. We have $M = \sinh(r)cosh(r)$ and average photon number $N = \sinh^2(r)$. The collective energy shifts Λ_{ij} and decay rates γ_{ij} due to the ordinary vacuum are the same as those given by [43, 42], which are shown as follow:

$$\begin{aligned}\Lambda_{ij} =& \frac{3}{4}\sqrt{\gamma_i\gamma_j}\{-(1-\cos^2\alpha)\frac{\cos(k_0 r_{ij})}{k_0 r_{ij}} \\ &+(1-3\cos^2\alpha)[\frac{\sin(k_0 r_{ij})}{(k_0 r_{ij})^2}+\frac{\cos(k_0 r_{ij})}{(k_0 r_{ij})^3}]\} \\ \gamma_{ij} =& \sqrt{\gamma_i\gamma_j}F(k_0 r_{ij})\end{aligned}$$

where $\gamma = \frac{\omega_0^3\mu^2}{3\pi\epsilon_0\hbar c^3}$ is the spontaneous decay rate of the atom in ordinary vacuum. Different from the thermal reservoir terms, the squeezed vacuum can contribute to the additional collective two-photon decay rate of the system which is given by

$$\gamma'_{ij} = \gamma e^{2ik_0 R}F(k_0|\boldsymbol{r}_i + \boldsymbol{r}_j|). \tag{3.26}$$

Thus, the collective decay due to the squeezed vacuum depends on the position of the center of mass of the emitters instead of their separation. One may think this reult is identical to the privious work[9, 10] except the phase $e^{2ik_0 R}$, but that is not true. No matter how the coordinate system is built, to reach the neat form of Eq.(3.26), $\boldsymbol{r}_i$ must still be interpreted as the displacement from

the center of squeezing sources to the ith atom. When their center of mass is at equal distances from all squeezing sources (i.e., $r_i + r_j = 0$), the decay induced by the squeezing is the strongest due to the perfectly constructive interference of the two-photon excitation from all directions. It decreases when it deviates from the center due to the destructive interference.

One way to verify the validity of our theory is to prove the positive definition of Eq.(3.25). The above master equation can be transformed to the Lindblad form [44] and the density matrix is positive. The phase factor $e^{2ik_{0z}R}$ can be effectively regarded as an controllable phase of M, which can be incorporated into θ. The master equation can be transformed as

$$\frac{d\rho^S}{dt} = -i\sum_i [H, \rho^S] + \sum_{m,n} h_{nm}(L_n \rho L_m^\dagger - \frac{1}{2}(\rho L_m^\dagger L_n + L_m^\dagger L_n \rho)) \tag{3.27}$$

where

$$\begin{aligned}
&H = \sum_{i \neq j} \Lambda_{ij} S_i^+ S_j^- \\
&L_1 = S_1^+, L_2 = S_2^+, L_3 = S_3^-, L_4 = S_4^- \\
&h = \begin{bmatrix}
\gamma_{11}\sinh^2 r & \gamma_{12}\sinh^2 r & \gamma'_{11}\sinh r\cosh r & \gamma'_{12}\sinh r\cosh r \\
\gamma_{12}\sinh^2 r & \gamma_{11}\sinh^2 r & \gamma'_{12}\sinh r\cosh r & \gamma'_{11}\sinh r\cosh r \\
\gamma'_{11}\sinh r\cosh r & \gamma'_{12}\sinh r\cosh r & \gamma_{11}\cosh^2 r & \gamma_{12}\cosh^2 r \\
\gamma'_{12}\sinh r\cosh r & \gamma'_{11}\sinh r\cosh r & \gamma_{12}\cosh^2 r & \gamma_{11}\cosh^2 r
\end{bmatrix}
\end{aligned} \tag{3.28}$$

here for simplicity, we have already used the relations: $\gamma'_{12} = \gamma'_{21}$, $\gamma_{12} = \gamma_{21}$, $\gamma_{11} = \gamma_{22}$, $\gamma'_{11} = \gamma'_{22}$. The last relation $\gamma'_{11} = \gamma'_{22}$ is not always satisfied, but without it we cannot diagonalize matrix h analytically. Hence we set $r_i + r_j = 0$. Now matrix h can be diagonalized:

$$h = u^\dagger \begin{bmatrix}
\zeta_1 & & & \\
& \zeta_2 & & \\
& & \zeta_3 & \\
& & & \zeta_4
\end{bmatrix} u \tag{3.29}$$

where u is a unitary matrix, and

$$\begin{aligned}
\zeta_1 &= \frac{1}{2}[(\gamma_{11}-\gamma_{12})(1+2\sinh^2 r) - \sqrt{(\gamma_{11}-\gamma_{12})^2 + 4\sinh^2 r\cosh^2 r(\gamma'_{11}-\gamma'_{12})^2}] \\
\zeta_2 &= \frac{1}{2}[(\gamma_{11}-\gamma_{12})(1+2\sinh^2 r) + \sqrt{(\gamma_{11}-\gamma_{12})^2 + 4\sinh^2 r\cosh^2 r(\gamma'_{11}-\gamma'_{12})^2}] \\
\zeta_3 &= \frac{1}{2}[(\gamma_{11}+\gamma_{12})(1+2\sinh^2 r) - \sqrt{(\gamma_{11}+\gamma_{12})^2 + 4\sinh^2 r\cosh^2 r(\gamma'_{11}+\gamma'_{12})^2}] \\
\zeta_4 &= \frac{1}{2}[(\gamma_{11}+\gamma_{12})(1+2\sinh^2 r) + \sqrt{(\gamma_{11}+\gamma_{12})^2 + 4\sinh^2 r\cosh^2 r(\gamma'_{11}+\gamma'_{12})^2}]
\end{aligned} \tag{3.30}$$

We noticed that since $|\gamma_{11}-\gamma_{12}| = |\gamma'_{11}-\gamma'_{12}|$ for $r_i + r_j = 0$, none of the eigenvalues is negative, so the density matrix is completely positive for any initial condition. For arbitrary r_i, r_j, we can only get the positive eigenvalues numerically.

It is worth noting that the master equation derived from the traditional reservoir theories[8, 9, 10] does not have the positive definition in the first place. In fact, the coefficients in their equations are modified by hand to enforce the positive definition.

3.2 Master equation in the quasi-one-dimensional waveguide

In practice, it is very difficult to squeeze all photon modes in 3D case. Since squeezing in 1D is experimentally achievable [28, 29], in this section we discuss the dynamics of the waveguide-QED in the squeezed vacuum. Here, we consider a perfect rectangular waveguide with negligible loss out of the waveguide as is shown in Fig. 3.2(a). We assume that the cross section of the waveguide is a square with dimensions $a \times b$. The origin of the coordinate system is chosen to be at the center of the two squeezing sources with the positions of the sources to be $(0, 0, \pm R)$. The emitters are located along the longitudinal centerline of the waveguide at $(0, 0, r_i)$ ($i = 1, 2, \cdots, N_a$) with the squeezed vacuum injected from both ends by the parametric process. Compared with the 3D case, the master equation in the 1D case is the same as Eq. (3.25) except that the values of $\gamma_{ij}, \gamma'_{ij}, \Lambda_{ij}$ are different.

Different from the free-space case, the square waveguide can only support certain photon modes. Generally, the allowed modes in the waveguide are very complex which need to be expressed in terms of the Dyadic Green functions[45]. Here we consider the simplest case, which

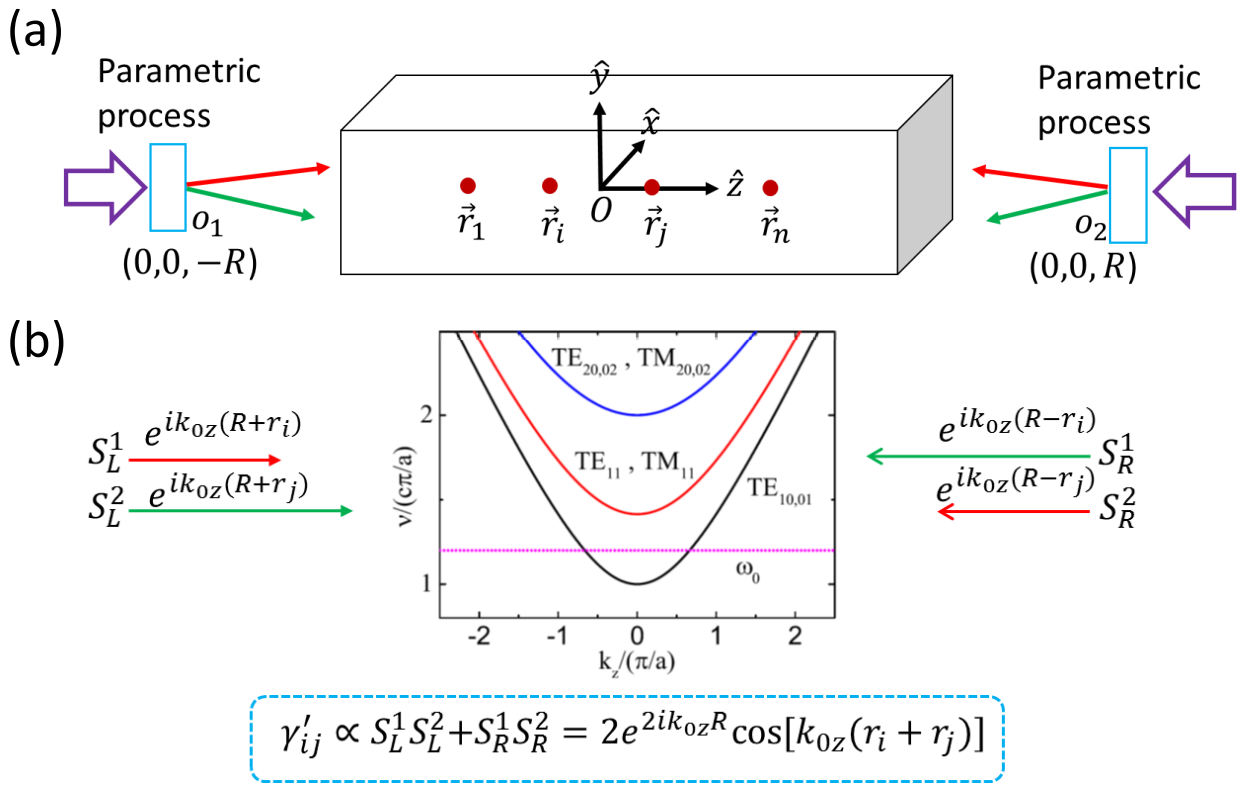

Figure 3.2: (a) Schematic setup for waveguide-QED in the 1D squeezed vacuum where the vacuum is squeezed from both directions. (b) The dispersion relations inside the waveguide. Here the atomic transition frequency is $\frac{1.2c\pi}{a}$, which is below the cut-off frequency of TE_{11} mode. Considering the fact that the atomic dipole moment is along y-axis and $E_y \neq 0$ only for TE_{10}, we only need to consider TE_{10} mode in our calculation.

is the perfect reflective rectangular waveguide with cross section $a \times b$. The rectangular waveguide can support both TE and TM electric field modes and they are given as follows(To get a neat expression of field equation, we set the origin of our coordinate system at the corner of the waveguide):

$$
\begin{aligned}
E_z^{TM} &= E_0 sin\frac{m\pi x}{a} sin\frac{n\pi y}{b} e^{ik_z z}, & H_z^{TE} &= H_0 \cos\frac{m\pi x}{a} \cos\frac{n\pi y}{b} e^{ik_z z} \\
E_x^{TM} &= E_0 \frac{ik_z}{h_{mn}^2}\frac{m\pi}{a} \cos\frac{m\pi x}{a} sin\frac{n\pi y}{b} e^{ik_z z}, & E_x^{TE} &= H_0 \frac{i\omega_k \mu}{h_{mn}^2}\frac{n\pi}{a} \cos\frac{m\pi x}{a} sin\frac{n\pi y}{b} e^{ik_z z} \\
E_y^{TM} &= E_0 \frac{ik_z}{h_{mn}^2}\frac{n\pi}{a} sin\frac{m\pi x}{a} \cos\frac{n\pi y}{b} e^{ik_z z}, & E_y^{TE} &= -H_0 \frac{i\omega_k \mu}{h_{mn}^2}\frac{m\pi}{a} sin\frac{m\pi x}{a} \cos\frac{n\pi y}{b} e^{ik_z z} \\
H_x^{TM} &= E_0 \frac{i\omega_k \epsilon}{h_{mn}^2}\frac{n\pi}{a} sin\frac{m\pi x}{a} \cos\frac{n\pi y}{b} e^{ik_z z}, & H_x^{TE} &= -H_0 \frac{ik_z}{h_{mn}^2}\frac{m\pi}{a} sin\frac{m\pi x}{a} \cos\frac{n\pi y}{b} e^{ik_z z} \\
H_y^{TM} &= -E_0 \frac{i\omega_k \epsilon}{h_{mn}^2}\frac{m\pi}{a} \cos\frac{m\pi x}{a} sin\frac{n\pi y}{b} e^{ik_z z}, & H_y^{TE} &= -H_0 \frac{ik_z}{h_{mn}^2}\frac{n\pi}{a} \cos\frac{m\pi x}{a} sin\frac{n\pi y}{b} e^{ik_z z}
\end{aligned}
\tag{3.31}
$$

where $h_{mn} = \sqrt{(\frac{m\pi}{a})^2 + (\frac{n\pi}{b})^2}$, $\epsilon(\mu)$ is the permittivity (permeability), and H_0, E_0 are arbitrary constants. For quantized modes, we have $E_0 = \sqrt{4\hbar h_{mn}^2/\epsilon^2 \mu\nu LS}$ and $H_0 = \sqrt{4\hbar h_{mn}^2/\epsilon\mu^2\nu LS}$[46]. The dispersion relation inside the waveguide is given by $\omega_k^2/c^2 = (m\pi/a)^2 + (n\pi/b)^2 + k_z^2$. For simplicity, we here consider the waveguide with square cross section, i.e., $a = b$ and the dispersion curves of different modes are shown in Fig. 3.2(b). For square waveguide, $TE_{mn}(TM_{mn})$ and $TE_{nm}(TM_{nm})$ modes are degenerate, and TE_{10} and TE_{01} have the lowest energy.

We assume that the all emitters' transition frequencies are the same and they are below the cutoff frequency of TE_{11} and TM_{11} modes. Since the rectangular waveguide cannot support the TM_{10} and TM_{01} mode, the emitter can only couple to the TE_{01} or TE_{10} modes. Here, without loss of generality we assume that the transition dipole moment of the emitter is in the y direction. Thus, it can only couple to the TE_{10} mode. The emitters are assumed to be located at the center of the waveguide cross section, i.e., $(\frac{a}{2}, \frac{a}{2}, r_i)$ and $(\frac{a}{2}, \frac{a}{2}, r_j)$. In this case, the mode function for TE_{10} mode is given by $\boldsymbol{u}_{k_z}(\boldsymbol{r}_i) = \sqrt{\frac{\omega_{k_z}\hbar}{\epsilon_0 LS}}\hat{y}e^{ik_z(\boldsymbol{r}-\boldsymbol{o}_{k_z})}$ with $S = a^2$. By reducing the cross section, we can increase the amplitude of the mode function and therefore the coupling strength. are shown in

Fig. 3.2(b). To simplify the problem, we assume that the transtion dipole moment of the emitter is along the y direction and the size of the waveguide satisfies $\lambda_0/2 < a < \lambda_0/\sqrt{2}$ where $\lambda_0 = 2\pi c/\omega_0$ with ω_0 being the transition frequency of the emitter. In this case, the emitter is mainly coupled to the TE_{10} mode (Fig. 3.2(b)). The density of states of EM field in the waveguide is $D(\nu) = \frac{L}{\pi c^2}\frac{\nu}{\sqrt{(\frac{\nu}{c})^2-(\frac{\pi}{a})^2}}$. The coupling strength between the emitter and the TE_{10} mode is therefore given by $g \equiv \boldsymbol{\mu}\cdot\boldsymbol{E}/\hbar = \mu\sqrt{\nu/\epsilon_0 LS\hbar}$ [46]. The single emitter decay rate due to the waveguide modes is

$$\gamma_{1d} = 2\pi\sum_{\nu}|g(\nu)|^2\delta(\omega_0-\nu) = \frac{2\mu^2\omega_0^2}{\hbar\epsilon_0 Sc^2k_{0z}} \equiv \eta\gamma_0, \tag{3.32}$$

where $\eta = 3\lambda_0\lambda_{0z}/(2\pi a^2)$ is the enhancement factor, $\lambda_{0z} = 2\pi/k_{0z}$ is the effective longitudinal wavelength and γ_0 is the spontaneous decay rate in the free space. Around the cutoff frequency, we have $k_{0z} \to 0$ and therefore $\eta \to \infty$, i.e., the spontaneous decay rate can be greatly enhanced. The dispersion relations

Then we need to derive the master equation in the waveguide case. Compared with the free space case, the only modification to the calculation for the waveguide is $\sum_{\boldsymbol{k}s} \to \sum_{k_z}$ in Eq.(3.13). We here calculate the first and the second term in Eq.(3.13) as an example. For the second term,

we have

$$
\begin{aligned}
&-\sum_{k_z}\int_0^t d\tau \boldsymbol{\mu}_i\cdot\boldsymbol{u}_{\boldsymbol{k}s}(r_i)S_i^+e^{i\omega_0 t}\boldsymbol{\mu}_j^*\cdot\boldsymbol{u}^*_{\boldsymbol{k}'s'}(r_j)S_j^-e^{-i\omega_0(t-\tau)}e^{-i\omega_{\boldsymbol{k}'s'}\tau}\cosh^2 r\rho^S(t-\tau)\delta_{\boldsymbol{k}\boldsymbol{k}'}\delta_{ss'}\\
=&-\frac{L}{2\pi}\int_{-\infty}^{\infty}dk_z\int_0^t d\tau e^{i\omega_0\tau}e^{-i\omega_{k_z}\tau}\frac{\omega_k\mu^2}{\epsilon_0 LS\hbar}e^{ik_z(r_i-r_j)}\cosh^2 rS_i^+S_j^-\rho^S(t-\tau)\\
\approx&-\frac{L}{2\pi}\int_0^{\infty}dk_z\int_0^t d\tau e^{i\omega_0\tau}e^{-i[\omega_0+c^2k_{0z}(k_z-k_{0z})/\omega_0]\tau}\frac{\omega_k\mu^2}{\epsilon_0 LS\hbar}[e^{ik_z(r_i-r_j)}+e^{-ik_z(r_i-r_j)}]\cosh^2 rS_i^+S_j^-\rho^S(t-\tau)\\
\approx&-\frac{L}{2\pi}\int_{-k_{0z}}^{\infty}d\delta k_z\int_0^t d\tau e^{-i\tau c^2k_{0z}\delta k_z/\omega_0}\frac{\omega_k\mu^2}{\epsilon_0 LS\hbar}[e^{i(k_{0z}+\delta k_z)(r_i-r_j)}+e^{-i(k_{0z}+\delta k_z)(r_i-r_j)}]\cosh^2 rS_i^+S_j^-\rho^S(t-\tau)\\
\approx&-\frac{L}{2\pi}\int_{-\infty}^{\infty}d\delta k_z\int_0^t d\tau e^{-i(c^2k_{0z}\delta k_z/\omega_0)\tau}\frac{\omega_k\mu^2}{\epsilon_0 LS\hbar}[e^{i(k_{0z}+\delta k_z)(r_i-r_j)}+e^{-i(k_{0z}+\delta k_z)(r_i-r_j)}]\cosh^2 rS_i^+S_j^-\rho^S(t-\tau)\\
\approx&-\frac{L}{2\pi}\int_0^t d\tau\frac{\omega_0\mu^2}{\epsilon_0 LS\hbar}2\pi[e^{ik_{0z}(r_i-r_j)}\delta((r_i-r_j)-\frac{c^2k_{0z}}{\omega_0}\tau)+e^{-ik_{0z}(r_i-r_j)}\delta((r_i-r_j)+\frac{c^2k_{0z}}{\omega_0}\tau)]\\
&\times\cosh^2 rS_i^+S_j^-\rho^S(t-\tau)\\
\approx&-\frac{L}{2\pi}e^{ik_{0z}r_{ij}}\frac{\omega_0\mu^2}{\epsilon_0 LS\hbar}2\pi\frac{\omega_0}{c^2k_{0z}}\cosh^2 rS_i^+S_j^-\rho^S(t)\\
\approx&-[\frac{\gamma_{1d}}{2}\cos(k_{0z}r_{ij})+i\frac{\gamma_{1d}}{2}sin(k_{0z}r_{ij})]\cosh^2 rS_i^+S_j^-\rho^S(t)\\
\equiv&-(\frac{\gamma_{ij}}{2}+i\Lambda_{ij})\cosh^2 rS_i^+S_j^-\rho^S(t)
\end{aligned}
\tag{3.33}
$$

where emitter separation $r_{ij}=|r_i-r_j|$, $\gamma_{1d}=2\mu^2\omega_0^2/\hbar\epsilon_0Sc^2k_{0z}$ is the spontaneous decay rate in the waveguide, $\gamma_{ij}=\gamma_{1d}\cos(k_{0z}r_{ij})$ is the collective decay rate, and $\Lambda_{ij}=\gamma_{1d}\sin(k_{0z}r_{ij})/2$ is the collective energy shift. In the third line we expand $\omega_k=c\sqrt{(\frac{\pi}{a})^2+(k_z)^2}$ around $k_z=k_{0z}$ since resonant modes provide dominant contributions. In the fifth line we extend the integration $\int_{-k_{0z}}^{\infty}dk_z\to\int_{-\infty}^{\infty}dk_z$ because the main contribution comes from the components around $\delta k_z=0$. In the next line, Weisskopf-Wigner approximation is used. Thus, we have obtained γ_{ij} and Λ_{ij}.

Next we need to calculate the first term (squeezing term) in Eq.(3.13):

$$
\begin{aligned}
&\sum_{k_z}\int_0^t d\tau\{\boldsymbol{\mu}_i\cdot\boldsymbol{u}_{2\boldsymbol{k}_0-\boldsymbol{k}}(r_i)S_i^+\boldsymbol{\mu}_j\cdot\boldsymbol{u}_{\boldsymbol{k}}(r_j)S_j^+e^{i(\omega_{\boldsymbol{k}}-\omega_0)\tau}[-\sinh(r)\cosh(r)]\rho^S(t-\tau)\\
=&-\frac{L}{2\pi}\int_0^{2k_{0z}}dk_z\int_0^t d\tau e^{i(\omega_{k_z}-\omega_0)\tau}e^{i(2k_{0z}-k_z)(r_i-o_1)}e^{ik_z(r_j-o_1)}\\
&\times\frac{\sqrt{\omega_{k_z}\omega_{2k_{0z}-k_z}}\mu^2}{\epsilon_0LS\hbar}\sinh(r)\cosh(r)S_i^+S_j^+\rho^S(t-\tau)\\
&-\frac{L}{2\pi}\int_{-2k_{0z}}^0dk_z\int_0^t d\tau e^{i(\omega_{k_z}-\omega_0)\tau}e^{i(-2k_{0z}-k_z)(r_i-o_2)}e^{ik_z(r_j-o_2)}\\
&\times\frac{\sqrt{\omega_{k_z}\omega_{-2k_{0z}-k_z}}\mu^2}{\epsilon_0LS\hbar}\sinh(r)\cosh(r)S_i^+S_j^+\rho^S(t-\tau)
\end{aligned}
\tag{3.34}
$$

For $i=j$, Eq.(5.8) reduces to

$$
\begin{aligned}
&\sum_{k_z}\int_0^t d\tau\{\boldsymbol{\mu}_i\cdot\boldsymbol{u}_{2\boldsymbol{k}_0-\boldsymbol{k}}(r_i)S_i^+\boldsymbol{\mu}_j\cdot\boldsymbol{u}_{\boldsymbol{k}}(r_j)S_j^+e^{i(\omega_{\boldsymbol{k}}-\omega_0)\tau}[-\sinh(r)\cosh(r)]\rho^S(t-\tau)\\
&=-\frac{L}{2\pi}\int_0^{2k_{0z}}dk_z\int_0^t d\tau e^{i\frac{c^2k_{0z}}{\omega_0}(k_z-k_{0z})\tau}e^{i2k_{0z}(r_i-o_1)}\frac{\sqrt{\omega_{k_z}\omega_{2k_{0z}-k_z}}\mu^2}{\epsilon_0LS\hbar}\sinh(r)\cosh(r)S_i^+S_j^+\rho^S(t-\tau)\\
&-\frac{L}{2\pi}\int_{-2k_{0z}}^0dk_z\int_0^t d\tau e^{i\frac{c^2k_{0z}}{\omega_0}(k_z-k_{0z})\tau}e^{-i2k_{0z}(r_i-o_2)}\frac{\sqrt{\omega_{k_z}\omega_{-2k_{0z}-k_z}}\mu^2}{\epsilon_0LS\hbar}\sinh(r)\cosh(r)S_i^+S_j^+\rho^S(t-\tau)\\
&=-\frac{L}{2\pi}[e^{i2k_{0z}(r_i-o_1)}+e^{-i2k_{0z}(r_i-o_2)}]\frac{\omega_{k_{0z}}\mu^2}{\epsilon_0LS\hbar}\int_0^t d\tau 2\pi\delta(\frac{c^2k_{0z}}{\omega_0}\tau)\sinh(r)\cosh(r)S_i^+S_j^+\rho^S(t-\tau)\\
&=-\frac{L}{2\pi}[e^{i2k_{0z}(r_i-o_1)}+e^{-i2k_{0z}(r_i-o_2)}]\frac{\omega_{k_{0z}}\mu^2}{\epsilon_0LS\hbar}\int_0^t d\tau 2\pi\delta(\frac{c^2k_{0z}}{\omega_0}\tau)\sinh(r)\cosh(r)S_i^+S_j^+\rho^S(t-\tau)\\
&=-e^{i2k_{0z}R}\frac{\omega_0^2\mu^2}{\epsilon_0\hbar Sc^2k_{0z}}\cos(2k_{0z}r_i)\sinh(r)\cosh(r)S_i^+S_j^+\rho^S(t)\\
&=-e^{i2k_{0z}R}\frac{\gamma_{1d}}{2}\cos(2k_{0z}r_i)\sinh(r)\cosh(r)S_i^+S_j^+\rho^S(t)
\end{aligned}
\tag{3.35}
$$

where we have used the fact that the origin of coordinate system is at equal distant from two sources(i.e., $o_2=-o_1=R$) in the second last line. Thus, we have $\gamma'_{ii}=\gamma_{1d}\cos(2k_{0z}r_i)$. For

$i \neq j$, Eq. (5.8) reduces to

$$
\begin{aligned}
&\sum_{k_z}\int_0^t d\tau\{\boldsymbol{\mu}_i\cdot\boldsymbol{u}_{2\boldsymbol{k}_0-\boldsymbol{k}}(r_i)S_i^+\boldsymbol{\mu}_j\cdot\boldsymbol{u}_{\boldsymbol{k}}(r_j)S_j^+e^{i(\omega_{\boldsymbol{k}}-\omega_0)\tau}[-\sinh(r)\cosh(r)]\rho^S(t-\tau)\\
=&-\frac{L}{2\pi}\int_0^{2k_{0z}}dk_z\int_0^t d\tau e^{i\frac{c^2k_{0z}}{\omega_0}(k_z-k_{0z})\tau}e^{i2k_{0z}(r_c-o_1)}e^{-i(k_z-k_{0z})(r_i-r_j)}\\
&\times\frac{\sqrt{\omega_{k_z}\omega_{2k_{0z}-k_z}}\mu^2}{\epsilon_0LS\hbar}\sinh(r)\cosh(r)S_i^+S_j^+\rho^S(t-\tau)\\
&-\frac{L}{2\pi}\int_{-2k_{0z}}^0dk_z\int_0^t d\tau e^{i\frac{c^2k_{0z}}{\omega_0}(-k_z-k_{0z})\tau}e^{-i2k_{0z}(r_c-o_2)}e^{-i(k_z+k_{0z})(r_i-r_j)}\\
&\times\frac{\sqrt{\omega_{k_z}\omega_{-2k_{0z}-k_z}}\mu^2}{\epsilon_0LS\hbar}\sinh(r)\cosh(r)S_i^+S_j^+\rho^S(t-\tau)\\
=&-\frac{L}{2\pi}\int_0^{2k_{0z}}dk_z\int_0^t d\tau e^{i\frac{c^2k_{0z}}{\omega_0}(k_z-k_{0z})\tau}e^{i2k_{0z}(r_c-o_1)}e^{-i(k_z-k_{0z})(r_i-r_j)}\\
&\times\frac{\sqrt{\omega_{k_z}\omega_{2k_{0z}-k_z}}\mu^2}{\epsilon_0LS\hbar}\sinh(r)\cosh(r)S_i^+S_j^+\rho^S(t-\tau)\\
&-\frac{L}{2\pi}\int_0^{2k_{0z}}dk_z\int_0^t d\tau e^{i\frac{c^2k_{0z}}{\omega_0}(k_z-k_{0z})\tau}e^{-i2k_{0z}(r_c-o_2)}e^{-i(-k_z+k_{0z})(r_i-r_j)}\\
&\times\frac{\sqrt{\omega_{-k_z}\omega_{-2k_{0z}+k_z}}\mu^2}{\epsilon_0LS\hbar}\sinh(r)\cosh(r)S_i^+S_j^+\rho^S(t-\tau)\\
=&-\frac{L}{2\pi}e^{i2k_{0z}(r_c-o_1)}\frac{\omega_{k_{0z}}\mu^2}{\epsilon_0LS\hbar}\int_{-\infty}^{\infty}dk_z\int_0^t d\tau e^{i\frac{c^2k_{0z}}{\omega_0}(k_z-k_{0z})\tau}e^{-i(k_z-k_{0z})(r_i-r_j)}\\
&\times\sinh(r)\cosh(r)S_i^+S_j^+\rho^S(t-\tau)\\
&-\frac{L}{2\pi}e^{-i2k_{0z}(r_c-o_2)}\frac{\omega_{k_{0z}}\mu^2}{\epsilon_0LS\hbar}\int_{-\infty}^{\infty}dk_z\int_0^t d\tau e^{i\frac{c^2k_{0z}}{\omega_0}(k_z-k_{0z})\tau}e^{i(k_z-k_{0z})(r_i-r_j)}\\
&\times\sinh(r)\cosh(r)S_i^+S_j^+\rho^S(t-\tau)\\
=&-\frac{L}{2\pi}e^{i2k_{0z}R}\frac{\omega_0\mu^2}{\epsilon_0LS\hbar}\int_0^t d\tau 2\pi[e^{i2k_{0z}r_c}\delta(r_i-r_j-\frac{c^2k_{0z}}{\omega_0}\tau)+e^{-i2k_{0z}r_c}\delta(r_i-r_j+\frac{c^2k_{0z}}{\omega_0}\tau)]\\
&\times\sinh(r)\cosh(r)S_i^+S_j^+\rho^S(t-\tau)\\
=&-e^{i2k_{0z}R}\frac{\omega_0^2\mu^2}{\epsilon_0\hbar Sc^2k_{0z}}e^{i2k_{0z}r_csgn(i-j)}S_i^+S_j^+\rho^S(t)\to-\frac{\gamma_{1d}}{2}e^{i2k_{0z}R}\cos(k_{0z}(r_i+r_j))S_i^+S_j^+\rho^S(t)
\end{aligned}
\tag{3.36}
$$

where $sgn(i-j)$ is the sign function. The last arrow is because we need to sum over i,j, so the imaginary part of $e^{i2k_{0z}r_csgn(i-j)}$ vanishes and the neat result is that $\gamma'_{ij}=e^{i2k_{0z}R}\gamma_{1d}\cos(k_{0z}(r_i+$

$r_j)$). As for $S_i^+\rho^S(t)S_j^+$ terms, the combination of the last two terms in Eq.(3.11) will make the imaginary part of $e^{i2k_{0z}r_c sgn(i-j)}$ vanish. Thus, we have $\gamma'_{ij} = e^{i2k_{0z}R}\gamma_{1d}\cos(k_{0z}(r_i + r_j))$. If one needs to get $\gamma_{ij}, \gamma'_{ij}$ and Λ_{ij}in the unidirectional waveguide case, we just need to discard the second terms in the parenthesis of Eq.(5.7) and Eq.(5.10).

In conclusion, the master equation in the 1D waveguide is also given by Eq. (3.25), but the coefficients are replaced by:

$$\begin{aligned}
\gamma_{ij} &= \gamma_{1d}\cos(k_{0z}r_{ij}) \\
\Lambda_{ij} &= \frac{\gamma_{1d}}{2}\sin(k_{0z}r_{ij}) \\
\gamma'_{ij} &= \gamma_{1d}\cos[k_{0z}(r_i + r_j)]
\end{aligned} \tag{3.37}$$

where $k_{0z} = \sqrt{(\frac{\omega_0}{c})^2 - (\frac{c\pi}{a})^2}$ is the wave vector along the waveguide direction and $r_{ij} = |r_i - r_j|$ is the separation between two emitters. It is worth noting that Eq. (3.25) is valid not only for the rectangular waveguide, but also for arbitrary type of waveguide with arbitrary atomic transition frequency. The only difference for different types of waveguide and different transition frequency is the value of γ_{1d} in Eq. (5.13).

Similar to the 3D case, the two-photon decay rate induced by the squeezed vacuum depends on the center of mass of the emitters. This can be explained by the interference shown in Fig. 3.2(b). The emitters can absorb two photons from the squeezing sources either from the left or the right. These two processes can interfere with each others and we have

$$\gamma_{ij}^{'} \propto S_L^1 S_L^2 + S_R^1 S_R^2 = 2e^{2ik_{0z}R}\cos[k_{0z}(r_i + r_j)]$$

which is a periodic function with period λ_{0z}. Thus, when the center of mass happens to be at the antinodes (nodes) of the standing wave, the two-photon decay rate is maximized (minimized).

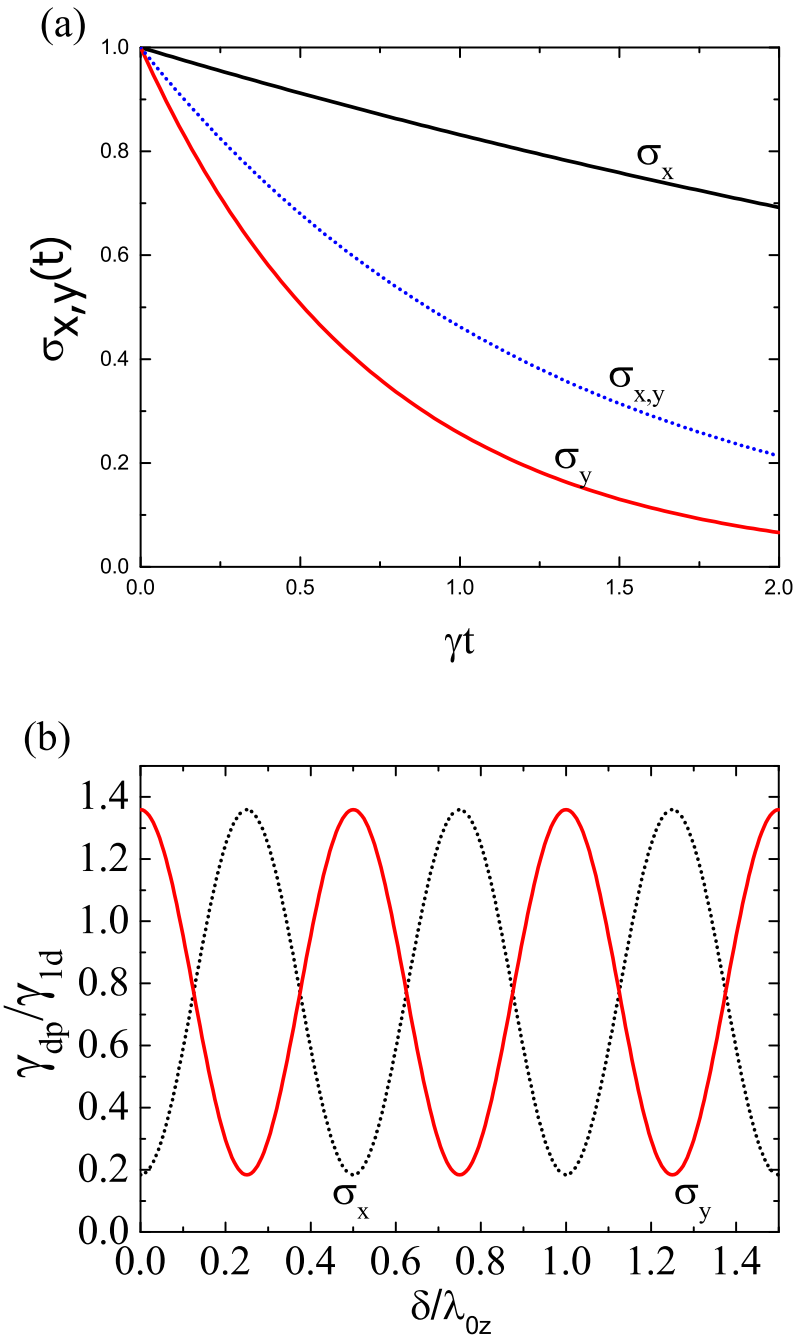

Figure 3.3: (a) The dephasing dynamics of a single emitter in the squeezed vacuum. The black and red solid curves are the results of σ_x and σ_y, respectively. The blue dotted line is the result when there is no squeezing (thermal reservoir). (b) The dephasing rates of σ_x and σ_y as a function of the emitter position. For (a)&(b), the squeezing parameters are chosen to be $r = 0.5$.

3.3 Dynamics of a single qubit

In this section, we will show the difference between the traditional theory and our theory when applied to the single two-level atom case. We still assume that the atom is located at $(0, 0, \delta)$, with the transition dipole moment along the y-axis. By eliminating the terms with $i \neq j$, the master equation shown in Eq.(3.25) is reduced to the single-atom case which is given by

$$\begin{aligned}\frac{d\rho^S}{dt} &= \sinh(r)\cosh(r)\gamma'(e^{2ik_{0z}R}S^+\rho^S S^+ + H.c.) \\ &- \frac{1}{2}\gamma\cosh^2(r)(\rho^S S^+S^- + S^+S^-\rho^S - 2S^-\rho^S S^+) \\ &- \frac{1}{2}\gamma\sinh^2(r)(\rho^S S^-S^+ + S^-S^+\rho^S - 2S^+\rho^S S^-)\end{aligned} \tag{3.38}$$

with $\gamma = \gamma_{1d}$ and $\gamma' = \gamma_{1d}\cos(2k_0\delta)$. It is worth noting that the squeezing terms like $S^+\rho^S S^+$ and $S^-\rho^S S^-$ in Eq. (5.15) only affect the non-diagonal terms but not the diagonal terms. Thus, for single emitter, the squeezing can only modify the dephasing rate rather than the population decay rate. We also notice that the dephasing rate due to the squeezed vacuum is dependent on the emitter position because the interference between the two squeezing sources generates a standing wave.

The dynamical equations for the expectation value of σ_+ and σ_- are given by

$$\frac{d}{dt}\begin{pmatrix}\langle\sigma_+\rangle \\ \langle\sigma_-\rangle\end{pmatrix} = U\begin{pmatrix}\langle\sigma_+\rangle \\ \langle\sigma_-\rangle\end{pmatrix} \tag{3.39}$$

where

$$U = \gamma_{1d}\begin{pmatrix}-(N+\frac{1}{2}) & Me^{-2ik_{0z}R}\cos(2k_{0z}\delta) \\ Me^{2ik_{0z}R}\cos(2k_{0z}\delta) & -(N+\frac{1}{2})\end{pmatrix}. \tag{3.40}$$

The eigenvalues of U are $\gamma_{dp,\pm} = [N + \frac{1}{2} \pm M\cos(2k_{0z}\delta)]\gamma_{1d}$ which are the dephasing rate. In fact, such a position-dependent property of the dephasing rate can be associated with the variance in the quadrature phases of the squeezed field at the site of the atom. Considering

the operator $X(\delta,\alpha,\beta) = \frac{1}{2\sqrt{2}}(e^{i(k_{0z}+k_z)\delta}a_{k_{0z}+k_z}e^{i\alpha} + e^{i(k_{0z}-k_z)\delta}a_{k_{0z}-k_z}e^{i\beta} + H.c.)$ which describes the entangled modes of the two-mode squeezing, we can find its variance $\Delta X(\delta,\alpha,\beta) = \frac{1}{2}[N+\frac{1}{2}-M\cos(2k_{0z}\delta+\alpha+\beta)]$. Therefore, we have the relation that $\gamma_{dp,+} = 2\Delta X(\delta,\alpha+\beta=0)$ and $\gamma_{dp,-} = 2\Delta X(\delta,\alpha+\beta=\pi)$.

We can see that when there is no squeezing, i.e., $M = 0$, both σ_x and σ_y have the same dephasing rate $\cosh^2(r)\gamma_{1d}/2$ (blue dotted line in Fig. 3.3(a)). However, if there is squeezing, i.e., $M \neq 0$, σ_x and σ_y have different dephasing rates with one being enhanced and the other one being suppressed (solid lines in Fig. 3.3(a)). The dephasing rate can be tuned by changing the position of the emitter. In Fig. 3.3(b), it is shown that the dephasing rates of σ_x and σ_y vary periodically as the emitter position changes. At some regions, σ_x decays faster than σ_y, while at other regions, σ_x decays slower than σ_y. This result challenges the traditional conclusion where dephasing rate is a position-independent constant[4, 30].

The power spectrum of the resonance fluorescence can also be calculated and the result is similar to Ref. [32] with the simple replacements of M by $M\gamma'$ and the phase of M by $e^{2ik_{0z}R}$.

3.4 Dynamics of multiple qubits coupled by the dipole-dipole interaction

Next, we consider the two-emitter case where dipole-dipole interaction can occur and two-photon process is allowed. In Fig. 3.4(a), we show the dynamics of the transverse polarization σ_x and σ_y. Here, we compare two different emitter separations $r_{12} = 0.5\lambda_{0z}$ and $r_{12} = 1.0\lambda_{0z}$. In both cases, the x and y polarizations have the same decay dynamics in the thermal reservoir. However, in the squeezed vacuum, the two orthogonal polarizations have different decay rates with one being enhanced and the other being suppressed. When $r_{12} = 0.5\lambda_{0z}$, σ_x decays faster than that in the thermal reservoir, but σ_y decays much slower than that in the thermal reservoir. While opposite result occurs when $r_{12} = 1.0\lambda_{0z}$. This is similar to the one-emitter case.

Different from the one-emitter case, as is shown in Fig. 3.4(b), the squeezed vacuum can affect the population decay of the two-emitter system. This is because two-photon process is allowed in the two-emitter system. Without the squeezed vacuum, the system is finally in the thermal equilibrium state (dotted lines). However, the squeezed vacuum can deplete the populations on

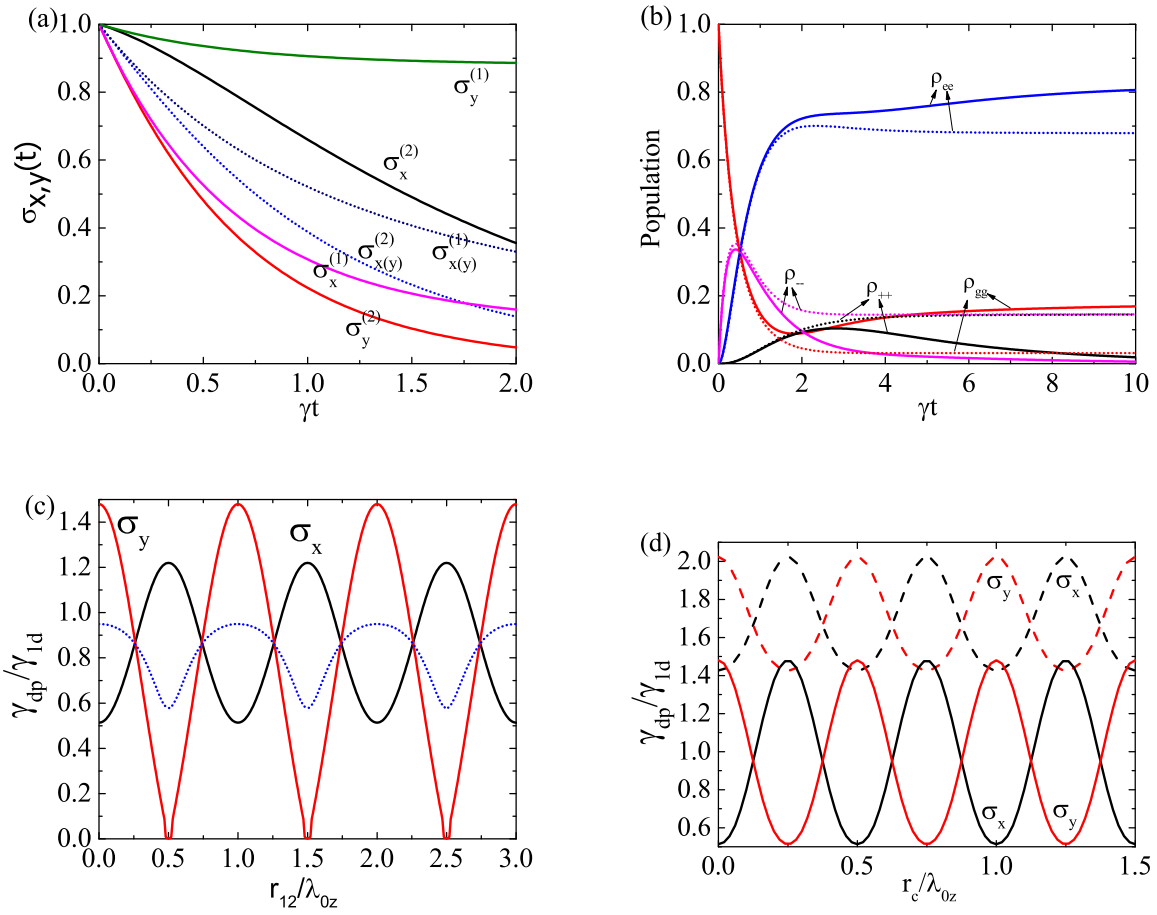

Figure 3.4: Two-emitter case: Transverse polarization decay of the first emitter as a function of time. (a) $r_{12} = 0.5\lambda_{0z}$ for superscript (1) and $r_{12} = 1.0\lambda_{0z}$ for superscript (2), $r = 0.5$ and $r_c = 0$; (b) population decay as a function of time when $r_{12} = 0.5\lambda_{0z}$, $r = 0.5$ and $r_c = 0$. Solid lines are the results in squeezed vacuum and the dotted lines are the results in the thermal reservoir with $N = \sinh^2(r)$. Here the dynamics of ρ_{++} and ρ_{--} are highly identical. (c) Dephasing rate as a function of atom separation with the center of mass fixed at $r_c = 0$. (d) Dephasing rate as a function of center of mass position with atom separation fixed at $r_{ij} = \lambda_{0z}$, where the two-atom case is plotted in solid lines and the five-atom case is plotted in dashed lines.

$|++\rangle$ and $|--\rangle$ with $|\pm\rangle = \frac{1}{\sqrt{2}}(|e_1\rangle|g_2\rangle \pm |g_1\rangle|e_2\rangle)$. In fact, the atomic pair evolves into an entanglement state in this case and we will discuss it later.

We also study the dephasing rate as a function of emitter separation and position of the center of mass which are shown in Fig. 3.4(c) and (d) respectively. Here the dephasing rate is defined to be the inverse of time for $\sigma_x(\sigma_y)$ to damp to $1/e$ of its initial value. Similar to the one-emitter case, the dephasing rate is a periodic function of both r_{12} and r_c. However, due to the dipole-dipole interaction, the dephasing rate is no longer a constant even in the thermal reservoir (dotted line in Fig. 3.4(c)) so that the value ranges of σ_x and σ_y are no longer the same in the squeezed vacuum(solid lines in Fig. 3.4(c)). It is noted that when $r_{12} = 0.5n\lambda_{0z}$ (n is any integer) σ_y does not decay to $1/e$ of its initial value due to the subradiance effect. When we fix the atom separation and change the center of mass(Fig. 3.4(d)), the dephasing rate changes periodically and harmonically like one-emitter case. Therefore, the dephasing rate is tunable by changing the atom separation or position of center of mass. Usually, the positions of the atoms are not easy to be tuned. However, we can easily tune the position of the squeezing sources to effectively change the center of mass of the atoms. Figure 3.4(d) also shows the result when there are five emitters (dashed lines). The dephasing rate is significantly increased when N_a increases due to the collective effect, which depends on the number of atoms but not its parity.

3.5 Generalization to multi-level atoms

In this section, we will consider a more general case for atoms of arbitrary number of energy levels in the squeezed vacuum reservoir. For the rectangular waveguide, there is no TM_{01} or TM_{10} mode. Assuming $b < a$, TE_{10} is the ground mode with the lowest cutoff frequency. For simplicity, we assume that all electronic transitions only coupled to TE_{10} mode.

The atom-field system is described by the Hamiltonian

$$H = H_A + H_F + H_{AF} \tag{3.41}$$

where $H_A = \sum_{l=1}^{N_a} \sum_{e=a,b,c} \hbar\omega_{e,l} |e_l\rangle \langle e_l|$ is the atomic Hamiltonian, and $|e_l\rangle$ is the energy state of

the lth atom with energy $\hbar\omega_{e,l}$. The Hamiltonian of the EM field is $H_F = \sum_{\boldsymbol{ks}} \hbar\omega_{\boldsymbol{ks}}(\hat{a}^\dagger_{\boldsymbol{ks}}\hat{a}_{\boldsymbol{ks}} + \frac{1}{2})$ where $\hat{a}_{\boldsymbol{ks}}$ and $\hat{a}^\dagger_{\boldsymbol{ks}}$ are the annihilation and creation operators of the filed mode with wavevector $\boldsymbol{k}$, polarization s (in waveguide, it represents TE_{mn} or TM_{mn}), and frequency $\omega_{\boldsymbol{k},s}$. The interaction Hamiltonian in the electric-dipole approximation is $H_{AF} = -i\hbar\sum_{\boldsymbol{ks}}\sum_{i=1,2}\sum_{l=1}^{N_a}[\boldsymbol{\mu}_{l,i} \cdot \boldsymbol{u}_{\boldsymbol{ks}}(\boldsymbol{r}_{l,i})S^+_{l,i}\hat{a}_{\boldsymbol{ks}} + \boldsymbol{\mu}^*_{l,i} \cdot \boldsymbol{u}_{\boldsymbol{ks}}(\boldsymbol{r}_{l,i})S^-_{l,i}\hat{a}_{\boldsymbol{ks}} - H.c.]$ where $\boldsymbol{\mu}_{l,i}$ is the electric dipole moment for the ith transition of the lth atom, where $i = 1$ denotes the transition from $|a\rangle$ to $|b\rangle$, and $i = 2$ denotes the transition from $|b\rangle$ to $|c\rangle$. Here, $S^+_{l,i}$ and $S^-_{l,i}$ are the raising and lowering operator for the transition i of the lth atom. The mode function of the squeezed vacuum in the TE_{10} mode is given by

$$\boldsymbol{u}_{\boldsymbol{ks}}(\boldsymbol{r}_i) = \sqrt{\frac{\omega_{\boldsymbol{ks}}}{2\epsilon_0\hbar V}}\boldsymbol{x}e^{i\boldsymbol{k}\cdot(\boldsymbol{r}_i-\boldsymbol{o}_{\boldsymbol{ks}})} \tag{3.42}$$

Thus, the interaction Hamiltonian is where

$$D(t) = \sum_{l,i}[\boldsymbol{\mu}_{l,i} \cdot \boldsymbol{u}_{\boldsymbol{k},s}(r_{l,i})S^\dagger_{l,i}(t) + \boldsymbol{\mu}^*_{l,i} \cdot \boldsymbol{u}_{\boldsymbol{k},s}(r_{l,i})S^-_{l,i}(t)] \tag{3.43}$$

The reduced master equation of atoms in the reservoir is:

$$\begin{aligned}\frac{d\rho^S}{dt} =& -\frac{1}{\hbar^2}\int_0^t d\tau Tr_F\{[V(t),[V(t-\tau),\rho^S(t-\tau)\rho^F\}\\ =& -\frac{1}{\hbar^2}\int_0^t d\tau Tr_F\{V(t)V(t-\tau)\rho^S(t-\tau)\rho^F + \rho^S(t-\tau)\rho^F V(t-\tau)V(t)\\ &- V(t)\rho^S(t-\tau)\rho^F V(t-\tau) - V(t-\tau)\rho^S(t-\tau)\rho^F V(t)\}\end{aligned} \tag{3.44}$$

Here we just show how to deal with the first term in Eq. (3.11), the remaining terms can be

calculated in the same way. For the first term, we have

$$
\begin{aligned}
&-\frac{1}{\hbar^2}\int_0^t d\tau Tr_F\{V(t)V(t-\tau)\rho^S(t-\tau)\rho^F\} \\
=&\int_0^t d\tau \sum_{\boldsymbol{ks},\boldsymbol{k's'}} \{D(t)D(t-\tau)Tr_F[\rho^F a_{ks}(t)a_{k's'}(t-\tau)] - D(t)D^+(t-\tau)Tr_F[\rho^F a_{ks}(t)a^\dagger_{k's'}(t-\tau)] \\
&- D^+(t)D(t-\tau)Tr_F[\rho^F a^\dagger_{ks}(t)a_{k's'}(t-\tau)] + D^+(t)D^+(t-\tau)Tr_F[\rho^F a^\dagger_{ks}(t)a^\dagger_{k's'}(t-\tau)]\}\rho^S(t-\tau)\}.
\end{aligned}
\tag{3.45}
$$

Under the rotating wave approximation(RWA), we have

$$
\begin{aligned}
&-\frac{1}{\hbar^2}\int_0^t d\tau Tr_F\{V(t)V(t-\tau)\rho^S(t-\tau)\rho^F\} \\
=&\sum_{ijlm}\sum_{\boldsymbol{ks},\boldsymbol{k's'}}\int_0^t d\tau\{\boldsymbol{\mu}_{l,i}\cdot\boldsymbol{u}_{\boldsymbol{ks}}(r_{l,i})S^+_{l,i}e^{i\omega_i t}\boldsymbol{\mu}_{m,j}\cdot\boldsymbol{u}_{\boldsymbol{k's'}}(r_{m,j})S^+_{m,j}e^{i\omega_j(t-\tau)} \\
&\quad\times e^{-i(\omega_{\boldsymbol{ks}}+\omega_{\boldsymbol{k's'}})t+i\omega_{\boldsymbol{k's'}}\tau}[-M\delta_{\boldsymbol{k'},2\boldsymbol{k}_0-\boldsymbol{k}}\delta_{ss'}] \\
&-\boldsymbol{\mu}_{l,i}\cdot\boldsymbol{u}_{\boldsymbol{ks}}(r_{l,i})S^+_{l,i}e^{i\omega_i t}\boldsymbol{\mu}^*_{m,j}\cdot\boldsymbol{u}^*_{\boldsymbol{k's'}}(r_{m,j})S^-_{m,j}e^{-i\omega_j(t-\tau)}e^{-i\omega_{\boldsymbol{k's'}}\tau}\cosh^2 r\delta_{\boldsymbol{kk'}}\delta_{ss'} \\
&-\boldsymbol{\mu}^*_{l,i}\cdot\boldsymbol{u}_{\boldsymbol{ks}}(r_{l,i})S^-_{l,i}e^{-i\omega_i t}\boldsymbol{\mu}_{m,j}\cdot\boldsymbol{u}^*_{\boldsymbol{k's'}}(r_{m,j})S^+_{m,j}e^{i\omega_j(t-\tau)}e^{-i\omega_{\boldsymbol{k's'}}\tau}\cosh^2 r\delta_{\boldsymbol{kk'}}\delta_{ss'} \\
&-\boldsymbol{\mu}^*_{l,i}\cdot\boldsymbol{u}^*_{\boldsymbol{ks}}(r_{l,i})S^-_{l,i}e^{-i\omega_i t}\boldsymbol{\mu}_{m,j}\cdot\boldsymbol{u}_{\boldsymbol{k's'}}(r_{m,j})S^+_{m,j}e^{i\omega_j(t-\tau)}e^{i\omega_{\boldsymbol{k's'}}\tau}\sinh^2 r\delta_{\boldsymbol{kk'}}\delta_{ss'} \\
&-\boldsymbol{\mu}_{l,i}\cdot\boldsymbol{u}^*_{\boldsymbol{ks}}(r_{l,i})S^+_{l,i}e^{i\omega_i t}\boldsymbol{\mu}^*_{m,j}\cdot\boldsymbol{u}_{\boldsymbol{k's'}}(r_{m,j})S^-_{m,j}e^{-i\omega_j(t-\tau)}e^{i\omega_{\boldsymbol{k's'}}\tau}\sinh^2 r\delta_{\boldsymbol{kk'}}\delta_{ss'} \\
&+\boldsymbol{\mu}^*_{l,i}\cdot\boldsymbol{u}^*_{\boldsymbol{ks}}(r_{l,i})S^-_{l,i}e^{-i\omega_i t}\boldsymbol{\mu}^*_{m,j}\cdot\boldsymbol{u}^*_{\boldsymbol{k's'}}(r_{m,j})S^-_{m,j}e^{-i\omega_j(t-\tau)}e^{i(\omega_{\boldsymbol{ks}}+\omega_{\boldsymbol{k's'}})t-i\omega_{\boldsymbol{k's'}}\tau} \\
&\quad\times[-M\delta_{\boldsymbol{k'},2\boldsymbol{k}_0-\boldsymbol{k}}\delta_{ss'}]\}\rho^S(t-\tau)
\end{aligned}
\tag{3.46}
$$

where l, m are used for labeling different atoms, and i, j are used for transitions within an atom. Here we just calculate the first and second term. Since all atoms are identical, $\omega_{l,i} = \omega_i$, $|\boldsymbol{\mu}_{l,i}| = |\boldsymbol{\mu}_i|$, and $r_{l,i} = r_l$ can be used to simplify Eq. (3.46). For simplicity, we define μ_j to be the

projection of $\boldsymbol{\mu_j}$ on the x axis. For the second term(thermal term), we have

$$
\begin{aligned}
&-\sum_{k_z}\int_0^t d\tau \boldsymbol{\mu}_{l,i}\cdot\boldsymbol{u}_{\boldsymbol{k}s}(r_l)S^+_{l,i}e^{i\omega_i t}\boldsymbol{\mu}^*_{m,j}\cdot\boldsymbol{u}^*_{\boldsymbol{k}'s'}(r_m)S^-_{m,j}e^{-i\omega_j(t-\tau)}e^{-i\omega_{\boldsymbol{k}'s'}\tau}\cosh^2 r\rho^S(t-\tau)\delta_{\boldsymbol{k}\boldsymbol{k}'}\delta_{ss'}\\
=&-\frac{L}{2\pi}e^{i(\omega_i-\omega_j)t}\int_{-\infty}^{\infty}dk_z\int_0^t d\tau e^{i\omega_j\tau}e^{-i\omega_{k_z}\tau}\frac{\omega_k\mu_i\mu_j}{\epsilon_0 LS\hbar}e^{ik_z(r_l-r_m)}\cosh^2 rS^+_{l,i}S^-_{m,j}\rho^S(t-\tau)\\
\approx&-\frac{L}{2\pi}e^{i(\omega_i-\omega_j)t}\int_0^{\infty}dk_z\int_0^t d\tau e^{i\omega_j\tau}e^{-i[\omega_j+c^2k_{jz}(k_z-k_{jz})/\omega_j]\tau}\frac{\omega_k\mu_i\mu_j}{\epsilon_0 LS\hbar}\\
&\times[e^{ik_z(r_l-r_m)}+e^{-ik_z(r_l-r_m)}]\cosh^2 rS^+_{l,i}S^-_{m,j}\rho^S(t-\tau)\\
\approx&-\frac{L}{2\pi}e^{i(\omega_i-\omega_j)t}\int_{-k_{0z}}^{\infty}d\delta k_z\int_0^t d\tau e^{-i\tau c^2k_{jz}\delta k_z/\omega_j}\frac{\omega_k\mu_i\mu_j}{\epsilon_0 LS\hbar}\\
&\times[e^{i(k_{jz}+\delta k_z)(r_l-r_m)}+e^{-i(k_{jz}+\delta k_z)(r_l-r_m)}]\cosh^2 rS^+_{l,i}S^-_{m,j}\rho^S(t-\tau)\\
\approx&-\frac{L}{2\pi}e^{i(\omega_i-\omega_j)t}\int_{-\infty}^{\infty}d\delta k_z\int_0^t d\tau e^{-i(c^2k_{jz}\delta k_z/\omega_j)\tau}\frac{\omega_k\mu_i\mu_j}{\epsilon_0 LS\hbar}\\
&\times[e^{i(k_{jz}+\delta k_z)(r_l-r_m)}+e^{-i(k_{jz}+\delta k_z)(r_l-r_m)}]\cosh^2 rS^+_{l,i}S^-_{m,j}\rho^S(t-\tau)\\
\approx&-\frac{L}{2\pi}e^{i(\omega_i-\omega_j)t}\int_0^t d\tau\frac{\omega_j\mu_i\mu_j}{\epsilon_0 LS\hbar}2\pi[e^{ik_{jz}(r_l-r_m)}\delta((r_l-r_m)-\frac{c^2k_{jz}}{\omega_0}\tau)+e^{-ik_{jz}(r_l-r_m)}\delta((r_l-r_m)+\frac{c^2k_{jz}}{\omega_0}\tau)]\\
&\times\cosh^2 rS^+_{l,i}S^-_{m,j}\rho^S(t-\tau)\\
\approx&-\frac{L}{2\pi}e^{ik_{jz}r_{lm}}\frac{\omega_j\mu_i\mu_j}{\epsilon_0 LS\hbar}2\pi\frac{\omega_j}{c^2k_{0z}}\cosh^2 rS^+_{l,i}S^-_{m,j}\rho^S(t)e^{i(\omega_i-\omega_j)t}\\
\approx&-[\frac{\sqrt{\gamma_i\gamma_j}}{2}\cos(k_{0z}r_{lm})+i\frac{\sqrt{\gamma_i\gamma_j}}{2}sin(k_{0z}r_{lm})]\cosh^2 rS^+_{l,i}S^-_{m,j}\rho^S(t)e^{i(\omega_i-\omega_j)t}
\end{aligned}
\tag{3.47}
$$

where emitter separation $r_{lm}=|r_l-r_m|$, collective decay rate $\gamma_i=2\mu_i^2\omega_i^2/\hbar\epsilon_0 Sc^2k_{iz}$, and collective energy shift $\Lambda_{ij}=\sqrt{\gamma_i\gamma_j}\sin(k_{0z}r_{ij})/2$. In the third line we expand $\omega_k=c\sqrt{(\frac{\pi}{a})^2+(k_z)^2}$ around $k_z=k_{0z}$ since resonant modes provide dominant contributions. In the fifth line we extend the integration $\int_{-k_{jz}}^{\infty}dk_z\rightarrow\int_{-\infty}^{\infty}dk_z$ because the main contribution comes from the components around $\delta k_z=0$. In the next line, Weisskopf-Wigner approximation is used.

Next we need to calculate the first term (squeezing term) in Eq. (3.46), putting aside the overall

factor $e^{i(\omega_i+\omega_j-2\omega_0)t}$, we have:

$$
\begin{aligned}
&\sum_{k_z}\int_0^t d\tau\{\boldsymbol{\mu}_{l,i}\cdot\boldsymbol{u}_{2\boldsymbol{k}_0-\boldsymbol{k}}(r_l)S^+_{l,i}\boldsymbol{\mu}_{m,j}\cdot\boldsymbol{u}_{\boldsymbol{k}}(r_m)S^+_{m,j}e^{i(\omega_{\boldsymbol{k}}-\omega_j)\tau}(-M)\rho^S(t-\tau)\\
=&-\frac{L}{2\pi}\int_0^{2k_{0z}}dk_z\int_0^t d\tau e^{i(\omega_{k_z}-\omega_j)\tau}e^{i(2k_{jz}-k_z)(r_l-o_1)}e^{ik_z(r_m-o_1)}\frac{\sqrt{\omega_{k_z}\omega_{2k_{0z}-k_z}}\mu_i\mu_j}{\epsilon_0LS\hbar}MS^+_{l,i}S^+_{m,j}\rho^S(t-\tau)\\
&-\frac{L}{2\pi}\int_{-2k_{0z}}^0dk_z\int_0^t d\tau e^{i(\omega_{k_z}-\omega_j)\tau}e^{i(-2k_{jz}-k_z)(r_l-o_2)}e^{ik_z(r_m-o_2)}\frac{\sqrt{\omega_{k_z}\omega_{-2k_{0z}-k_z}}\mu_i\mu_j}{\epsilon_0LS\hbar}MS^+_{l,i}S^+_{m,j}\rho^S(t-\tau)
\end{aligned}
\tag{3.48}
$$

For terms with $r_l=r_j$, Eq. (5.8) reduces to

$$
\begin{aligned}
&\sum_{k_z}\int_0^t d\tau\{\boldsymbol{\mu}_{l,i}\cdot\boldsymbol{u}_{2\boldsymbol{k}_0-\boldsymbol{k}}(r_l)S^+_{l,i}\boldsymbol{\mu}_{l,j}\cdot\boldsymbol{u}_{\boldsymbol{k}}(r_l)S^+_{l,j}e^{i(\omega_{\boldsymbol{k}}-\omega_j)\tau}(-M)\rho^S(t-\tau)\\
=&-\frac{L}{2\pi}\int_0^{2k_{0z}}dk_z\int_0^t d\tau e^{i\frac{c^2k_{jz}}{\omega_j}(k_z-k_{jz})\tau}e^{i2k_{0z}(r_l-o_1)}\frac{\sqrt{\omega_{k_z}\omega_{2k_{0z}-k_z}}\mu_i\mu_j}{\epsilon_0LS\hbar}MS^+_{l,i}S^+_{l,j}\rho^S(t-\tau)\\
&-\frac{L}{2\pi}\int_{-2k_{0z}}^0dk_z\int_0^t d\tau e^{i\frac{c^2k_{jz}}{\omega_j}(k_z-k_{jz})\tau}e^{-i2k_{0z}(r_l-o_2)}\frac{\sqrt{\omega_{k_z}\omega_{-2k_{0z}-k_z}}\mu_i\mu_j}{\epsilon_0LS\hbar}MS^+_{l,i}S^+_{l,j}\rho^S(t-\tau)\\
=&-\frac{L}{2\pi}[e^{i2k_{0z}(r_l-o_1)}+e^{-i2k_{0z}(r_l-o_2)}]\frac{\sqrt{\omega_i\omega_j}\mu_i\mu_j}{\epsilon_0LS\hbar}\int_0^t d\tau 2\pi\delta(\frac{c^2k_{jz}}{\omega_j}\tau)MS^+_{l,i}S^+_{l,j}\rho^S(t-\tau)\\
=&-e^{i2k_{jz}R}\frac{\omega_0^2\mu_i\mu_j}{\epsilon_0\hbar Sc^2k_{0z}}\cos(2k_{0z}r_l)MS^+_{l,i}S^+_{l,j}\rho^S(t)\\
=&-e^{i2k_{0z}R}\frac{\sqrt{\gamma_i\gamma_j}}{2}\cos(2k_{0z}r_l)MS^+_{l,i}S^+_{l,j}\rho^S(t)
\end{aligned}
\tag{3.49}
$$

where we have used the fact that the origin of coordinate system is at equal distant from two sources(i.e., $o_2=-o_1=R$) in the second last line. Incorporating index l into i, we have $\gamma'_{ij}=$

$\sqrt{\gamma_i\gamma_j}\cos(2k_{0z}r_i)$. For $r_i \neq r_j$, Eq. (5.8) reduces to

$$
\begin{aligned}
&\sum_{k_z}\int_0^t d\tau\{\boldsymbol{\mu}_{l,i}\cdot\boldsymbol{u}_{2\boldsymbol{k}_0-\boldsymbol{k}}(r_l)S^+_{l,i}\boldsymbol{\mu}_{m,j}\cdot\boldsymbol{u}_{\boldsymbol{k}}(r_m)S^+_{m,j}e^{i(\omega_{\boldsymbol{k}}-\omega_j)\tau}(-M)\rho^S(t-\tau)\\
=&-\frac{L}{2\pi}\int_0^{2k_{0z}}dk_z\int_0^t d\tau e^{i\frac{c^2k_{jz}}{\omega_j}(k_z-k_{jz})\tau}e^{i2k_{0z}(r_c-o_1)}e^{-i(k_z-k_{0z})(r_l-r_m)}\\
&\times\frac{\sqrt{\omega_{k_z}\omega_{2k_{0z}-k_z}}\mu_i\mu_j}{\epsilon_0LS\hbar}MS^+_{l,i}S^+_{m,j}\rho^S(t-\tau)\\
&-\frac{L}{2\pi}\int_{-2k_{0z}}^0dk_z\int_0^t d\tau e^{i\frac{c^2k_{jz}}{\omega_j}(-k_z-k_{jz})\tau}e^{-i2k_{0z}(r_c-o_2)}e^{-i(k_z+k_{0z})(r_l-r_m)}\\
&\times\frac{\sqrt{\omega_{k_z}\omega_{-2k_{0z}-k_z}}\mu_i\mu_j}{\epsilon_0LS\hbar}MS^+_{l,i}S^+_{m,j}\rho^S(t-\tau)\\
=&-\frac{L}{2\pi}e^{i2k_{0z}(r_c-o_1)}\frac{\sqrt{\omega_i\omega_j}\mu_i\mu_j}{\epsilon_0LS\hbar}\int_{-\infty}^{\infty}dk_z\int_0^t d\tau e^{i\frac{c^2k_{jz}}{\omega_j}(k_z-k_{jz})\tau}e^{-i(k_z-k_{0z})(r_l-r_m)}\\
&\times MS^+_{l,i}S^+_{m,j}\rho^S(t-\tau)\\
&-\frac{L}{2\pi}e^{-i2k_{0z}(r_c-o_2)}\frac{\sqrt{\omega_i\omega_j}\mu_i\mu_j}{\epsilon_0LS\hbar}\int_{-\infty}^{\infty}dk_z\int_0^t d\tau e^{i\frac{c^2k_{jz}}{\omega_j}(k_z-k_{jz})\tau}e^{i(k_z-k_{0z})(r_l-r_m)}\\
&\times MS^+_{l,i}S^+_{m,j}\rho^S(t-\tau)\\
\approx&-\frac{L}{2\pi}e^{i2k_{0z}R}\frac{\omega_0^2\mu_i\mu_j}{\epsilon_0LS\hbar}\int_0^t d\tau 2\pi[e^{i2k_{0z}r_c}\delta(r_l-r_m-\frac{c^2k_{0z}}{\omega_0}\tau)+e^{-i2k_{0z}r_c}\delta(r_l-r_m+\frac{c^2k_{0z}}{\omega_0}\tau)]\\
&\times MS^+_{l,i}S^+_{m,j}\rho^S(t-\tau)\\
\approx&-e^{i2k_{0z}R}\frac{\omega_0^2\mu_i\mu_j}{\epsilon_0\hbar Sc^2k_{0z}}e^{i2k_{0z}r_csgn(r_l-r_m)}S^+_{l,i}S^+_{m,j}\rho^S(t)\\
\to&-\frac{\sqrt{\gamma_i\gamma_j}}{2}e^{i2k_{0z}R}\cos(k_{0z}(r_l+r_m))S^+_{l,i}S^+_{m,j}\rho^S(t)
\end{aligned}
\tag{3.50}
$$

where $sgn(r_l-r_m)$ is the sign function. The last arrow is because we need to sum over i,j, so the imaginary part of $e^{i2k_{0z}r_csgn(i-j)}$ vanishes, so the neat result is that $\gamma'_{ijkl}=e^{i2k_{0z}R}\sqrt{\gamma_j\gamma_l}\cos(k_{0z}(r_i+r_k))$. As for $S_i^+\rho^S(t)S_j^+$ terms, the combination of the last two terms in Eq. (3.11) makes the imaginary part of $e^{i2k_{0z}r_csgn(r_l-r_m)}$ vanish. Doing similar calculations for the remaining terms, we

have the master equation

$$\begin{aligned}\frac{d\rho^S}{dt} =& -i\sum_{ijkl}\Lambda_{ijkl}[S^+_{i,j}S^-_{k.l},\rho^S]e^{i(\omega_j-\omega_l)t}\\ &-\frac{1}{2}\sum_{ijkl}\gamma_{ijkl}(1+N)(\rho^S S^+_{i,j}S^-_{k.l}+S^+_{i,j}S^-_{k.l}\rho^S-2S^-_{k.l}\rho^S S^+_{i,j})e^{i(\omega_j-\omega_l)t}\\ &-\frac{1}{2}\sum_{ijkl}\gamma_{ijkl}N(\rho^S S^-_{i,j}S^+_{k.l}+S^-_{i,j}S^+_{k,l}\rho^S-2S^+_{k,l}\rho^S S^-_{i,j})e^{-i(\omega_j-\omega_l)t}\\ &-\frac{1}{2}\sum_{\alpha=\pm}\sum_{ijkl}\gamma'_{ijkl}Me^{2\alpha ik_{0z}R}e^{i\alpha(\omega_j+\omega_l-2\omega_0)t}(\rho^S S^\alpha_{i,j}S^\alpha_{k.l}+S^\alpha_{i,j}S^\alpha_{k,l}\rho^S-2S^\alpha_{k,l}\rho^S S^\alpha_{i,j})\end{aligned} \tag{3.51}$$

with

$$\begin{aligned}\gamma_{ijkl} &= \sqrt{\gamma_j\gamma_l}\cos(k_{0z}r_{ik})\\ \Lambda_{ijkl} &= \frac{\sqrt{\gamma_j\gamma_l}}{2}\sin(k_{0z}r_{ik})\\ \gamma'_{ijkl} &= \sqrt{\gamma_j\gamma_l}\cos[k_{0z}(r_i+r_k)]\end{aligned} \tag{3.52}$$

The above equation reduces to Eq. (3.25) when $l=0$ indicating that the atom can be treated as a qubit.

4. THE STEADY STATE PROPERTIES OF ATOMS IN THE SQUEEZED VACUUM[1]

It is worth noting that in our scheme, the squeezed vacuum reservoir is not affected by the atomic behaviors because of there are a great number of modes in the reservoir. What's more, the squeezed vacuum is pumped into the waveguide endlessly so that the effects left by the atoms will be erased eventually. Therefore, the behaviors of the steady state of the atoms in the squeezed vacuum are expected to be quite different from those in the ordinary vacuum or thermal reservoir. In this section, we will study the properties of the steady state with different atomic structures.

4.1 Quantum entanglement of two qubits

Quantum entanglement is an important resource of the quantum information and quantum metrology [47, 48]. Preparation of the maximum entangled state is still a central topic of interest. It has been shown that stationary quantum entanglement can be dissipatively prepared by engineering the bath enviroment [49, 50, 51, 52]. By squeezing the enviroment, quantum entanglement between emitters can be also created [53, 34, 35]. However, it is shown in Ref. [34] that stationary maximum entanglement can not be reached by the squeezed vacuum for identical emitters. Here, we show that identical emitters coupled to the 1D waveguide can also be driven to a stationary maximum entangled NOON state by the squeezed vacuum as long as the center of mass is put at the proper position.

The quantum entanglement can be measured by the concurrence which is defined as [54]: $\mathscr{C} \equiv max\{0, \lambda_1 - \lambda_2 - \lambda_3 - \lambda_4\}$ in which $\lambda_1, \lambda_2, \lambda_3, \lambda_4$ are eigenvalues, in decreasing order, of the Hermitian matrix $R = \sqrt{\sqrt{\rho}\widetilde{\rho}\sqrt{\rho}}$ with $\widetilde{\rho} = (\sigma_y \bigotimes \sigma_y)\rho^*(\sigma_y \bigotimes \sigma_y)$. For a pure two-qubit state $|\Psi\rangle = \alpha|ee\rangle + \beta|eg\rangle + \gamma|ge\rangle + |gg\rangle$ with $|\alpha|^2 + |\beta|^2 + |\gamma|^2 + |\delta|^2 = 1$, the concurrence is given by $\mathscr{C} = max\{0, 2|\alpha\delta - \beta\gamma|\}$. According to the master equation Eq. (3.25) describing qubits in the waveguide, the concurrence of two qubits as a function of time for different initial states can

[1]Part of this section is reprinted with permission from: "Waveguide QED in the Squeezed Vacuum" by Jieyu You et al, 2018. Physical Review A, 97, 023810, Copyright 2018 by the American Physical Society and "Steady-state population inversion of multiple Ks-type atoms by the squeezed vacuum in a waveguide" by Jieyu You, Zeyang Liao, and M. Suhail Zubairy, 2019. Physical Review A, 100, 013843, Copyright 2019 by the American Physical Society.

be calculated, which is shown in Fig. 4.1(a) where $r = 1, r_c = 0$, and $r_{12} = 0.25\lambda_{0z}$. Different curves correspond to different initial states. We can see that no matter what the initial state is, the two-emitter state will be driven to a very high entangled state. To see what the stationary state is, we also show the fidelity of the emitter state with respect to the maximum entangled state $\frac{1}{\sqrt{2}}(|gg\rangle - |ee\rangle)$ which is shown in Fig. 4.1(b). We can see that the stationary state is very close to it. Therefore, under these parameters the two emitters can be driven to the maximum entangled state which may find important applications in quantum information and quantum computation.

To find the stationary state analytically, we rewrite the master equation in Eq. (3.25) as

$$\begin{aligned}
\dot{\rho}_{gg} &= -2N\gamma\rho_{gg} + (N+1)\gamma_+\rho_{++} + (N+1)\gamma_-\rho_{--} \\
&\quad + M\gamma_{12}^{'}\rho_u, \qquad (4.1) \\
\dot{\rho}_{ee} &= -2(N+1)\gamma\rho_{ee} + N\gamma_+\rho_{++} + N\gamma_-\rho_{--} \\
&\quad + M\gamma_{12}^{'}\rho_u, \qquad (4.2) \\
\dot{\rho}_{++} &= -(2N+1)\gamma_+\rho_{++} + (N+1)\gamma_+\rho_{ee} + N\gamma_+\rho_{gg} \\
&\quad - M\gamma_{+}^{'}\rho_u, \qquad (4.3) \\
\dot{\rho}_{--} &= -(2N+1)\gamma_-\rho_{--} + (N+1)\gamma_-\rho_{ee} + N\gamma_-\rho_{gg} \\
&\quad - M\gamma_{-}^{'}\rho_u. \qquad (4.4) \\
\dot{\rho}_u &= -(2N+1)\gamma_{11}\rho_u - 2M\gamma_{+}^{'}\rho_{++} - 2M\gamma_{-}^{'}\rho_{--} \\
&\quad + 2M\gamma_{12}^{'}(\rho_{ee} + \rho_{gg}). \qquad (4.5)
\end{aligned}$$

where $\rho_{ee} = \langle ee|\rho|ee\rangle$, $\rho_{gg} = \langle gg|\rho|gg\rangle$, $\rho_{\pm\pm} = \langle \pm|\rho|\pm\rangle$ with $|\pm\rangle = \frac{1}{\sqrt{2}}(|e_1\rangle|g_2\rangle \pm |g_1\rangle|e_2\rangle)$, $\rho_u = e^{-2ik_{0z}R}\langle ee|\rho|gg\rangle + e^{2ik_{0z}R}\langle gg|\rho|ee\rangle$, and $\gamma = \gamma_{1d}$, $\gamma_\pm = \gamma_{1d}(1 \pm \cos(k_{0z}r_{12}))$, $\gamma_{12}^{'} = \gamma_{1d}\cos(2k_{0z}r_c)$, $\gamma_\pm^{'} = \gamma_{1d}\{\cos[2k_{0z}r_c] \pm \frac{1}{2}[\cos(2k_{0z}r_1) + \cos(2k_{0z}r_2)]\}$ with $r_c = \frac{(r_1+r_2)}{2}$. Then the

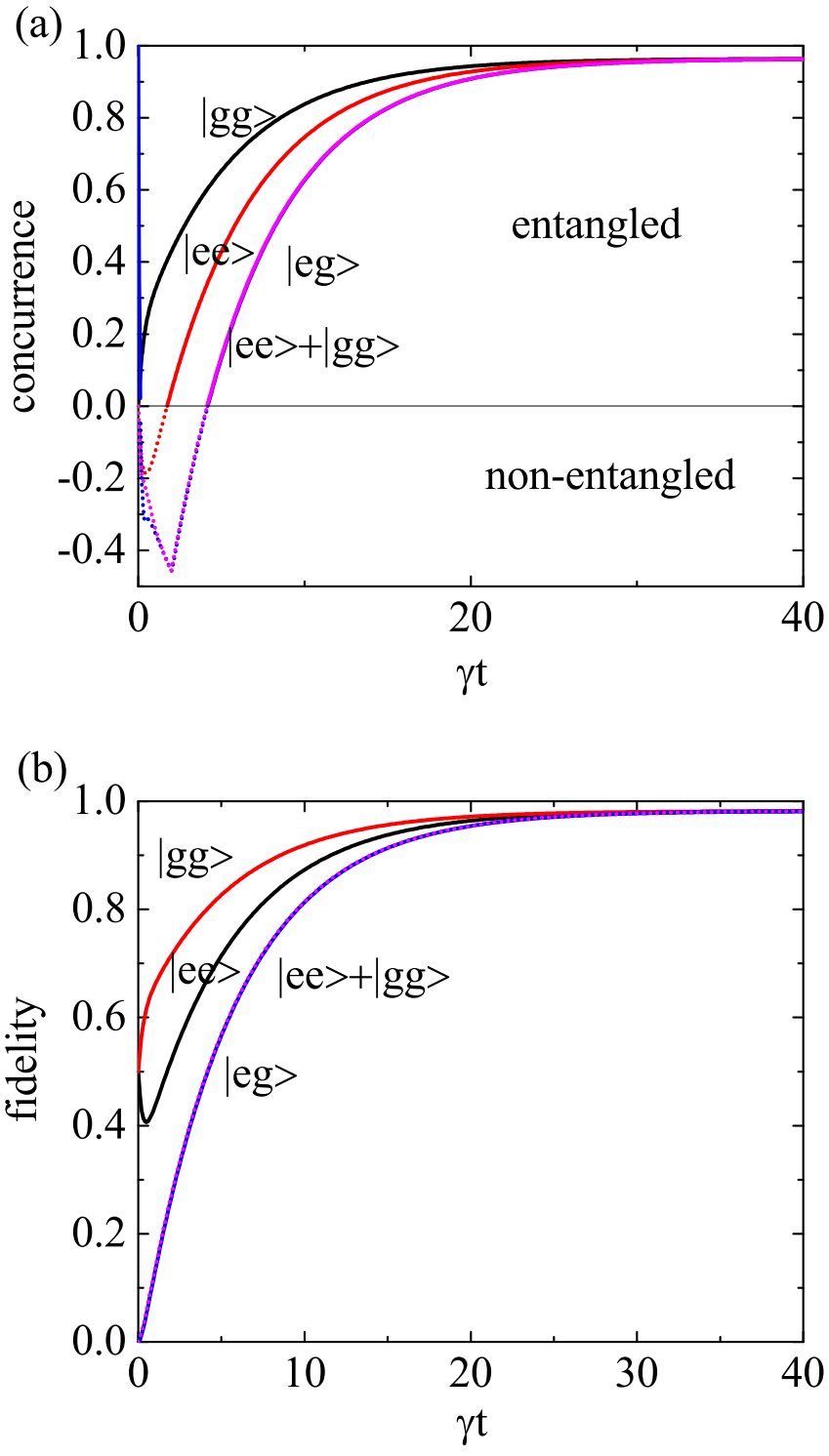

Figure 4.1: (a) Concurrence evolution of different initial states in squeezed vacuum, where $r = 1$, $r_c = 0$, and $r_{12} = 0.25\lambda_{0z}$. (b) Fidelity evolution of different initial states in the same environment.

steady state solutions are given by

$$\begin{aligned}
\rho_{ee} &= \frac{N[-1-N-2N^2+(-1+N+2N^2)\cos(4k_{0z}r_c)]}{2(1+2N)[-1-2N-2N^2+2N(1+N)\cos(4k_{0z}r_c)]} \\
\rho_{++} &= -\frac{N(1+N)sin^2(2k_{0z}r_c)}{-1-2N-2N^2+2N(1+N)\cos(4k_{0z}r_c)} \\
\rho_{--} &= -\frac{N(1+N)sin^2(2k_{0z}r_c)}{-1-2N-2N^2+2N(1+N)\cos(4k_{0z}r_c)} \\
\rho_{u} &= \frac{-2\sqrt{N(1+N)}\cos(2k_{0z}r_c)}{(1+2N)[-1-2N-2N^2+2N(1+N)\cos(4k_{0z}r_c)]}
\end{aligned} \tag{4.6}$$

where we have used the relation $M^2 = N(N+1)$. Obviously, the population given by Eq. (5.16) differs from that given by thermal reservoir: $\rho_{ee(gg)} = \rho^{th}_{ee(gg)} + \Delta\rho, \rho_{++(--)} = \rho^{th}_{++(--)} - \Delta\rho$ with $\Delta\rho = \frac{N(N+1)\cos^2(2k_{0z}r_c)}{(1+2N)^2(1+2N+2N^2-2N(1+N)\cos(4k_{0z}r_c))}$ and $\rho^{th}_{ee} = \frac{N^2}{(1+2N)^2}$, $\rho^{th}_{++} = \rho^{th}_{--} = \frac{N(N+1)}{(1+2N)^2}$, $\rho^{th}_{gg} = \frac{(1+N)^2}{(1+2N)^2}$ which obey the Boltzmann distribution. It is interesting that the steady state depends only on the center of mass but not on the separation between the two emitters. Meanwhile, it is worth noting that the dark state cannot always be reached since the ergodicity cannot be guaranteed under every condition. For example, when $\cos(k_{0z}r_{12}) = 1$, $|+\rangle$ becomes a dark state, while it is $|-\rangle$ when $\cos(k_{0z}r_{12}) = -1$.

Eq. (5.16) shows that as r_c gets closer to $\frac{n}{4}\lambda_{0z}$, the magnitude of $\gamma'_{\pm}$ gets closer to ± 1 which leads to smaller population on $|+\rangle$ and $|-\rangle$ as well as bigger concurrence. When the position of the center mass $r_c = \frac{n}{4}\lambda_{0z}$, the steady states are given by

$$\begin{aligned}
\rho_{gg} &= \frac{N+1}{(1+2N)}, \\
\rho_{ee} &= \frac{N}{(1+2N)}, \\
\rho_{++} &= \rho_{--} = 0, \\
\rho_{u} &= (-1)^{n+1}\frac{2\sqrt{N(1+N)}}{(1+2N)}.
\end{aligned} \tag{4.7}$$

which corresponds to the state $|\Psi_s\rangle = \frac{1}{\sqrt{2N+1}}(\sqrt{N+1}|gg\rangle + (-1)^{n+1}\sqrt{N}|ee\rangle)$. The concurrence of this state is given by $\mathscr{C} = |\rho_u| - (\rho_{++} + \rho_{--}) = \frac{2\sqrt{N(N+1)}}{(2N+1)}$, which monotonically increases

with the average photon number N. When $N \to \infty$, $\mathscr{C} \to 1$ which is a maximum-entangled state $\frac{1}{\sqrt{2}}(|gg\rangle - |ee\rangle)$ ($\frac{1}{\sqrt{2}}(|gg\rangle + |ee\rangle)$) with even(odd) n.

Fig. 4.2(a) shows the dependence of the stationary quantum entanglement on the photon number and the center-of-mass position. It is clearly seen that when r_c is close to $\frac{n}{4}\lambda_{0z}$ the system can be prepared in a high entangled state, while the entanglement can never be formed when $r_c = \frac{2n+1}{8}\lambda_{0z}$ because the dipole-dipole interaction γ'_{12} vanishes. In experiments, the center of mass position of emitters may be hard to control, but it can be effectively controllable by setting the positions squeezing sources. Thus, as long as the pump beam in SPDC is strong enough to guarantee the average photon number of the squeezed vacuum, the emitters can definitely evolve into a NOON state. While the dephasing rate is not very sensitive to the fluctuations of the emitter positions, the stationary quantum entanglement significantly depends on their center of mass. Only when the center of mass position is around $n\lambda/4$, the quantum entanglement is nonzero. In Fig. 4.2(b), we show half the range of center of mass where the quantum entanglement is non-zero. The larger the squeezing is, the more sensitive the quantum entanglement is to the fluctuation of center-of-mass. For example, when $N = 1$, a deviation of about 0.04λ from $n\lambda/4$ will make the entanglement vanish.

4.2 Resonance fluorescence of a group of atoms

In this section, we study how the squeezing can affect the resonance fluorescence of the waveguide-QED system. In the following we study how the collective interaction, squeezing phase, squeezing degree, emitter separation, and the center of mass affect the resonance fluorescence of this system.

The power spectrum of the resonance fluorescence is given by [30, 55, 56]

$$S(\omega) \propto Re \int_0^\infty d\tau Tr[\sigma^-(\tau)\sigma^+(0)]e^{i\omega\tau}. \tag{4.8}$$

where we assume that the detector is perpendicular to the waveguide and $\sigma^\pm = \sigma_1^\pm + \sigma_2^\pm$ for the two-emitter example. The two-time correlation function in the integration can be calculated by

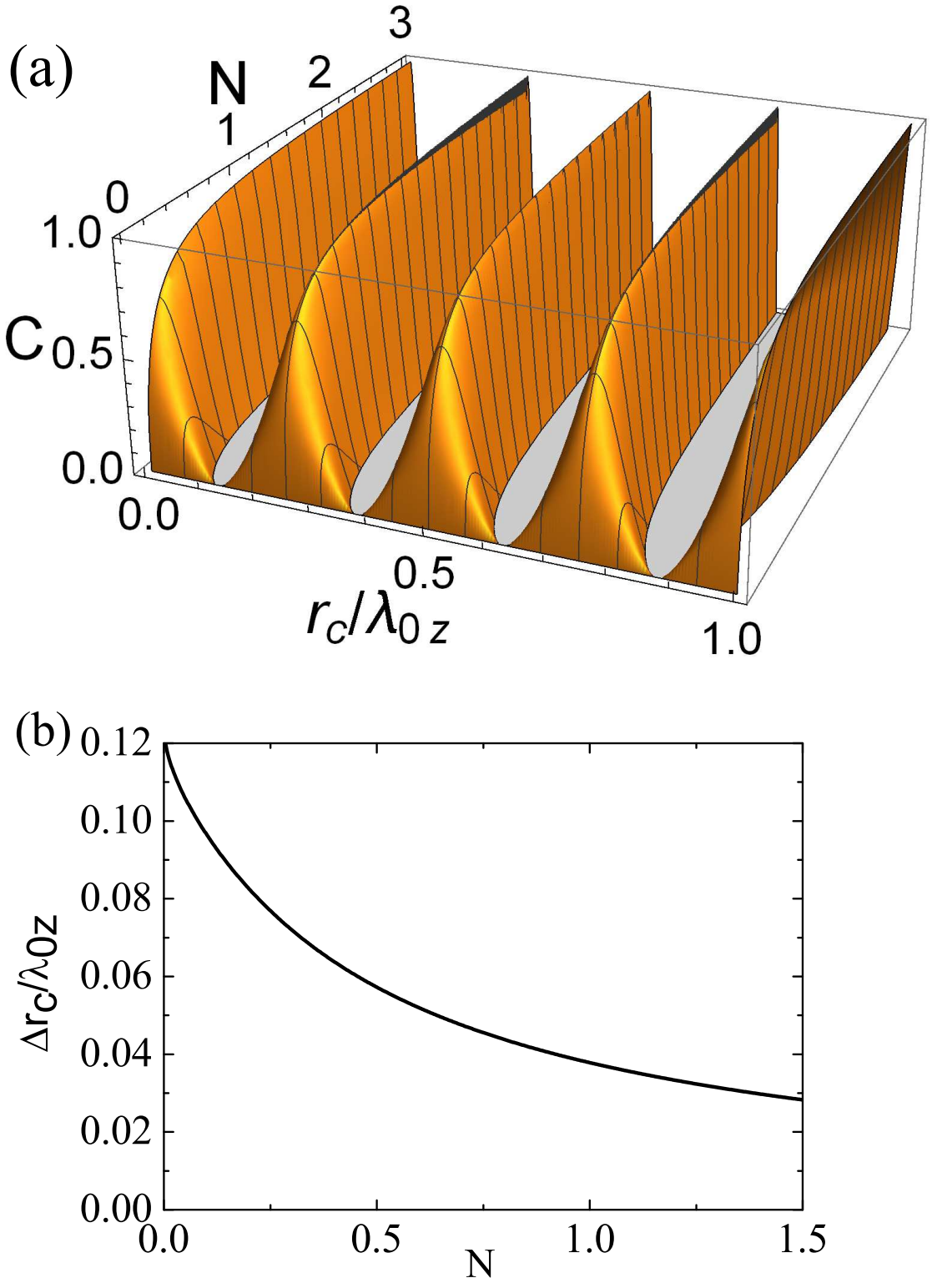

Figure 4.2: (a) Concurrence of the steady state as a function of average photon number $N = \sinh(r)^2$ and the position of the center mass $r_c = \frac{r_1+r_2}{2}$.(b) The impact of r_c's fluctuations on concurrence for different average photon number N. Δr_c is the distance from $\frac{n}{4}\lambda_{0z}$ to the position where the entanglement vanishes.

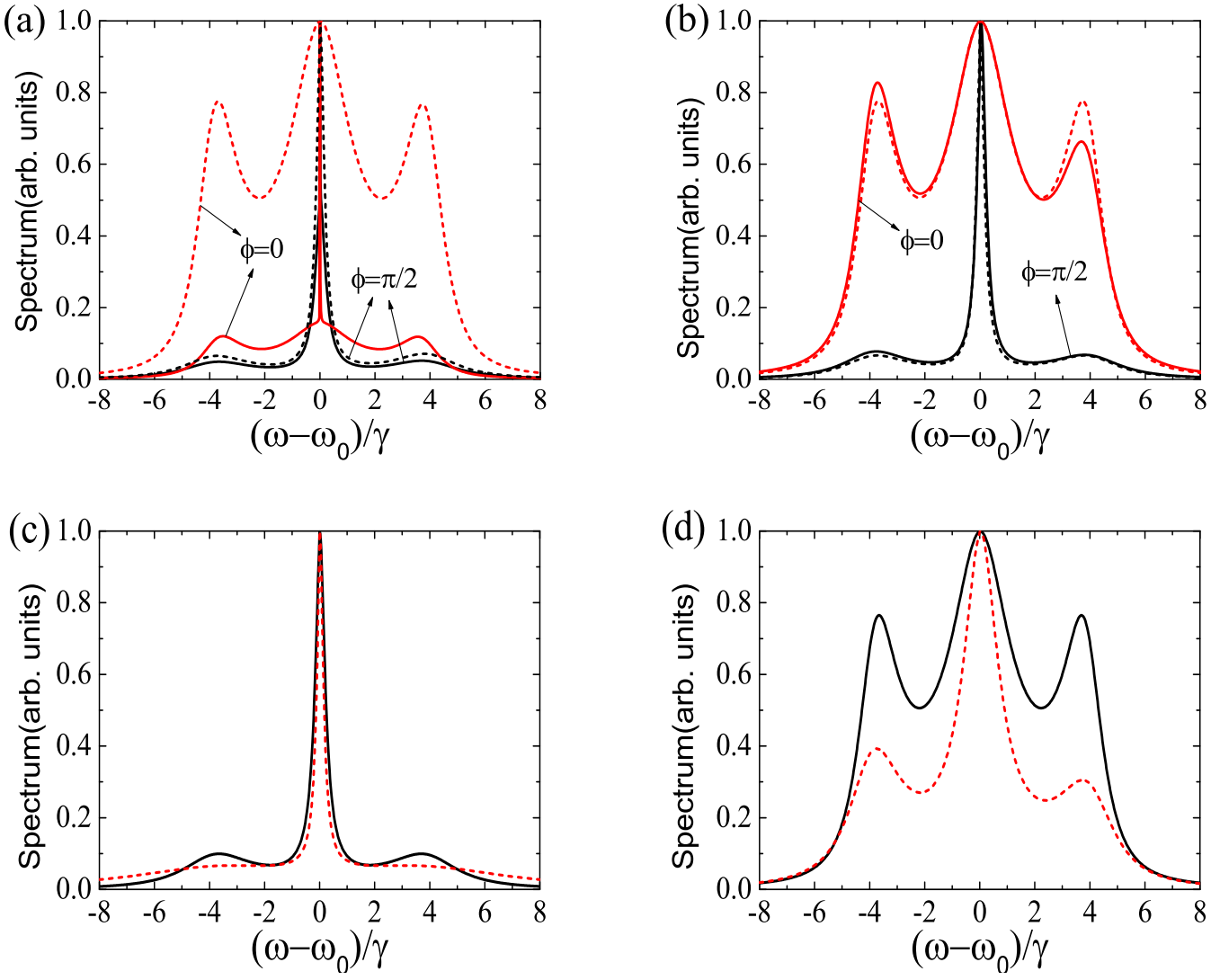

Figure 4.3: Resonance fluorescence spectrum of the two-emitter system inside a 1D waveguide. For better comparison, the spectra are normalized to the intensity at $\omega = \omega_0$ with the coherent elastic scattering singularity removed. Coherent driving Rabi frequency is $\Omega_R = 4\gamma$. In (a) and (b), the solid curves are the spectra for the coupled emitters, while the dashed curves are the spectra without emitter-emitter coupling. Parameters: (a) $r_1 = 0, r_2 = 0.01\lambda_{0z}$, squeezing parameter $r = 0.5$. (b) $r_1 = 0, r_2 = 0.25\lambda_{0z}, r = 0.5$. (c) $r_1 = 0, r_2 = \lambda_{0z}, \phi = \pi/2, r = 0.5$ for black line, $r = 1$ for red line. (d) $r_1 = -0.125\lambda_{0z}, r_2 = 0.125\lambda_{0z}$ for the red line, $r_1 = -0.25\lambda_{0z}, r_2 = 0.25\lambda_{0z}$ for the black line. $\phi = 0, r = 0.5$.

the quantum regression theorem. Usually, the analytical result is difficult to get. However, we can resort to the numerical method to calculate the resonance fluorescence [57].

To observe the resonance fluorescence, we need to apply an external coherent driving field. The master equation is given by

$$\frac{d\rho}{dt} = -i[V, \rho] + \mathcal{L}\rho \tag{4.9}$$

where $\mathcal{L}\rho$ is the right hand side of Eq.(3.25) and $V = \frac{\Omega_R}{2} e^{-i\alpha}(e^{-ik_{0z}r_1}\sigma_1^- + e^{-ik_{0z}r_2}\sigma_2^-) + H.c.$ is the interaction between the driving field and the emitters with Rabi frequency $\Omega_R = \frac{\boldsymbol{d}\cdot\boldsymbol{E}}{\hbar}$. From Eq. (5.19) we can evolve and obtain the steady state of the system ρ_{ss}. Next we use $(\sigma_1^- + \sigma_2^-)\rho_{ss}$ as the initial condition to solve a density matrix $c(t)$ which obeys the same equation of motion as ρ in Eq. (5.19). The resonance fluorescence spectrum is then given by [57]

$$S(\omega) \propto Re \int_0^\infty d\tau Tr[c(\tau)(\sigma_1^+ + \sigma_2^+)]e^{i\omega\tau}. \tag{4.10}$$

In Fig. 4.3(a) and Fig. 4.3(b) we compare the resonance fluorescence spectrum with and without the dipole-dipole interaction for different squeezing phases and emitter separations. When $r_{12} = 0.01\lambda_{0z}$ and $\phi = 0$, we can see that the spectrum is very different with and without dipole-dipole interaction. Without dipole-dipole interaction, the spectrum is very similar to the typical Mollow triplet (red dashed line). However, with dipole-dipole interaction, there is a very narrow peak around the center frequency (red solid line). This is due to the subradiant state induced by the dipole-dipole interaction. On the contrary, when $\phi = \pi/2$ the spectrum with and without the dipole-dipole interaction is very similar (black solid and dashed lines). From Fig. 4.3(b) we see that with dipole-dipole interaction, the spectrum can be asymmetric, i.e., the positive and negative sidebands are different.

In Fig. 4.3(c) we compare the spectrum with different squeezing degrees. We can see that greater squeezing parameter leads to the power spectrum in weak-driving-field limit(sidebands disappear). FIG. 4.3(d) shows that different emitter separation has different spectrum. This is not

only due to atomic interaction which is described by $\gamma_{12}, \gamma'_{12}, \Lambda_{12}$, but also due to their positions which determine the values of γ'_{ii}, i.e., the effective phase and magnitude of M. Comparing the red solid curve in Fig. 4.3(b) and the red dashed curve in Fig. 4.3(d) we can see that different center-of-mass position can also have different resonance fluorescence.

4.3 The steady state population inversion of a single Ξ-type atom by the squeezed vacuum

The concept of population inversion is of fundamental importance in laser physics because the population inversion is a key step of generating laser. However, the population inversion can never exist for a system at thermal equilibrium because of the spontaneous emission. The achievement of population inversion therefore requires pushing the system into a non-equilibrated state [31]. Thus, the spontaneous emission must be inhibited in order to maintain the population inversion in a steady state. In 1993, Ficek and Drummond studied the dynamical properties of a single three-level atom in the squeezed vacuum where they showed that a single three-level atom in the cascade configuration coupled to squeezed modes in a cavity can reach steady state with level population inversion relative to the ordinary laser spectroscopy [37, 38, 39]. In their model, they found a population inversion of about 78%. Here, instead of a cavity, we consider that the case in quasi-one-dimensional waveguide. The dynamic equation can be reduced from Eq. (3.51) with $r_i = r_k$, $r_i = r_j = 0$ and the resonant condition $\omega_1 + \omega_2 = 2\omega_0$. It follows from Eq. (3.51) that various matrix elements satisfy the following equation:

$$\dot{\rho}_{aa} = -\gamma_1 ch^2 \rho_{aa} + \gamma_1 sh^2 \rho_{bb} - \frac{1}{2}\sqrt{\gamma_1\gamma_2} M(\rho_{ac} + \rho_{ca}) \tag{4.11a}$$

$$\begin{aligned}\dot{\rho}_{bb} = {} & \gamma_1(ch^2\rho_{aa} - sh^2\rho_{bb}) + \gamma_2(sh^2\rho_{cc} - ch^2\rho_{bb}) \\ & + \sqrt{\gamma_1\gamma_2} M(\rho_{ac} + \rho_{ca})\end{aligned} \tag{4.11b}$$

$$\dot{\rho}_{cc} = \gamma_2 ch^2 \rho_{bb} - \gamma_2 sh^2 \rho_{cc} - \frac{1}{2}\sqrt{\gamma_1\gamma_2} M(\rho_{ac} + \rho_{ca}) \tag{4.11c}$$

$$\begin{aligned}\Re[\dot{\rho}_{ac}] = {} & -\frac{1}{2}(\gamma_1 ch^2 + \gamma_2 sh^2)\Re[\rho_{ac}] \\ & - \frac{1}{2}\sqrt{\gamma_1\gamma_2} M(\rho_{aa} - 2\rho_{bb} + \rho_{cc})\end{aligned} \tag{4.11d}$$

$$\begin{aligned}\Re[e^{i\delta\omega t}\dot{\rho}_{ba}] = & -\frac{1}{2}\sqrt{\gamma_1\gamma_2}(M-2sh^2)sh\Re[e^{i\delta\omega t}\rho_{bc}] \\ & -\frac{1}{2}((\gamma_1+\gamma_2)ch^2+\gamma_1 sh^2-\gamma_1 M)\Re[e^{i\delta\omega t}\rho_{ba}]\end{aligned} \tag{4.11e}$$

$$\begin{aligned}\Re[e^{i\delta\omega t}\dot{\rho}_{bc}] = & \frac{1}{2}\sqrt{\gamma_1\gamma_2}(2ch^2-M)\Re[(e^{-i\delta\omega t}\rho_{ab}] \\ & -\frac{1}{2}((\gamma_1+\gamma_2)sh^2+\gamma_2 ch^2-2\gamma_2 M)\Re[e^{i\delta\omega t}\rho_{bc}]\end{aligned} \tag{4.11f}$$

where $\Re$ means real part, $ch = \cosh(r)$, $sh = \sinh(r)$, and $\gamma_1 = \gamma_{ab}(\gamma_2 = \gamma_{bc})$ is the decay rate from $|a\rangle$ to $|b\rangle(|b\rangle$ to $|c\rangle)$ in ordinary vacuum due to the waveguide modes. Equations (4.11e) and (4.11f) are for the off-diagonal elements ρ_{ab}, ρ_{bc}. The steady state solution of these two equations is $\rho_{ab} = \rho_{bc} = 0$ because they are homogeneous linear equations. The first four equations Eqs. (4.11a)-(4.11d) also have a steady state solution when they are combined with the normalization condition $\rho_{aa} + \rho_{bb} + \rho_{cc} = 1$. It is also worth noting that Eqs. (4.11a)-(4.11d) are independent of $\delta\omega$, so the difference between ω_{ab} and ω_{bc} does not influence the steady state of the single atom case as long as both ω_{ab} and ω_{bc} are within the squeezing bandwidth. Thus, considering the minimum uncertainty squeezed vacuum where $M = \cosh(r)\sinh(r)$, the steady state solution is:

$$\begin{aligned}\rho_{aa} &= \frac{sh^2\gamma_2}{ch^2\gamma_1+sh^2\gamma_2}, \\ \rho_{cc} &= \frac{ch^2\gamma_1}{ch^2\gamma_1+sh^2\gamma_2}, \\ \rho_{ac} &= \rho_{ca} = -\frac{chsh\sqrt{\gamma_1\gamma_2}}{ch^2\gamma_1+sh^2\gamma_2}, \\ \rho_{bb} &= \rho_{ba} = \rho_{bc} = 0,\end{aligned} \tag{4.12}$$

which is in fact a pure state of a superposition of $|a\rangle$ and $|c\rangle$.

$$|\psi_{ss}\rangle = \frac{sh\sqrt{\gamma_2}}{\sqrt{ch^2\gamma_1+sh^2\gamma_2}}|a\rangle - \frac{ch\sqrt{\gamma_1}}{\sqrt{ch^2\gamma_1+sh^2\gamma_2}}|c\rangle. \tag{4.13}$$

Since there is no population in the state $|b\rangle$, population inversion can always occur between states $|a\rangle$ and $|b\rangle$ in the steady state. If $\tanh r > \sqrt{\frac{\gamma_1}{\gamma_2}}$, population inversion can also occur between the

state $|a\rangle$ and $|c\rangle$. This result is similar to the result in Ref. [39]. However, in our scheme, the population inversion can approach 100% with zero population in the ground state and the middile state if $\gamma_2 \gg \gamma_1$. In comparision, the population inversion in the cavity case shown in Ref. [39] is about of 78%.

The steady state population distribution for different ratios of $\frac{\gamma_{ab}}{\gamma_{bc}}$ is shown in Fig. 4.4(a). The mechanism of this population inversion can be interpreted with the help of Fig. 4.5. In Fig. 4.5 we show that the direct transition between $|a\rangle$, $|b\rangle$, and $|c\rangle$ are allowed just like the thermal reservoir case. However, in the squeezed vacuum, there are additional paths for the population flow: atom in any of these three states can evolve into the other two through an intermediate "state" ρ_{ac}. Although ρ_{ac} is an off-diagonal element rather than a state, it can be used to elucidate our idea. When $\gamma_{ab} \ll \gamma_{bc}$, the transition rate for the $|a\rangle \rightarrow |b\rangle$ transition is negligible compared to γ_{bc} and $\sqrt{\gamma_{ab}\gamma_{bc}}$. Thus the atom in the state $|c\rangle$ can be excited to $|a\rangle$ through $|c\rangle \rightarrow |b\rangle \rightarrow \rho_{ac} \rightarrow |a\rangle$, but $|a\rangle$ can not decay back to $|c\rangle$, which results in the population trapping in the level $|a\rangle$. This phenomenon is similar to the coherent population trapping, but here we achieve the trapping for Ξ structure with the squeezed vacuum reservoir, which cannot be realized with coherent pump due to spontaneous emission. Since it is hard to achieve perfect squeezing with $M = \sqrt{N(N+1)}$ in experiments, we also study the effect of different values of M on the steady state population with parameters $\gamma_{ab} = \frac{1}{4}\gamma_{bc}$ and $r = 1$, which is shown in Fig. 4.4(b). In general, there is population in all three energy levels. Although the steady state population distribution is very sensitive to the value of M, the population inversion between $|a\rangle$ and $|b\rangle$ still holds for $M = 0.8\sqrt{N(N+1)}$. Only when M is larger than 0.95 can the population inversion occur between the state $|a\rangle$ and the state $|c\rangle$.

4.4 The steady state population inversion of multiple Ξ-type atoms by the squeezed vacuum

In the last section, we demonstrated that arbitrary population inversion can occur for a single Ξ-type atom driven by the squeezed vacuum reservoir. However, with Eq. (4.12), this result can not be simply generalized to the multi-atom case since $\gamma'_{ijij} = \sqrt{\gamma_j\gamma_j}\cos[2k_{0z}r_i]$, i.e., different atoms have different γ'_{ijij} for the usual case unless all the atoms are perioidically distributed with period

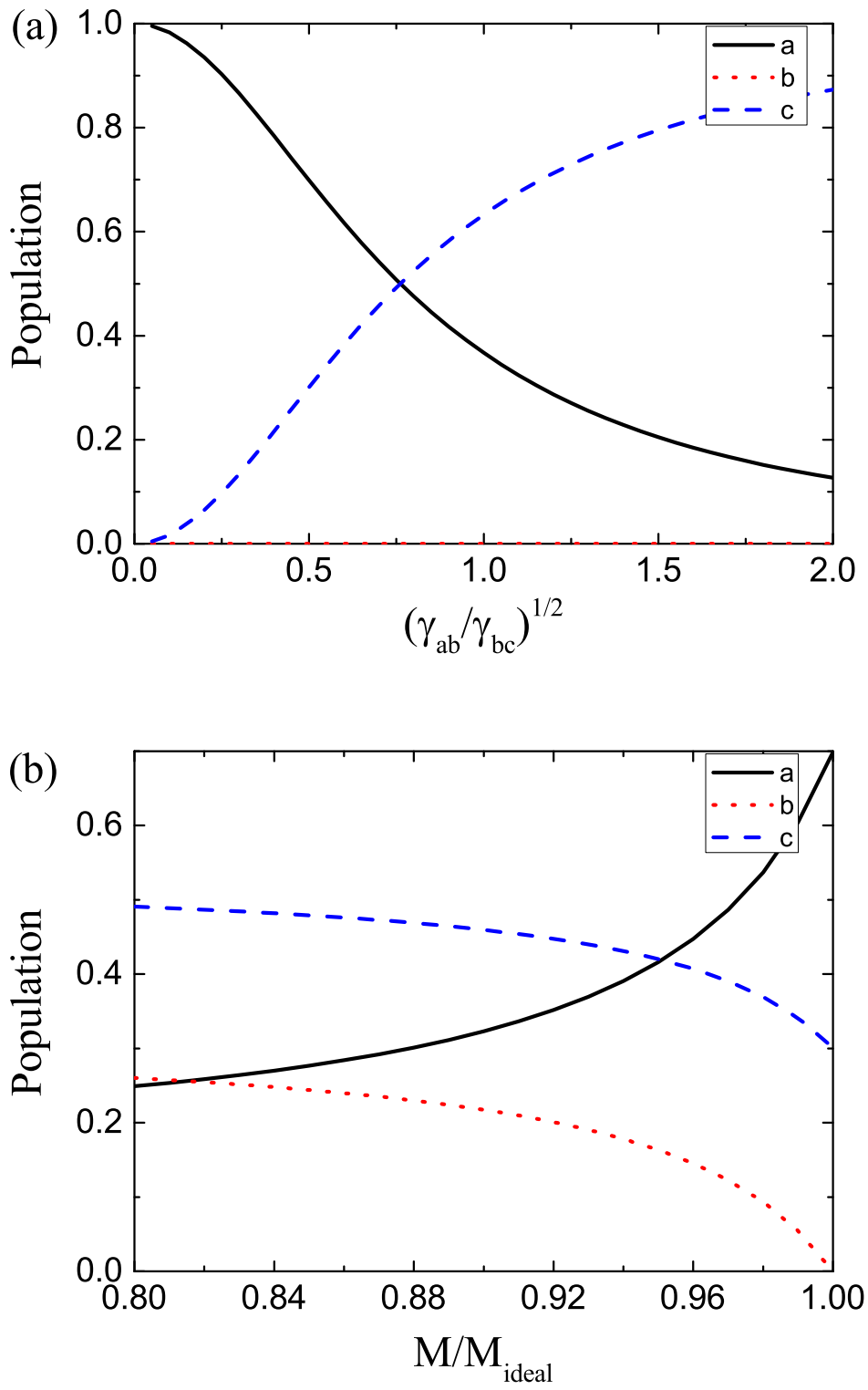

Figure 4.4: (a) The steady state population distribution for different μ_{ab} and μ_{bc}. The squeezing parameter $r = 1$ and the squeezing is perfect ($M = \sqrt{N(N+1)}$). (b) The steady state population distribution for non-ideal squeezed vacuum which is characterized by the ratio of M and $\sqrt{N(N+1)}$. The squeezing parameter $r = 1$, and $\gamma_{ab} = \frac{1}{4}\gamma_{bc}$.

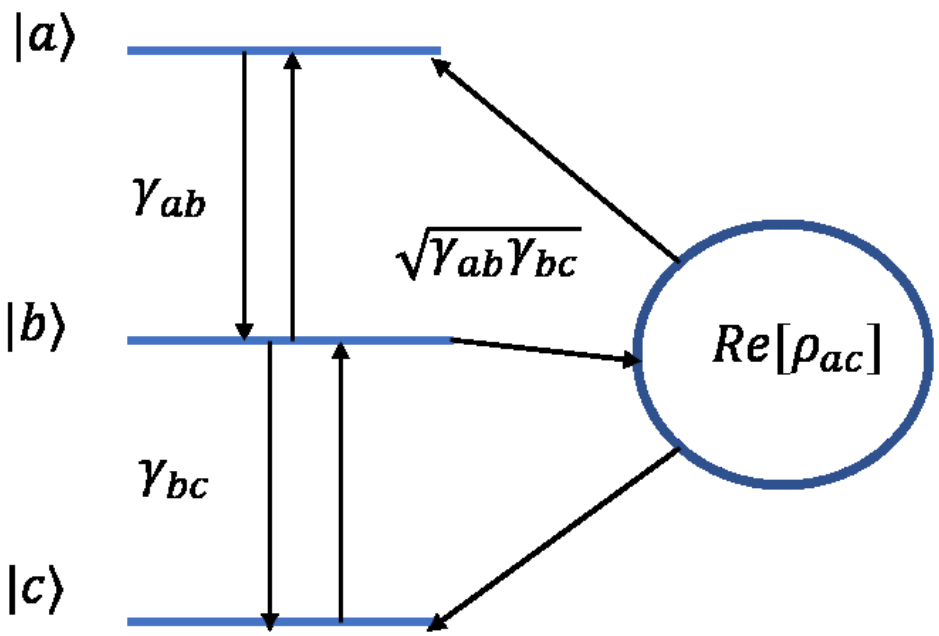

Figure 4.5: The allowed population flow in the squeezed vacuum.

$n\lambda/2$. The squeezing term in Eq. (3.51) vanishes for atoms located around $r_i = \frac{\pi}{4k_{0z}} + \frac{n\pi}{2k_{0z}}$. Thus, for a group of randomly located atoms, if we want to achieve steady state population inversion in the squeezed vacuum, we need to modify our scheme. Here we consider the following correlation functions:

$$\begin{aligned}
\left\langle a^{\dagger}_{\boldsymbol{k},s} a_{\boldsymbol{k}',s'} \right\rangle &= \sinh^2 r \delta_{\boldsymbol{k}'\boldsymbol{k}} \delta_{ss'} \\
\left\langle a_{\boldsymbol{k},s} a^{\dagger}_{\boldsymbol{k}',s'} \right\rangle &= \cosh^2 r \delta_{\boldsymbol{k}'\boldsymbol{k}} \delta_{ss'} \\
\left\langle a^{\dagger}_{\boldsymbol{k},s} a^{\dagger}_{\boldsymbol{k}',s'} \right\rangle &= -e^{-i\theta} \cosh(r) \sinh(r) \delta_{\boldsymbol{k}',-(2\boldsymbol{k}_0-\boldsymbol{k})} \delta_{ss'} \\
\langle a_{\boldsymbol{k},s} a_{\boldsymbol{k}',s'} \rangle &= -e^{i\theta} \cosh(r) \sinh(r) \delta_{\boldsymbol{k}',-(2\boldsymbol{k}_0-\boldsymbol{k})} \delta_{ss'}
\end{aligned} \tag{4.14}$$

which indicates that the photons are entangled with those from the opposite direction. In principle, we can split the squeezed vacuum into two beams by a trianglar prism and inject them into opposite

ends of the waveguide. Then the coefficients in the master equation shown in Eq. (3.51) become

$$\begin{aligned}
\gamma_{ijkl} &= \sqrt{\gamma_i\gamma_k}\cos(k_{0z}r_{jl}),\\
\Lambda_{ijkl} &= \frac{\sqrt{\gamma_i\gamma_k}}{2}\sin(k_{0z}r_{jl}),\\
\gamma'_{ijkl} &= \sqrt{\gamma_i\gamma_k}\cos(k_{0z}r_{jl}).
\end{aligned} \tag{4.15}$$

We can see that γ'_{ijij} is now independent of the atomic position because $r_{jj} = 0$. The resulting master equation is the traditionally studied master equation for atoms in squeezed reservoir [34]. The detailed derivation of these coefficients will be derived later. Based on the master equation in Eq. (3.25) with coefficients given by above, we can show that a single atom can reach population inversion anywhere in the waveguide. When there are multiple atoms in the waveguide where the dipole-dipole interaction should be considered, our calculation shows that the population inversion can still occur for all the atoms. In fact, it is very interesting that the final state of the multiple-atom case is just the direct product of the steady state of independent atoms despite of the dipole-dipole interaction. This result can be proved by the mathematical induction.

Considering the fact that $|\omega_1 - \omega_2| \gg \gamma_i$, it is reasonable to apply the secular approximation on Eq. (3.51) such that those terms with $e^{\pm i(\omega_1-\omega_2)t}$ and $e^{\pm i(2\omega_i-2\omega_0)t}$ are dropped and the master equation is then given by

$$\begin{aligned}
\frac{d\rho^S}{dt} =& -i\sum_{i,k,j}\Lambda_{ijkl}[S^+_{i,j}S^-_{k.j},\rho^S]\\
&-\frac{1}{2}\sum_{i,j,k}\gamma_{ijkl}(1+N)\Big(\{\rho^S,S^+_{i,j}S^-_{k,j}\}-2S^-_{k,j}\rho^S S^+_{i,j}\Big)\\
&-\frac{1}{2}\sum_{i,j,k}\gamma_{ijkl}N\Big(\{\rho^S,S^-_{i,j}S^+_{k,j}\}-2S^+_{k,j}\rho^S S^-_{i,j}\Big)\\
&-\frac{1}{2}\sum_{\alpha=\pm}\sum_{i,k,j\neq l}\gamma'_{ijkl}M\Big(\{\rho^S,S^\alpha_{i,j}S^\alpha_{k,l}\}-2S^\alpha_{k,l}\rho^S S^\alpha_{i,j}\Big)
\end{aligned} \tag{4.16}$$

In the following, we use mathemtics induction to prove that steady state of this system is direct product of the steady state of a single atom. Assume that the steady state of N-atom system is $\rho^S =$

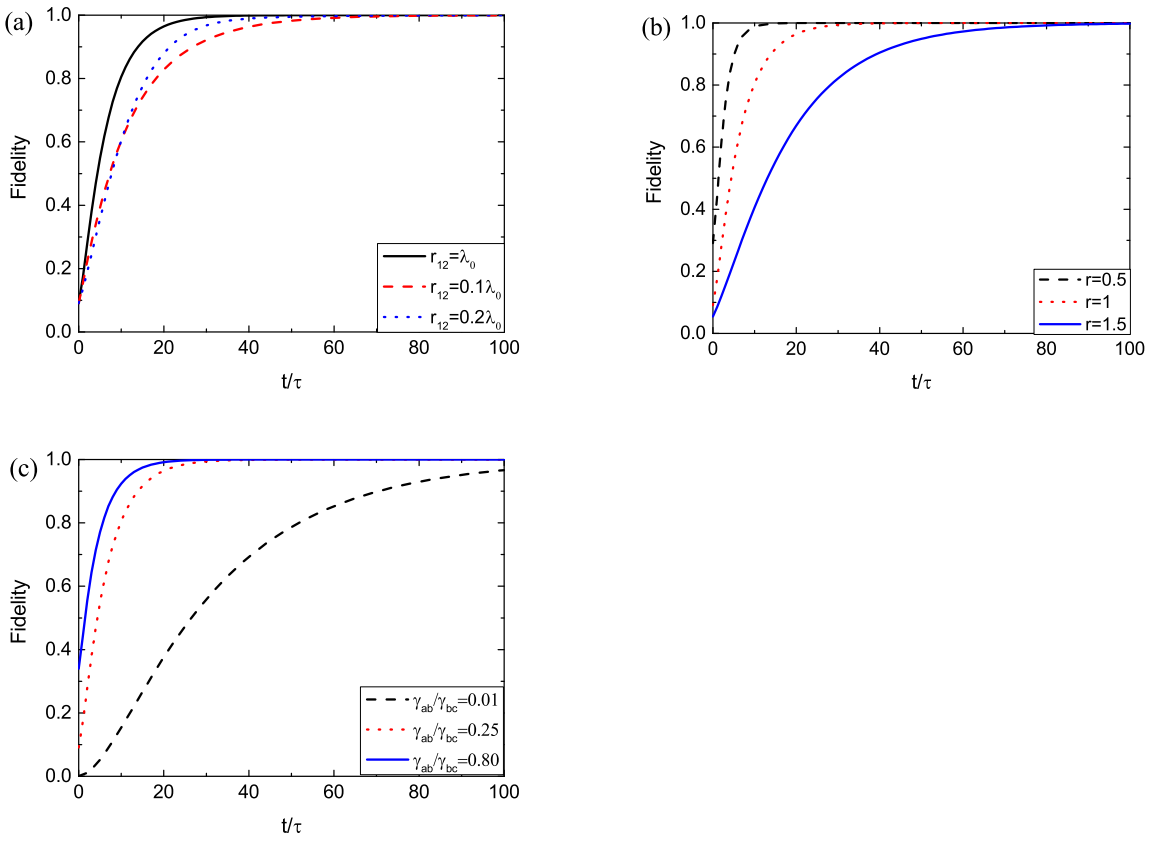

Figure 4.6: (a) Fidelity evolution with different atomic separations. The atomic separations of λ_0, $0.1\lambda_0$, $0.2\lambda_0$ are plotted. Squeezing parameter $r = 1$, decay rate $\frac{\gamma_1}{\gamma_2} = \frac{1}{4}$ and time unit $\tau = 1/\sqrt{\gamma_{ab}\gamma_{bc}}$ is the geometric mean of the transition $|a\rangle \rightarrow |b\rangle$ and $|b\rangle \rightarrow |c\rangle$'s spontaneous emission rates in ordinary vacuum. (b) Fidelity evolution with different squeezing parameters. Decay rate $\frac{\gamma_1}{\gamma_2} = \frac{1}{4}$, and atomic separation $r_{12} = \lambda_0$. (c) Fidelity evolution with different decay rates. Squeezing parameter $r = 1$, and atomic separation $r_{12} = \lambda_0$.

$\rho_1\rho_2...\rho_N$ where $\rho_i = (A|a_i\rangle + C|c_i\rangle)(A\langle a_i| + C\langle c_i|)$ and $A = \frac{sh\sqrt{\gamma_2}}{\sqrt{ch^2\gamma_1+sh^2\gamma_2}}, C = -\frac{ch\sqrt{\gamma_1}}{\sqrt{ch^2\gamma_1+sh^2\gamma_2}}$. Then for $(N+1)$-atom case, the extra terms induced by the $(N+1)th$ atom on the right hand side of Eq. (4.16) are composed of three parts: $i = k = N+1$ terms, $i = N+1, k = 1, 2, \cdots, N$ terms, and $i = 1, 2, \cdots, N, k = N+1$ terms. The $i = k = N+1$ terms are the exact terms for the the $(N+1)th$ atom as a single independent atom, so the net result of this term is 0. The terms with $i = N+1, k = 1, 2, \cdots, N$ are

$$\begin{aligned}
&- i\sum_{j,k}\Lambda_{N+1,j,k,j}[S^+_{N+1,j}S^-_{k.j}, \rho^S] \\
&- \frac{1}{2}\sum_{j,k}\gamma_{N+1,j,k,j}ch^2\Big(\{\rho^S, S^+_{N+1,j}S^-_{k,j}\} - 2S^-_{k,j}\rho^S S^+_{N+1,j}\Big) \\
&- \frac{1}{2}\sum_{j,k}\gamma_{N+1,j,k,j}sh^2\Big(\{\rho^S, S^-_{N+1,j}S^+_{k,j}\} - 2S^+_{k,j}\rho^S S^-_{N+1,j}\Big) \\
&- \sum_{\alpha=\pm}\sum_{i,k,j\neq l}\gamma'_{N+1,j,k,j}\frac{M}{2}\Big(\{\rho^S, S^\alpha_{N+1,j}S^\alpha_{k,l}\} - 2S^\alpha_{k,l}\rho^S S^\alpha_{N+1,j}\Big).
\end{aligned} \tag{4.17}$$

For the energy shift term (the first term) in expression (5.12), we have

$$\begin{aligned}
S^+_{N+1,j}S^-_{k.j}\rho^S &= \rho_1...(S^-_{k.j}\rho_k)...\rho_N(S^+_{N+1,j}\rho_{N+1}) = 0 \\
\rho^S S^+_{N+1,j}S^-_{k.l} &= \rho_1...(\rho_k S^-_{k.l})...\rho_N(\rho_{N+1}S^+_{N+1,j}) = 0
\end{aligned} \tag{4.18}$$

For the thermal terms (the second and third terms) in expression (5.12), we have

$$\begin{aligned}
\rho^S S^+_{N+1,j} S^-_{k,j} =& S^+_{N+1,j} S^-_{k,j} \rho^S = 0 \\
\rho^S S^-_{N+1,j} S^+_{k,j} =& S^-_{N+1,j} S^+_{k,j} \rho^S = 0 \\
S^-_{k,j} \rho^S S^+_{N+1,j} =& \rho_1 ... (S^-_{k.j} \rho_k) ... \rho_N (\rho_{N+1} S^+_{N+1,j}) \\
=& \rho_1 ... (S^-_{k.1} \rho_k) ... \rho_N (\rho_{N+1} S^+_{N+1,1}) \\
=& \rho_1 ... (A|b_k\rangle)(A\langle a_k| + C\langle c_k|) .. \rho_N \\
& \otimes (A|a_{N+1}\rangle + C|c_{N+1}\rangle)(A\langle b_{N+1}|) \\
S^+_{k,j} \rho^S S^-_{N+1,j} =& \rho_1 ... (S^+_{k.j} \rho_k) ... \rho_N (\rho_{N+1} S^-_{N+1,j}) \\
=& \rho_1 ... (S^+_{k.2} \rho_k) ... \rho_N (\rho_{N+1} S^-_{N+1,2}) \\
=& \rho_1 ... (C|b_k\rangle)(A\langle a_k| + C\langle c_k|) ... \rho_N \\
& \otimes (A|a_{N+1}\rangle + C|c_{N+1}\rangle)(C\langle b_{N+1}|)
\end{aligned} \tag{4.19}$$

For the squeezed vacuum terms(the fourth term), we have

$$\begin{aligned}
\rho^S S^\alpha_{N+1,j} S^\alpha_{k,l} &= S^\alpha_{N+1,j} S^\alpha_{k,l} \rho^S = 0 \\
S^+_{k,1} \rho^S S^+_{N+1,2} &= \rho_1 ... (S^+_{k,1} \rho_k) ... \rho_N (\rho_{N+1} S^+_{N+1,2}) = 0 \\
S^+_{k,2} \rho^S S^+_{N+1,1} &= \rho_1 ... (S^+_{k,2} \rho_k) ... \rho_N (\rho_{N+1} S^+_{N+1,1}) \\
&= \rho_1 ... (C|b_k\rangle)(A\langle a_k| + C\langle c_k|) ... \rho_N \\
&\otimes (A|a_{N+1}\rangle + C|c_{N+1}\rangle)(A\langle b_{N+1}|), \\
S^-_{k,1} \rho^S S^-_{N+1,2} &= \rho_1 ... (S^-_{k,1} \rho_k) ... \rho_N (\rho_{N+1} S^-_{N+1,2}) \\
&= \rho_1 ... (A|b_k\rangle)(A\langle a_k| + C\langle c_k|) ... \rho_N \\
&\otimes (A|a_{N+1}\rangle + C|c_{N+1}\rangle)(C\langle b_{N+1}|) \\
S^-_{k,2} \rho^S S^-_{N+1,1} &= \rho_1 ... (S^-_{k,2} \rho_k) ... \rho_N (\rho_{N+1} S^-_{N+1,1}) = 0
\end{aligned} \tag{4.20}$$

On substituting from Eqs. (5.13)-(5.15) into expression (5.12), we have

$$
\begin{aligned}
&\sum_k \gamma_{N+1,1,k,1}(ch^2) S^-_{k,1}\rho^S S^+_{N+1,1} + \sum_{j,k}\gamma_{N+1,2,k,2} sh^2 S^+_{k,2}\rho^S S^-_{N+1,2} \\
&\quad + \sum_{\alpha=\pm}\sum_{i,k,j\neq l}\gamma'_{N+1,j,k,l} chsh S^\alpha_{k,l}\rho^S S^\alpha_{N+1,j} \\
=&\sum_k \gamma_{N+1,1,k,1}(ch^2)\rho_1...(A|b_k\rangle)(A\langle a_k| + C\langle c_k|)..\rho_N(A|a_{N+1}\rangle + C|c_{N+1}\rangle)(A\langle b_{N+1}|) \\
&+ \sum_k \gamma_{N+1,2,k,2} sh^2 \rho_1...(C|b_k\rangle)(A\langle a_k| + C\langle c_k|)...\rho_N(A|a_{N+1}\rangle + C|c_{N+1}\rangle)(C\langle b_{N+1}|) \\
&+ \sum_k \gamma'_{N+1,j,k,l} chsh[\rho_1...(C|b_k\rangle)(A\langle a_k| + C\langle c_k|)...\rho_N(A|a_{N+1}\rangle + C|c_{N+1}\rangle)(A\langle b_{N+1}|) \\
&+ \rho_1...(A|b_k\rangle)(A\langle a_k| + C\langle c_k|)...\rho_N(A|a_{N+1}\rangle + C|c_{N+1}\rangle)(C\langle b_{N+1}|)] \\
=&\sum_k (\gamma_{N+1,1,k,1} ch^2 A^2 + \gamma_{N+1,2,k,2} sh^2 C^2 + 2\gamma'_{N+1,j,k,l} chshCA) \\
&\times \rho_1...(|b_k\rangle)(A\langle a_k| + C\langle c_k|)..\rho_N(A|a_{N+1}\rangle + C|c_{N+1}\rangle)(\langle b_{N+1}|).
\end{aligned}
\tag{4.21}
$$

It is not difficutlt to prove that $ch^2A^2\gamma_{N+1,1,k,1} + sh^2C^2\gamma_{N+1,2,k,2} + 2chshCA\gamma'_{N+1,j,k,l} = 0$ by substituting the expressions of A, B, C. Hence, the extra terms with the atom index $i = N+1$ and $k = 1 \sim N$ when we add the $N+1$th atom are 0. Similarly, the terms with $i = 1 \sim N$ and $k = N+1$ also vanish. Thus, we prove that the right hand side of Eq. (4.16) is zero when the state of the system is direct product of the steady state of single atom. This indicates that direct product of the steady state of single atom is the steady state of the multiple atoms driven by the squeezed vacuum. It is interesting to note that while introducing the dipole-dipole interaction between the atoms affects the evolution of the system, the final steady state still remains unaffected. Therefore, for multiple atoms, a population inversion of almost 100% can also be achieved even the dipole-dipole interaction is considered, under the condition that the dipole direction for all atoms are properly oriented to satisfy $\gamma_{ab} \ll \gamma_{bc}$. Actually, in the normal squeezed vacuum with correlation shown in Eq. (2.40), the steady state of the atoms can also be direct product of the steady state of a single atom if all the atoms are in the nodes of the standing wave.

To verify the above proof, we will do the numerical simulation to show that the steady state

of multiple atoms is indeed the direct product of steady state of single atom. Since the cost for numerical simulation increases exponentially as the number of atoms increases, we only show the fidelity of two-atom state with respect to theoretical steady state as a function of time in Fig. 4.6, where the system is initially in the ground state. From Fig. 4.6(a), we can see that different atom separations have different evolution dynamics because they have different dipole-dipole interactions. However, we can see that the system finally evolves into the following equation regardless of the atomic separation, squeezing parameter, and the ratio of decay rate γ_{ab}/γ_{bc}:

$$\begin{aligned} |\psi_s s\rangle =& \Big(\frac{sh\sqrt{\gamma_2}}{\sqrt{ch^2\gamma_1 + sh^2\gamma_2}} |a_1\rangle - \frac{ch\sqrt{\gamma_1}}{\sqrt{ch^2\gamma_1 + sh^2\gamma_2}} |c_1\rangle \Big) \\ & \otimes \Big(\frac{sh\sqrt{\gamma_2}}{\sqrt{ch^2\gamma_1 + sh^2\gamma_2}} |a_2\rangle - \frac{ch\sqrt{\gamma_1}}{\sqrt{ch^2\gamma_1 + sh^2\gamma_2}} |c_2\rangle \Big) \end{aligned} \tag{4.22}$$

From Fig. 4.6(b), we see that the system takes less time to evolve into the steady state for a smaller squeezing parameter. Fig. 4.6(c) shows that while smaller γ_{ab} results in higher population inversion, it takes much longer for the system to evolve into the steady state.

In the previous sections, we studied the interactions between the squeezed vacuum and atoms, or fermions with discrete energy levels. In this section, we study the interactions between the squeezed vacuum and the harmonic oscillators, or bosons with continuous energy levels. A practical model is a leaky cavity, where the modes inside and outside the cavity are essentially harmonic oscillators, and their coupling can be described by the Q factor[30].

5.1 General master equation of cavity-cavity interaction

In this section, we will derive the master equation for two single-mode leaky cavities placed inside the waveguide with the squeezed vacuum injected from both ends. The schematic setup is shown in Fig. 5.1. Then we will study how the modes inside the cavity will evolve under the influence of the squeezed vacuum. The free Hamiltonian of cavity and waveguide modes is:

$$H_0 = \sum_i \hbar\omega_i(a_i^\dagger a_i + \frac{1}{2}) + \hbar\sum_{k,s}\omega_k(a_{k,s}^\dagger a_{k,s} + \frac{1}{2}) \tag{5.1}$$

where a_k stands for the modes in the waveguide and a_i is the field operator of the single mode inside ith the cavity. The waveguide is saturated with the squeezed vacuum with the center frequency ω_0. The interaction Hamiltonian between the cavity mode and waveguide modes is:

$$V = -i\hbar\sum_{\boldsymbol{k}s}[Da_{\boldsymbol{k}s} - D^+a_{\boldsymbol{k}s}^\dagger] \tag{5.2}$$

where

$$D = \sum_i [g_{i,k,s}^* a_i^\dagger + g_{i,k,s}a_i] \tag{5.3}$$

Here we define $g_{i,k,s} = |g_{i,k,s}|e^{-ik_z r_i}$ where r_i is just a phenomenological parameter describing the location of cavity. The reduced master equation of atoms in the reservoir is[30]

$$\begin{aligned}\frac{d\rho^S}{dt} =& -\frac{1}{\hbar^2}\int_0^t d\tau Tr_F\{[V(t),[V(t-\tau),\rho^S(t-\tau)\rho^F\} \\ =& -\frac{1}{\hbar^2}\int_0^t d\tau Tr_F\{V(t)V(t-\tau)\rho^S(t-\tau)\rho^F + \rho^S(t-\tau)\rho^F V(t-\tau)V(t) \\ & - V(t)\rho^S(t-\tau)\rho^F V(t-\tau) - V(t-\tau)\rho^S(t-\tau)\rho^F V(t)\}.\end{aligned} \tag{5.4}$$

Here we just show how to deal with the first term in Eq.(5.4), the remaining terms can be calculated in the same way. For the first term, we have

$$\begin{aligned}& -\frac{1}{\hbar^2}\int_0^t d\tau Tr_F\{V(t)V(t-\tau)\rho^S(t-\tau)\rho^F\} \\ =& \int_0^t d\tau \sum_{\boldsymbol{k}s,\boldsymbol{k}'s'}\{D(t)D(t-\tau)Tr_F[\rho^F a_{ks}(t)a_{k's'}(t-\tau)] - D(t)D^+(t-\tau)Tr_F[\rho^F a_{ks}(t)a^\dagger_{k's'}(t-\tau)] \\ & - D^+(t)D(t-\tau)Tr_F[\rho^F a^\dagger_{ks}(t)a_{k's'}(t-\tau)] + D^+(t)D^+(t-\tau)Tr_F[\rho^F a^\dagger_{ks}(t)a^\dagger_{k's'}(t-\tau)]\}\rho^S(t-\tau)\}.\end{aligned} \tag{5.5}$$

Under the rotating wave approximation(RWA), we have

$$\begin{aligned}& -\frac{1}{\hbar^2}\int_0^t d\tau Tr_F\{V(t)V(t-\tau)\rho^S(t-\tau)\rho^F\} \\ =& \sum_{ij}\sum_{\boldsymbol{k}s,\boldsymbol{k}'s'}\int_0^t d\tau\{g^*_{i,k,s}a^\dagger_i e^{i\omega_i t}g^*_{j,k',s'}a^\dagger_j e^{i\omega_j(t-\tau)}e^{-i(\omega_{\boldsymbol{k}s}+\omega_{\boldsymbol{k}'s'})t+i\omega_{\boldsymbol{k}'s'}\tau}[-\sinh(r)\cosh(r)\delta_{\boldsymbol{k}',2\boldsymbol{k}_0-\boldsymbol{k}}\delta_{ss'}] \\ & - g^*_{i,k,s}a^\dagger_i e^{i\omega_i t}g_{j,k',s'}a_j e^{-i\omega_j(t-\tau)}e^{-i\omega_{\boldsymbol{k}'s'}\tau}\cosh^2 r\delta_{\boldsymbol{k}\boldsymbol{k}'}\delta_{ss'} \\ & - g_{i,k,s}a_i e^{-i\omega_i t}g^*_{j,k',s'}a^\dagger_j e^{i\omega_j(t-\tau)}e^{-i\omega_{\boldsymbol{k}'s'}\tau}\cosh^2 r\delta_{\boldsymbol{k}\boldsymbol{k}'}\delta_{ss'} \\ & - g_{i,k,s}a_i e^{-i\omega_i t}g^*_{j,k',s'}a^\dagger_j e^{i\omega_j(t-\tau)}e^{i\omega_{\boldsymbol{k}'s'}\tau}\sinh^2 r\delta_{\boldsymbol{k}\boldsymbol{k}'}\delta_{ss'} \\ & - g^*_{i,k,s}a^\dagger_i e^{i\omega_i t}g_{j,k',s'}a_j e^{-i\omega_j(t-\tau)}e^{i\omega_{\boldsymbol{k}'s'}\tau}\sinh^2 r\delta_{\boldsymbol{k}\boldsymbol{k}'}\delta_{ss'} \\ & + g_{i,k,s}a_i e^{-i\omega_i t}g_{j,k',s'}a_j e^{-i\omega_j(t-\tau)}e^{i(\omega_{\boldsymbol{k}s}+\omega_{\boldsymbol{k}'s'})t-i\omega_{\boldsymbol{k}'s'}\tau}[-\sinh(r)\cosh(r)\delta_{\boldsymbol{k}',2\boldsymbol{k}_0-\boldsymbol{k}}\delta_{ss'}]\}\rho^S(t-\tau)\end{aligned} \tag{5.6}$$

Here we just calculate the first and second term to show how to get the master equation. For the second term, we have

$$
\begin{aligned}
&-\sum_{k_z}\int_0^t d\tau g^*_{i,k,s}a_i^\dagger e^{i\omega_i t}g_{j,k',s'}a_j e^{-i\omega_j(t-\tau)}e^{-i\omega_{\boldsymbol{k}'s'}\tau}\cosh^2 r\rho^S(t-\tau)\delta_{\boldsymbol{k}\boldsymbol{k}'}\delta_{ss'}\\
=&-\frac{L}{2\pi}e^{i(\omega_i-\omega_j)t}\int_{-\infty}^{\infty}dk_z\int_0^t d\tau e^{i\omega_j\tau}e^{-i\omega_{k_z}\tau}|g_{i,\boldsymbol{k},s}g_{j,\boldsymbol{k},s}|\\
&\times e^{ik_z(r_i-r_j)}\cosh^2 r a_i^\dagger a_j\rho^S(t-\tau)\\
\approx&-\frac{L}{2\pi}e^{i(\omega_i-\omega_j)t}\int_0^{\infty}dk_z\int_0^t d\tau e^{i\omega_j\tau}e^{-i[\omega_j+c^2k_{jz}(k_z-k_{jz})/\omega_j]\tau}|g_{i,\boldsymbol{k},s}g_{j,\boldsymbol{k},s}|\\
&\times[e^{ik_z(r_i-r_j)}+e^{-ik_z(r_i-r_j)}]\cosh^2 r a_i^\dagger a_j\rho^S(t-\tau)\\
\approx&-\frac{L}{2\pi}e^{i(\omega_i-\omega_j)t}\int_{-k_{0z}}^{\infty}d\delta k_z\int_0^t d\tau e^{-i\tau c^2k_{jz}\delta k_z/\omega_j}|g_{i,\boldsymbol{k},s}g_{j,\boldsymbol{k},s}|\\
&\times[e^{i(k_{jz}+\delta k_z)(r_i-r_j)}+e^{-i(k_{jz}+\delta k_z)(r_i-r_j)}]\cosh^2 r a_i^\dagger a_j\rho^S(t-\tau)\\
\approx&-\frac{L}{2\pi}e^{i(\omega_i-\omega_j)t}\int_{-\infty}^{\infty}d\delta k_z\int_0^t d\tau e^{-i(c^2k_{jz}\delta k_z/\omega_j)\tau}|g_{i,\boldsymbol{k},s}g_{j,\boldsymbol{k},s}|\\
&\times[e^{i(k_{jz}+\delta k_z)(r_i-r_j)}+e^{-i(k_{jz}+\delta k_z)(r_i-r_j)}]\cosh^2 r a_i^\dagger a_j\rho^S(t-\tau)\\
\approx&-\frac{L}{2\pi}e^{i(\omega_i-\omega_j)t}\int_0^t d\tau|g_{i,\boldsymbol{k},s}g_{j,\boldsymbol{k},s}|2\pi[e^{ik_{jz}(r_i-r_j)}\delta((r_i-r_j)-\frac{c^2k_{jz}}{\omega_0}\tau)\\
&+e^{-ik_{jz}(r_i-r_j)}\delta((r_i-r_j)+\frac{c^2k_{jz}}{\omega_0}\tau)]\cosh^2 r a_i^\dagger a_j\rho^S(t-\tau)\\
\approx&-\frac{L}{2\pi}e^{ik_{jz}r_{ij}}|g_{i,\boldsymbol{k},s}g_{j,\boldsymbol{k},s}|2\pi\frac{\omega_j}{c^2k_{0z}}\cosh^2 r a_i^\dagger a_j\rho^S(t)e^{i(\omega_i-\omega_j)t}\\
\approx&-[\frac{\sqrt{\gamma_i\gamma_j}}{2}\cos(k_{0z}r_{ij})+i\frac{\sqrt{\gamma_i\gamma_j}}{2}sin(k_{0z}r_{ij})]\cosh^2 r a_i^\dagger a_j\rho^S(t)e^{i(\omega_i-\omega_j)t}\\
\equiv&-(\frac{\sqrt{\gamma_i\gamma_j}}{2}+i\Lambda_{ij})\cosh^2 r a_i^\dagger a_j\rho^S(t)e^{i(\omega_i-\omega_j)t}
\end{aligned}
\tag{5.7}
$$

where $r_{ij}=|r_i-r_j|$ is also a phenomenological parameter indicating the relative position between cavities. $\gamma_i=L|g_{i,k_0}|^2$ is the leaking rate for the ith cavity, and $\Lambda_{ij}=\sqrt{\gamma_i\gamma_j}\sin(k_{0z}r_{ij})/2$ is the energy shift. In the third line we expand $\omega_k=c\sqrt{(\frac{\pi}{a})^2+(k_z)^2}$ around $k_z=k_{0z}$ since resonant modes provide dominant contributions. In the fifth line we extend the integration $\int_{-k_{0z}}^{\infty}dk_z\rightarrow\int_{-\infty}^{\infty}dk_z$ because the main contribution comes from the components around $\delta k_z=0$. In the next line, Weisskopf-Wigner approximation is used.

Next we need to calculate the first term (squeezing term) in Eq.(5.6):

$$
\begin{aligned}
& e^{i(\omega_i+\omega_j-2\omega_0)t}\sum_{k_z}\int_0^t d\tau\{g^*_{i,2\boldsymbol{k}_0-\boldsymbol{k}}a_i^\dagger g^*_{j,\boldsymbol{k}}a_j^\dagger e^{i(\omega_{\boldsymbol{k}}-\omega_j)\tau}[-\sinh(r)\cosh(r)]\rho^S(t-\tau) \\
=& -\frac{L}{2\pi}e^{i(\omega_i+\omega_j-2\omega_0)t}\int_0^{2k_{0z}}dk_z\int_0^t d\tau e^{i(\omega_{k_z}-\omega_j)\tau}e^{i(2k_{iz}-k_z)(r_i-o_1)}e^{ik_z(r_j-o_1)} \\
& \times|g_{i,2\boldsymbol{k}_0-\boldsymbol{k}}g_{j,\boldsymbol{k}}|\sinh(r)\cosh(r)a_i^\dagger a_j^\dagger\rho^S(t-\tau) \\
& -\frac{L}{2\pi}e^{i(\omega_i+\omega_j-2\omega_0)t}\int_{-2k_{0z}}^0 dk_z\int_0^t d\tau e^{i(\omega_{k_z}-\omega_j)\tau}e^{i(-2k_{iz}-k_z)(r_i-o_2)}e^{ik_z(r_j-o_2)} \\
& \times|g_{i,2\boldsymbol{k}_0-\boldsymbol{k}}g_{j,\boldsymbol{k}}|\sinh(r)\cosh(r)a_i^\dagger a_j^\dagger\rho^S(t-\tau)
\end{aligned}
\tag{5.8}
$$

Putting the overall factor $e^{i(\omega_i+\omega_j-2\omega_0)t}$ aside, for $i=j$, Eq.(5.8) reduces to

$$
\begin{aligned}
& \sum_{k_z}\int_0^t d\tau\{g^*_{i,2\boldsymbol{k}_0-\boldsymbol{k}}a_i^\dagger g^*_{i,\boldsymbol{k}}a_i^\dagger e^{i(\omega_{\boldsymbol{k}}-\omega_i)\tau}[-\sinh(r)\cosh(r)]\rho^S(t-\tau) \\
&= -\frac{L}{2\pi}\int_0^{2k_{0z}}dk_z\int_0^t d\tau e^{i\frac{c^2k_{iz}}{\omega_i}(k_z-k_{iz})\tau}e^{i2k_{0z}(r_i-o_1)}|g_{i,2\boldsymbol{k}_0-\boldsymbol{k}}g_{i,\boldsymbol{k}}|\sinh(r)\cosh(r)a_i^\dagger a_i^\dagger\rho^S(t-\tau) \\
&- \frac{L}{2\pi}\int_{-2k_{0z}}^0 dk_z\int_0^t d\tau e^{i\frac{c^2k_{iz}}{\omega_i}(k_z-k_{iz})\tau}e^{-i2k_{0z}(r_i-o_2)}|g_{i,2\boldsymbol{k}_0-\boldsymbol{k}}g_{i,\boldsymbol{k}}|\sinh(r)\cosh(r)a_i^\dagger a_i^\dagger\rho^S(t-\tau) \\
&= -\frac{L}{2\pi}[e^{i2k_{0z}(r_i-o_1)}+e^{-i2k_{0z}(r_i-o_2)}]|g_{i,2\boldsymbol{k}_0-\boldsymbol{k}}g_{i,\boldsymbol{k}}|\int_0^t d\tau 2\pi\delta(\frac{c^2k_{iz}}{\omega_i}\tau)\sinh(r)\cosh(r)a_i^\dagger a_i^\dagger\rho^S(t-\tau) \\
&= -e^{i2k_{0z}R}\frac{\gamma_i}{2}\cos(2k_{0z}r_i)\sinh(r)\cosh(r)a_i^\dagger a_i^\dagger\rho^S(t)
\end{aligned}
\tag{5.9}
$$

where we have used the fact that the origin of coordinate system is at equal distance from two sources(i.e., $o_2=-o_1=R$) in the second last line. Thus, we have $\gamma'_{ii}=\gamma_i\cos(2k_{0z}r_i)$. For

$r_i \neq r_j$, Eq. (5.8) reduces to

$$
\begin{aligned}
&\sum_{k_z}\int_0^t d\tau\{g_{i,2\boldsymbol{k}_0-\boldsymbol{k}}a_i^\dagger g_{j,\boldsymbol{k}}a_j^\dagger e^{i(\omega_{\boldsymbol{k}}-\omega_j)\tau}[-\sinh(r)\cosh(r)]\rho^S(t-\tau)\\
=&-\frac{L}{2\pi}\int_0^{2k_{0z}}dk_z\int_0^t d\tau e^{i\frac{c^2k_{jz}}{\omega_j}(k_z-k_{jz})\tau}e^{i2k_{0z}(r_c-o_1)}e^{-i(k_z-k_{0z})(r_i-r_j)}\\
&\times|g_{i,2\boldsymbol{k}_0-\boldsymbol{k}}g_{j,\boldsymbol{k}}|\sinh(r)\cosh(r)a_i^\dagger a_j^\dagger\rho^S(t-\tau)\\
&-\frac{L}{2\pi}\int_{-2k_{0z}}^0 dk_z\int_0^t d\tau e^{i\frac{c^2k_{jz}}{\omega_j}(-k_z-k_{jz})\tau}e^{-i2k_{0z}(r_c-o_2)}e^{-i(k_z+k_{0z})(r_i-r_j)}\\
&\times|g_{i,2\boldsymbol{k}_0-\boldsymbol{k}}g_{j,\boldsymbol{k}}|\sinh(r)\cosh(r)a_i^\dagger a_j^\dagger\rho^S(t-\tau)\\
=&-\frac{L}{2\pi}e^{i2k_{0z}(r_c-o_1)}|g_{i,2\boldsymbol{k}_0-\boldsymbol{k}}g_{j,\boldsymbol{k}}|\int_{-\infty}^{\infty}dk_z\int_0^t d\tau e^{i\frac{c^2k_{jz}}{\omega_j}(k_z-k_{jz})\tau}\\
&\times e^{-i(k_z-k_{0z})(r_i-r_j)}\sinh(r)\cosh(r)a_i^\dagger a_j^\dagger\rho^S(t-\tau)\\
&-\frac{L}{2\pi}e^{-i2k_{0z}(r_c-o_2)}|g_{i,2\boldsymbol{k}_0-\boldsymbol{k}}g_{j,\boldsymbol{k}}|\int_{-\infty}^{\infty}dk_z\int_0^t d\tau e^{i\frac{c^2k_{jz}}{\omega_j}(k_z-k_{jz})\tau}\\
&\times e^{i(k_z-k_{0z})(r_i-r_j)}\sinh(r)\cosh(r)a_i^\dagger a_j^\dagger\rho^S(t-\tau)\\
\approx&-\frac{L}{2\pi}e^{i2k_{0z}R}|g_{i,2\boldsymbol{k}_0-\boldsymbol{k}}g_{j,\boldsymbol{k}}|\int_0^t d\tau 2\pi[e^{i2k_{0z}r_c}\delta(r_i-r_j-\frac{c^2k_{0z}}{\omega_0}\tau)\\
&+e^{-i2k_{0z}r_c}\delta(r_i-r_j+\frac{c^2k_{0z}}{\omega_0}\tau)]\sinh(r)\cosh(r)a_i^\dagger a_j^\dagger\rho^S(t-\tau)\\
\approx&-e^{i2k_{0z}R}L|g_{i,\boldsymbol{k}_0}g_{j,\boldsymbol{k}_0}|e^{i2k_{0z}r_c sgn(i-j)}a_i^\dagger a_j^\dagger\rho^S(t)\\
\to&-\frac{\sqrt{\gamma_i\gamma_j}}{2}e^{i2k_{0z}R}\cos(k_{0z}(r_i+r_j))a_i^\dagger a_j^\dagger\rho^S(t)
\end{aligned}
\tag{5.10}
$$

where $sgn(i-j)$ is the sign function. The last arrow is because we need to sum over i,j, so the imaginary part of $e^{i2k_{0z}r_c sgn(i-j)}$ vanishes and the neat result is that $\gamma'_{ij}=e^{i2k_{0z}R}\sqrt{\gamma_i\gamma_j}\cos(k_{0z}(r_i+r_j))$. As for $a_i^\dagger\rho^S(t)a_j^\dagger$ terms, the combination of the last two terms in Eq.(5.4) will make the imaginary part of $e^{i2k_{0z}r_c sgn(i-j)}$ vanish. Thus, we have $\gamma'_{ij}=e^{i2k_{0z}R}\sqrt{\gamma_i\gamma_j}\cos(k_{0z}(r_i+r_j))$.

Doing the above calculation for all terms in Eq.(5.4), we have the general equation for cavity-

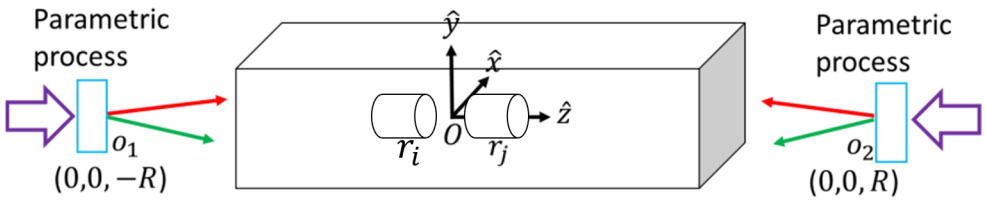

Figure 5.1: (a) Schematic setup: two single-mode cavities are placed inside the waveguide with the broadband squeezed vacuum incident from both ends.

cavity interaction in the squeezed vacuum as follows:

$$\begin{aligned}\dot{\rho} = &\sum_{ij}\gamma_{ij}\cosh^2 r(-\rho a_i^\dagger a_j - a_i^\dagger a_j\rho + 2a_i\rho a_j^\dagger)e^{i(\omega_i-\omega_j)t} \\ &+\sum_{ij}\gamma_{ij}\sinh^2 r(-\rho a_i a_j^\dagger - a_i a_j^\dagger\rho + 2a_i^\dagger\rho a_j)e^{-i(\omega_i-\omega_j)t} \\ &+\sum_{ij}\gamma_{ij}\cosh r\sinh r[(e^{i\theta}\rho a_i a_j + e^{i\theta}a_i a_j\rho - e^{i\theta}2a_i\rho a_j)e^{-i(\omega_i+\omega_j)t} + H.c.]\end{aligned} \tag{5.11}$$

5.2 Steady state of non-resonant cavities

First, we study two non-resonant cavities coupled to the squeezed vacuum reservoir. The eigen frequencies of these two cavities are $\omega_1 = \omega_0 - \delta\omega$ and $\omega_2 = \omega_0 + \delta\omega$. Under the rotating wave approximation(RWA), Eq.(5.11) becomes:

$$\begin{aligned}\dot{\rho} = &\sum_{i}\gamma(1+N)(-\rho a_i^\dagger a_i - a_i^\dagger a_i\rho + 2a_i\rho a_i^\dagger) \\ &+\sum_{i}\gamma N(-\rho a_i a_i^\dagger - a_i a_i^\dagger\rho + 2a_i^\dagger\rho a_i) \\ &+\sum_{i\neq j}\gamma M(e^{i\theta}\rho a_i a_j + e^{i\theta}a_i a_j\rho - 2e^{i\theta}a_i\rho a_j + h.c.)\end{aligned} \tag{5.12}$$

where we have assumed $\gamma_{ij} = \gamma$ for simplicity. The above equation can be re-arranged as:

$$\begin{aligned}\dot{\rho} = \sum_{i\neq j} \frac{\gamma}{2}[&-\rho(\cosh(r)a_i^\dagger - e^{i\theta}\sinh(r)a_j)(\cosh(r)a_i - e^{-i\theta}\sinh(r)a_j^\dagger) \\ &- (\cosh(r)a_i^\dagger - e^{i\theta}\sinh(r)a_j)(\cosh(r)a_i - e^{-i\theta}\sinh(r)a_j^\dagger)\rho \\ &+ 2(\cosh(r)a_i - e^{-i\theta}\sinh(r)a_j^\dagger)\rho(\cosh(r)a_i^\dagger - e^{i\theta}\sinh(r)a_j)]\end{aligned} \tag{5.13}$$

we use the following Bogoliubov transformation[58]:

$$\begin{aligned}S &= exp(\eta^\star a_i a_j - \eta a_i^\dagger a_j^\dagger) \\ A_i &= S^+ a_i S = \cosh(r)a_i - e^{-i\theta}\sinh(r)a_j^\dagger \\ A_i^+ &= S^+ a_i^+ S = \cosh(r)a_i^+ - e^{i\theta}\sinh(r)a_j\end{aligned} \tag{5.14}$$

so the master equation Eq.(5.13) becomes:

$$\dot{\rho} = \sum_i \gamma[-\rho A_i^\dagger A_i - A_i^\dagger A_i \rho + 2A_i \rho A_i^\dagger] \tag{5.15}$$

Next we redefine the density matrix: $\rho_s = S\rho S^\dagger$. Thus Eq.(5.15) becomes:

$$\begin{aligned}\dot{\rho}_s &= \sum_i \gamma[-\rho_s a_i^\dagger a_i - a_i^\dagger a_i \rho_s + 2a_i \rho_s a_i^\dagger] \\ &\equiv \sum_i \gamma[-a_i^{l\dagger} a_i^l \rho_s - a_i^{r\dagger} a_i^r \rho_s + 2a_i^r a_i^{l\dagger} \rho_s] \equiv L\rho_s\end{aligned} \tag{5.16}$$

Here we define superoperator $\{a_i^l, a_i^{l\dagger}\}(\{a_i^r, a_r^{l\dagger}\}$) only acting to the left(right) on density operator ρ [59, 60]. These operators have the following commutation relations:

$$[a_i^r, a_j^{r\dagger}] = \delta_{ij},\ [a_i^l, a_j^{l\dagger}] = -\delta_{ij},\ [a_i^l, a_j^{r\dagger}] = [a_i^l, a_j^r] = [a_i^{l\dagger}, a_j^r] = [a_i^{l\dagger}, a_j^{r\dagger}] = 0 \tag{5.17}$$

Thus, the steady state of Eq.(5.16) can be solved by solving $L\rho = 0$, which requires the diagnolization of superoperator L. Applying the similarity transformation $U = e^{-a_1^r a_1^{l\dagger} - a_2^r a_2^{l\dagger}}$ to Eq.(5.16)

, since we have $U^{-1}(a_i^{r\dagger}, a_i^l, a_i^r, a_i^{l\dagger})U = (a_i^{r\dagger} + a_i^{l\dagger}, a_i^r + a_i^l, a_i^r, a_i^{l\dagger})$, the right hand side of Eq.(5.16) becomes:

$$RHS = \sum_i \gamma U^{-1}[-a_i^{l\dagger}a_i^l - a_i^{r\dagger}a_i^r + 2a_i^r a_i^{l\dagger}]UU^{-1}\rho_s = \sum_i \gamma[-a_i^{l\dagger}a_i^l - a_i^{r\dagger}a_i^r]U^{-1}\rho_s \tag{5.18}$$

The only solution to $L\rho = 0$ is $U^{-1}\rho_s = |0,0\rangle\langle 0,0|$, which yields $\rho = S^\dagger \rho_S S = S^\dagger e^{-K_{-1}-K_{-2}}|0,0\rangle\langle 0,0|S = S^\dagger|0,0\rangle\langle 0,0|S$ which is the two mode squeezed vacuum.

5.3 Steady state of resonant cavities

Next we study the case where two cavities are identical, i.e., $\omega_1 = \omega_2 = \omega_0$. Then the master equation becomes:

$$\begin{aligned}
\dot{\rho} = &\sum_{ij} \gamma \cosh^2 r(-\rho a_i^\dagger a_j - a_i^\dagger a_j \rho + 2a_j \rho a_i^\dagger) \\
&+ \sum_{ij} \gamma \sinh^2 r(-\rho a_i a_j^\dagger - a_i a_j^\dagger \rho + 2a_j^\dagger \rho a_i) \\
&+ \sum_{ij} \gamma \cosh r \sinh r(e^{i\theta}\rho a_i a_j + e^{i\theta} a_i a_j \rho - e^{i\theta} 2a_i \rho a_j + h.c.)
\end{aligned} \tag{5.19}$$

This equation can be rearranged as follows:

$$\begin{aligned}
\dot{\rho} = \sum_{ij} \gamma[&-\rho(\cosh r a_i^\dagger - e^{i\theta}\sinh r a_i)(\cosh r a_j - e^{-i\theta}\sinh r a_j^\dagger) \\
&- (\cosh r a_i^\dagger - e^{i\theta}\sinh r a_i)(\cosh r a_j - e^{-i\theta}\sinh r a_j^\dagger)\rho \\
&+ 2(\cosh r a_j - e^{-i\theta}\sinh r a_j^\dagger)\rho(\cosh r a_i^\dagger - e^{i\theta}\sinh r a_i)]
\end{aligned} \tag{5.20}$$

We introduce the Bogoliubov transformation:

$$\begin{aligned}
S_i &= exp(\frac{1}{2}\eta^\star a_i^2 - \frac{1}{2}\eta a_i^{\dagger 2}) \\
A_i &= S_i^+ a_i S_i = \cosh(r) a_i - e^{-i\theta}\sinh(r) a_i^\dagger \\
A_i^+ &= S_i^+ a_i^+ S_i = \cosh(r) a_i^+ - e^{i\theta}\sinh(r) a_i
\end{aligned} \tag{5.21}$$

so master equation Eq.(5.20) becomes

$$\dot{\rho} = \sum_{ij} \gamma[-\rho A_i^\dagger A_j - A_i^\dagger A_j \rho + 2A_j \rho A_i^\dagger] \tag{5.22}$$

Next we define $\rho_s = S_1 S_2 \rho \dot{S_1^+} S_2^+$ so the master equation is reduced to:

$$\dot{\rho_s} = \sum_{ij} \gamma[-\rho_s a_i^\dagger a_j - a_i^\dagger a_j \rho_s + 2a_j \rho_s a_i^\dagger] \tag{5.23}$$

To diagnolize this Lindblad equation, we introduce the transformation:

$$\begin{array}{lcl} L_1 & = & \frac{1}{\sqrt{2}}(a_1 - a_2) \\ L_2 & & \frac{1}{\sqrt{2}}(a_1 + a_2) \end{array}$$

where $[L_i, L_j^\dagger] = \delta_{ij}$, and the master equation becomes:

$$\begin{aligned} \dot{\rho_s} &= \gamma[-2\rho_s L_2^\dagger L_2 - 2L_2^\dagger L_2 \rho_s + 4L_2 \rho_s L_2^\dagger] \\ &= \gamma[-2L_2^{r\dagger} L_2^r \rho_s - 2L_2^{l\dagger} L_2^l \rho_s + 4L_2^l L_2^{r\dagger} \rho_s] \\ &= L\rho \end{aligned} \tag{5.24}$$

Operator $L_2^\dagger$ has the following properties:

$$L_2^\dagger |0\rangle = \frac{1}{\sqrt{2}}(|01\rangle + |10\rangle) \equiv |1_{L_2}\rangle$$

$$L_2^\dagger \frac{1}{\sqrt{2}}(|01\rangle + |10\rangle) = \sqrt{2}[\frac{1}{2}(|02\rangle + \sqrt{2}|11\rangle + |20\rangle)] = \sqrt{2}|2_{L_2}\rangle$$

$$L_2^\dagger \frac{1}{2}(|02\rangle + \sqrt{2}|11\rangle + |20\rangle) = \sqrt{3}[\frac{1}{2\sqrt{2}}(|03\rangle + \sqrt{3}|12\rangle + \sqrt{3}|21\rangle + |30\rangle)] = \sqrt{3}|3_{L_2}\rangle$$

...

while the operator $L_1^\dagger$ has the following properties:

$$L_1^\dagger|0\rangle = \frac{1}{\sqrt{2}}(-|01\rangle + |10\rangle) \equiv |1_{L_1}\rangle$$

$$L_1^\dagger \frac{1}{\sqrt{2}}(-|01\rangle + |10\rangle) = \sqrt{2}[\frac{1}{2}(|02\rangle - \sqrt{2}|11\rangle + |20\rangle)] = \sqrt{2}|2_{L_1}\rangle$$

$$L_1^\dagger \frac{1}{2}(|02\rangle - \sqrt{2}|11\rangle + |20\rangle) = \sqrt{3}[\frac{1}{2\sqrt{2}}(-|03\rangle + \sqrt{3}|12\rangle - \sqrt{3}|21\rangle + |30\rangle)] = \sqrt{3}|3_{L_1}\rangle$$

...

Thus, L_1 and L_2 is just another representation of a_1 and a_2. Then we use the similarity transformation: $U = e^{-L_2^r L_2^{l\dagger}}$, which yields $U^{-1}(L_2^{r\dagger}, L_2^l, L_2^{l\dagger}, L_2^r)U = (L_2^{r\dagger} + L_2^{l\dagger}, L_2^l + L_2^r, L_2^{l\dagger}, L_2^r)$. Thus, the master equation Eq.(5.25) becomes:

$$RHS = \gamma U^{-1}[-L_2^{l\dagger}L_2^l - L_2^{r\dagger}L_2^r + 2L_2^r L_2^{l\dagger}]UU^{-1}\rho_s = \gamma[-L_2^{l\dagger}L_2^l - L_2^{r\dagger}L_2^r]U^{-1}\rho_s \qquad (5.25)$$

The solutions to the steady state are $\rho_s = e^{-L_2^r L_2^{l\dagger}}|0_{L_2}m_{L_1}\rangle\langle 0_{L_2}n_{L_1}| = |m_{L_1}\rangle\langle n_{L_1}|$ which yields $\rho = S_1^+ S_2^+ \frac{1}{\sqrt{m!}}(\frac{a_1^\dagger - a_2^\dagger}{\sqrt{2}})^m|0\rangle\langle 0|\frac{1}{\sqrt{n!}}(\frac{a_1 - a_2}{\sqrt{2}})^n S_1 S_2$. This solution degenerates to the single mode squzeed vacuum in two modes when $m = n = 0$. Generally, an initial state $\rho(0) = \sum_{mnpq} C_{mnpq}|mn\rangle\langle pq| = \sum_{mnpq} C'_{mnpq}|m_{L_1}p_{L_2}\rangle\langle n_{L_1}q_{L_2}|$ will evolve into $\sum_{mn} G_{mn}|m_{L_1}\rangle\langle n_{L_1}|$ where $G_{mn} = \sum_{mnp} C'_{mnpp}$.

Therefore, we have shown that the entangled modes in the squeezed vacuum can be physically separated by the resonant cavities, without any loss of entanglement between them.

6. SUMMARY AND CONCLUSIONS[1]

In this dissertation, we systematically studied the interactions between the squeezed vacuum and the atoms. We challenged the traditional reservoir theory which fails to consider the effect of the squeezing source. We put forward a new reservoir theory by modifying the mode function of the electromagnetic fields, which includes the position information of the squeezing source. Then we derived a master equation of the atomic dynamics based on the Weisskopf-Wigner approximation. In our formalism, the density matrix is naturally positive-definite. We then apply this theory to the 1D waveguide-QED system where the squeezing in one direction is experimentally achievable. We show that the enhancement and suppression of the dephasing rate caused by the squeezed vacuum is actually dependent its position in the waveguide. In single-atom case, the squeezing does not affect its population dynamics. However, in multi-atom case, the squeezing can strongly affect the population dynamics of the system because two-photon absorption and emission are allowed in multi-atom system. We also show that dipole-dipole interaction influences dephasing rate and we can tune the position of the squeezing source to tune the dephasing rate of the system. Moreover, we show that stationary entangled state can be achieved in this system independent of the initial state and the emitter separation. Particularly, when the center of mass is close to $n\lambda_{0z}/4$ and the squeezing is large, the system can be prepared in GHZ state. Moreover, we study the power spectrum of the resonance fluorescence. It is demonstrated that the phase of the squeezed vacuum, emitter separation, and the center-of-mass position can affect the bandwidth and the intensity of the sidebands.

We further generalized our theory to arbitrary atomic structures. We studied the Ξ-type atoms coupled to a broadband squeezed vacuum reservoir in a quasi-one-dimensional waveguide, with the overall transition frequency $\omega_{ac} = 2\omega_0$. We showed that a single atom evolves into a steady

[1]Part of this section is reprinted with permission from: "Waveguide QED in the Squeezed Vacuum" by Jieyu You et al, 2018. Physical Review A, 97, 023810, Copyright 2018 by the American Physical Society and "Steady-state population inversion of multiple Ks-type atoms by the squeezed vacuum in a waveguide" by Jieyu You, Zeyang Liao, and M. Suhail Zubairy, 2019. Physical Review A, 100, 013843, Copyright 2019 by the American Physical Society.

state which is a superposition of the second excited state and the ground state. If the decay rate from the second excited state to the first excited state is much smaller than that from the first excited state to the ground state, the population can be almost 100% trapped in the second excited state, which is a great improvement compared to the maximum ratio of 78% in Ref. [39]. What is more, we proved that the above result can be generalized to an arbitrary number of atoms interacting with each other via dipole-dipole interaction, and the system's final steady state is a direct product of that in the single-atom case with modified squeezed vacuum shown in Eq. (4.14). This is one of the most interesting results here and its physical insight still needs further studies. We also argued that the arbitrary ratio of the two transitions' decay rates can be effectively controlled by different waveguide structure. This population-inversed system is experimentally feasible since the experiments on the broadband squeezed vacuum coupled to the artificial atom in a 1D cavity have been widely conducted[26, 28, 29, 61, 62, 63].

REFERENCES

[1] E. M. Purcell, H. C. Torrey, and R. V. Pound, "Resonance Absorption by Nuclear Magnetic Moments in a Solid," *Phys. Rev.*, vol. 69, pp. 37–38, Jan 1946.

[2] C. W. Gardiner, "Inhibition of Atomic Phase Decays by Squeezed Light: A Direct Effect of Squeezing," *Phys. Rev. Lett.*, vol. 56, pp. 1917–1920, May 1986.

[3] M. J. Collett and C. W. Gardiner, "Squeezing of intracavity and traveling-wave light fields produced in parametric amplification," *Phys. Rev. A*, vol. 30, pp. 1386–1391, Sep 1984.

[4] J. Gea-Banacloche, M. O. Scully, and M. S. Zubairy, "Vacuum Fluctuations and Spontaneous Emission in Quantum Optics," *Physica Scripta*, vol. T21, pp. 81–85, Jan 1988.

[5] C. W. Gardiner, A. S. Parkins, and M. J. Collett, "Input and output in damped quantum systems. II. Methods in non-white-noise situations and application to inhibition of atomic phase decays," *J. Opt. Soc. Am. B*, vol. 4, pp. 1683–1699, Oct 1987.

[6] G. Palma and P. Knight, "Single atom dynamics in a broad band squeezed vacuum," *Optics Communications*, vol. 73, no. 2, pp. 131 – 135, 1989.

[7] G. M. Palma and P. L. Knight, "Phase-sensitive population decay: The two-atom Dicke model in a broadband squeezed vacuum," *Phys. Rev. A*, vol. 39, pp. 1962–1969, Feb 1989.

[8] G. S. Agarwal and R. R. Puri, "Cooperative behavior of atoms irradiated by broadband squeezed light," *Phys. Rev. A*, vol. 41, pp. 3782–3791, Apr 1990.

[9] Z. Ficek, "Spontaneous emission from two atoms interacting with a broadband squeezed vacuum," *Phys. Rev. A*, vol. 42, pp. 611–617, Jul 1990.

[10] Z. Ficek, "Pairwise atomic states: Two-atom system in a three-dimensional squeezed vacuum field," *Phys. Rev. A*, vol. 44, pp. 7759–7776, Dec 1991.

[11] E. V. Goldstein and P. Meystre, "Dipole-dipole interaction in squeezed vacua," *Phys. Rev. A*, vol. 53, pp. 3573–3581, May 1996.

[12] S. Das, G. S. Agarwal, and M. O. Scully, "Quantum Interferences in Cooperative Dicke Emission from Spatial Variation of the Laser Phase," *Phys. Rev. Lett.*, vol. 101, p. 153601, Oct 2008.

[13] J. T. Shen and S. Fan, "Coherent photon transport from spontaneous emission in one-dimensional waveguides," *Opt. Lett.*, vol. 30, pp. 2001–2003, Aug 2005.

[14] J.-T. Shen and S. Fan, "Coherent Single Photon Transport in a One-Dimensional Waveguide Coupled with Superconducting Quantum Bits," *Phys. Rev. Lett.*, vol. 95, p. 213001, Nov 2005.

[15] J.-T. Shen and S. Fan, "Strongly Correlated Two-Photon Transport in a One-Dimensional Waveguide Coupled to a Two-Level System," *Phys. Rev. Lett.*, vol. 98, p. 153003, Apr 2007.

[16] V. I. Yudson and P. Reineker, "Multiphoton scattering in a one-dimensional waveguide with resonant atoms," *Phys. Rev. A*, vol. 78, p. 052713, Nov 2008.

[17] H. Zheng, D. J. Gauthier, and H. U. Baranger, "Waveguide QED: Many-body bound-state effects in coherent and Fock-state scattering from a two-level system," *Phys. Rev. A*, vol. 82, p. 063816, Dec 2010.

[18] L. Zhou, H. Dong, Y.-x. Liu, C. P. Sun, and F. Nori, "Quantum supercavity with atomic mirrors," *Phys. Rev. A*, vol. 78, p. 063827, Dec 2008.

[19] T. Shi and C. P. Sun, "Lehmann-Symanzik-Zimmermann reduction approach to multiphoton scattering in coupled-resonator arrays," *Phys. Rev. B*, vol. 79, p. 205111, May 2009.

[20] "Coherent single-photon absorption by single emitters coupled to one-dimensional nanophotonic waveguides, author=Chen, Yuntian and Wubs, Martijn and Mørk, Jesper and Koenderink, A Femius," *New Journal of Physics*, vol. 13, no. 10, p. 103010, 2011.

[21] Z. Liao, X. Zeng, S.-Y. Zhu, and M. S. Zubairy, "Single-photon transport through an atomic chain coupled to a one-dimensional nanophotonic waveguide," *Phys. Rev. A*, vol. 92, p. 023806, Aug 2015.

[22] Y. Shen and J.-T. Shen, "Photonic-Fock-state scattering in a waveguide-QED system and their correlation functions," *Phys. Rev. A*, vol. 92, p. 033803, Sep 2015.

[23] Z. Liao, H. Nha, and M. S. Zubairy, "Dynamical theory of single-photon transport in a one-dimensional waveguide coupled to identical and nonidentical emitters," *Phys. Rev. A*, vol. 94, p. 053842, Nov 2016.

[24] Z. Liao, X. Zeng, H. Nha, and M. S. Zubairy, "Photon transport in a one-dimensional nanophotonic waveguide QED system," *Physica Scripta*, vol. 91, no. 6, p. 063004, 2016.

[25] D. Roy, C. M. Wilson, and O. Firstenberg, "Colloquium: Strongly interacting photons in one-dimensional continuum," *Rev. Mod. Phys.*, vol. 89, p. 021001, May 2017.

[26] Q. A. Turchette, N. P. Georgiades, C. J. Hood, H. J. Kimble, and A. S. Parkins, "Squeezed excitation in cavity QED: Experiment and theory," *Phys. Rev. A*, vol. 58, pp. 4056–4077, Nov 1998.

[27] i. m. c. E. Kocabaş, E. Rephaeli, and S. Fan, "Resonance fluorescence in a waveguide geometry," *Phys. Rev. A*, vol. 85, p. 023817, Feb 2012.

[28] K. W. Murch, S. J. Weber, K. M. Beck, E. Ginossar, and I. Siddiqi, "Reduction of the radiative decay of atomic coherence in squeezed vacuum," *Nature*, vol. 499, p. 62–65, Jul 2013.

[29] D. M. Toyli, A. W. Eddins, S. Boutin, S. Puri, D. Hover, V. Bolkhovsky, W. D. Oliver, A. Blais, and I. Siddiqi, "Resonance Fluorescence from an Artificial Atom in Squeezed Vacuum," *Phys. Rev. X*, vol. 6, p. 031004, Jul 2016.

[30] M. O. Scully and M. S. Zubairy, *Quantum Optics*. Cambridge University Press, 1997.

[31] O. Svelto, *Principles of Lasers*. Springer US, 2010.

[32] H. J. Carmichael, A. S. Lane, and D. F. Walls, "Resonance fluorescence from an atom in a squeezed vacuum," *Phys. Rev. Lett.*, vol. 58, pp. 2539–2542, Jun 1987.

[33] I. Kruse, K. Lange, J. Peise, B. Lücke, L. Pezzè, J. Arlt, W. Ertmer, C. Lisdat, L. Santos, A. Smerzi, and C. Klempt, "Improvement of an Atomic Clock using Squeezed Vacuum," *Phys. Rev. Lett.*, vol. 117, p. 143004, Sep 2016.

[34] R. Tanas and Z. Ficek, "Stationary two-atom entanglement induced by nonclassical two-photon correlations," *arXiv preprint quant-ph/0309195*, 2003.

[35] F.-L. Li, P. Peng, and Z.-Q. Yin, "Preparing entangled states of two atoms through the intensity-dependent interaction with the two-mode squeezed vacuum," *Journal of Modern Optics*, vol. 53, no. 14, pp. 2055–2066, 2006.

[36] J. You, Z. Liao, S.-W. Li, and M. S. Zubairy, "Waveguide quantum electrodynamics in squeezed vacuum," *Phys. Rev. A*, vol. 97, p. 023810, Feb 2018.

[37] Z. Ficek and P. D. Drummond, "Three-level atom in a broadband squeezed vacuum field. I. General theory," *Phys. Rev. A*, vol. 43, pp. 6247–6257, Jun 1991.

[38] Z. Ficek and P. D. Drummond, "Three-level atom in a broadband squeezed vacuum field. II. Applications," *Phys. Rev. A*, vol. 43, pp. 6258–6271, Jun 1991.

[39] Z. Ficek and P. D. Drummond, "Two-Photon Population Inversion by Squeezed Light in a Fabry-Perot Microcavity," *Europhysics Letters (EPL)*, vol. 24, pp. 455–460, Nov 1993.

[40] C. Gerry and P. Knight, *Introductory Quantum Optics*. Cambridge University Press, 2004.

[41] Wikipedia, "Spontaneous parametric down-conversion." `https://en.wikipedia.org/wiki/Spontaneous_parametric_down-conversion`, Dec 2019. Accessed Feb-25-2020.

[42] Z. Ficek and S. Swain, *Quantum interference and coherence: theory and experiments*, vol. 100. Springer Science & Business Media, 2005.

[43] G. S. Agarwal, "Quantum statistical theories of spontaneous emission and their relation to other approaches," in *Quantum Optics*, pp. 1–128, Springer, 1974.

[44] G. Lindblad, "On the generators of quantum dynamical semigroups," *Communications in Mathematical Physics*, vol. 48, no. 2, pp. 119–130, 1976.

[45] C. Tai, I. Antennas, P. Society, I. M. Theory, and T. Society, *Dyadic Green Functions in Electromagnetic Theory*. IEEE Press Series on Electromagnetic Waves, IEEE Press, 1994.

[46] M. B. Kim, G. Veronis, T.-W. Lee, H. Lee, and J. P. Dowling, "Spontaneous Emission from a Two-Level Atom in a Rectangular Waveguide," *arXiv*, 2013.

[47] R. Horodecki, P. Horodecki, M. Horodecki, and K. Horodecki, "Quantum entanglement," *Rev. Mod. Phys.*, vol. 81, pp. 865–942, Jun 2009.

[48] V. Giovannetti, S. Lloyd, and L. Maccone, "Advances in quantum metrology," *Nature Photonics*, vol. 5, no. 4, p. 222, 2011.

[49] B. Kraus, H. P. Büchler, S. Diehl, A. Kantian, A. Micheli, and P. Zoller, "Preparation of entangled states by quantum Markov processes," *Phys. Rev. A*, vol. 78, p. 042307, Oct 2008.

[50] S. Diehl, A. Micheli, A. Kantian, B. Kraus, H. Büchler, and P. Zoller, "Quantum states and phases in driven open quantum systems with cold atoms," *Nature Physics*, vol. 4, no. 11, p. 878, 2008.

[51] Y. Lin, J. Gaebler, F. Reiter, T. R. Tan, R. Bowler, A. Sørensen, D. Leibfried, and D. J. Wineland, "Dissipative production of a maximally entangled steady state of two quantum bits," *Nature*, vol. 504, no. 7480, p. 415, 2013.

[52] S.-L. Ma, Z. Liao, F.-L. Li, and M. S. Zubairy, "Dissipative production of controllable steady-state entanglement of two superconducting qubits in separated resonators," *EPL (Europhysics Letters)*, vol. 110, no. 4, p. 40004, 2015.

[53] B. Kraus and J. I. Cirac, "Discrete Entanglement Distribution with Squeezed Light," *Phys. Rev. Lett.*, vol. 92, p. 013602, Jan 2004.

[54] S. Hill and W. K. Wootters, "Entanglement of a pair of quantum bits," *Phys. Rev. Lett.*, vol. 78, pp. 5022–5025, Jun 1997.

[55] Z. Ficek and B. C. Sanders, "Quantum beats in two-atom resonance fluorescence," *Phys. Rev. A*, vol. 41, pp. 359–368, Jan 1990.

[56] Z. Liao, M. Al-Amri, and M. S. Zubairy, "Resonance-fluorescence-localization microscopy with subwavelength resolution," *Phys. Rev. A*, vol. 85, p. 023810, Feb 2012.

[57] K. Mølmer, Y. Castin, and J. Dalibard, "Monte Carlo wave-function method in quantum optics," *J. Opt. Soc. Am. B*, vol. 10, pp. 524–538, Mar 1993.

[58] N. Bogoliubov, "On the theory of superfluidity," *J. Phys*, vol. 11, no. 1, p. 23, 1947.

[59] S. J. Wang, M. C. Nemes, A. N. Salgueiro, and H. A. Weidenmüller, "Mean-field approximation to the master equation for sympathetic cooling of trapped bosons," *Phys. Rev. A*, vol. 66, p. 033608, Sep 2002.

[60] A. Jun-Hong, W. Shun-Jin, L. Hong-Gang, and J. Cheng-Long, "Production of squeezed state of single mode cavity field by the coupling of squeezed vacuum field reservoir in nonautonomous case," *Chinese Physics Letters*, vol. 21, no. 1, p. 1, 2004.

[61] N. Bergeal, R. Vijay, V. Manucharyan, I. Siddiqi, R. Schoelkopf, S. Girvin, and M. Devoret, "Analog information processing at the quantum limit with a Josephson ring modulator," *Nature Physics*, vol. 6, no. 4, p. 296, 2010.

[62] Z. Wang, S. Shankar, Z. Minev, P. Campagne-Ibarcq, A. Narla, and M. Devoret, "Cavity Attenuators for Superconducting Qubits," *arXiv preprint arXiv:1807.04849*, 2018.

[63] W. Qin, A. Miranowicz, P.-B. Li, X.-Y. Lü, J. Q. You, and F. Nori, "Exponentially Enhanced Light-Matter Interaction, Cooperativities, and Steady-State Entanglement Using Parametric Amplification," *Phys. Rev. Lett.*, vol. 120, p. 093601, Mar 2018.